January 1971

Hybrid Computer Simulation of the Accumulation and Melt Processes in a Snowpack

Keith O. Eggleston

Eugene K. Israelsen

J. Paul Riley

HYBRID COMPUTER SIMULATION OF THE ACCUMULATION AND MELT PROCESSES IN A SNOWPACK

by

Keith O. Eggleston
Eugene K. Israelsen
J. Paul Riley

The work reported by this project completion report was supported with funds provided by the United States Department of Commerce, Environmental Science Services Administration, Contract E-268-68(N), Investigation Period June 25, 1968 to December 31, 1969

Utah Water Research Laboratory
College of Engineering
Utah State University
Logan, Utah

June 1971 PRWG65-1

ABSTRACT

HYBRID COMPUTER SIMULATION OF THE ACCUMULATION AND MELT PROCESSES IN A SNOWPACK

This study represents the first phase of an investigation to develop an operational simulation model of the point snowmelt process based on a time increment of one day or less. Mathematical relationships for various phenomena involved in the snowmelt process were proposed and tested. These relationships were combined into a model which is applicable to any geographic location by determining appropriate constants for certain relationships. The model was synthesized on a hybrid computer and calibrated using field data from the Central Sierra Snow Laboratory. It was then tested with data from other well instrumented locations. Sensitivity tests were also conducted to study the relative effects of the various basic parameters and functions upon the melting process. Initial tests of the model proved encouraging and suggested merit in persuing a proposed subsequent phase of the project to incorporate the point snowmelt model into that of the total hydrologic system. Thus, watershed runoff hydrographs resulting from a melting snowpack will be simulated.

Eggleston, Keith O.; Israelsen, Eugene K.; and Riley, J. Paul; HYBRID COMPUTER SIMULATION OF THE ACCUMULATION AND MELT PROCESSES IN A SNOWPACK. Project completion report to the Weather Bureau, Environmental Science Services Administration, United States Department of Commerce, February 1970, Washington, D. C., 77 p.

KEYWORDS--*point snowmelt/ *snowmelt modeling/ *simulation/ *snow hydrology/ hydrologic models/ runoff/ *flood prediction/ *snow laboratory/ *hydrologic research/ hydrology/ *hybrid computer/ precipitation/ weather modification/ *snowpack management/ water yields/

ACKNOWLEDGMENTS

This publication is a completion report for a project which was supported primarily with funds provided by the Environmental Science Services Administration of the United States Department of Commerce. The authors gratefully acknowledge this support and the helpful suggestions provided by Eugene L. Peck, Eric A. Anderson and other personnel of this Agency throughout the study.

Appreciation is also expressed to Dr. Jay M. Bagley, Director of the Utah Water Research Laboratory for the computer and other facilities at the laboratory which contributed significantly to the success of the project.

Keith O. Eggleston
Eugene K. Israelsen
J. Paul Riley

NOMENCLATURE

Symbol	Definition
A	Albedo, or reflectivity of the snowpack surface
ALB1	Solar radiation absorbed at the snow surface (1 - A)
C_c	Elevation correction factor applicable to the particular time increment
C_v	Vegetation canopy density
CSSL	Central Sierra Snow Laboratory
DECD	Degree days in digital program used in calculating snowmelt
DIN	Density of the new snow
D(t)	Depth of the snowpack in inches at a given time, t
$D_a(t)$	Apparent depth of snowpack
E_{cr}	Potential evapotranspiration in inches per day
E_o	Different values according to the position of the snow layer under consideration
EVAP	Evaporation from the snowpack in inches per unit time
E_s	Mean elevation of the watershed zone in thousands of feet
E_v	Mean elevation of the valley floor in thousands of feet
F	Melt rate factor (in/time)
HOS2	Total water available from the surface as a function of surface melt and rain
k	Constant equal to 21 cm^3/gr
k_a	Time constant
k_c	Coefficient which is a function of physiology and stage of growth of the crop
k_f	Coefficient which regulates the rate of liquid water freezing as a function of time
k_m	Constant of proportionality
k_s	Proportionality constant
k_{sc}	Settlement time constant for the snowpack
k_t	Equal to $0.0173\ T_a - 0.314$
k_v	Vegetation transmission coefficient for radiation
$L_c(t)$	Liquid water holding capacity in inches at a given time (t)
L_w	Total liquid water in the snowpack
M	Number of depth zones into which the pack has been divided
M_r	Total snowmelt in inches per unit time, t
M_{rg}	Melt rate at the snow ground interface in inches per unit time, t
M_{rp}	Melt rate at the snow surface due to rain falling on the snowpack in inches per unit of time, t
M_{rs}	Snowmelt rate at the surface
P	Percent of daylight hours
P_{rg}	Precipitation reaching the ground or snow surface, in inches
Q_e	Gain or loss of latent heat caused by evaporation, condensation, and sublimation
$Q_{fr}(t)$	Quantity of liquid water held in the pack that freezes at time, t
Q_i	Gain or loss of latent heat caused by freezing or melting
Q_n	Sensible heat transfer
Q_o	Change in heat storage for the snowpack
Q_r	Net radiation heat transfer
Q_s	Net transfer of heat by conduction at the snow ground interface
Q_w	Net heat transfer by a gain or loss of water

NOMENCLATURE (Continued)

Symbol	Definition
RI_h	Radiation index for a horizontal surface at the same latitude as the particular watershed or zone under study
RI_s	Radiation index for a particular watershed zone possessing a known degree and aspect of slope
RO_o	Initial density
SNAC	Depth of new snow accumulation
T_a	Mean daily air temperature
TEMSS	Temperature of the snow surface, in ^oF
T_j	Temperature of snow at point j, in ^oF
T_{j+1}	Temperature of snow at point j+1, in ^oF
T_{j-1}	Temperature of snow at point j-1, in ^oF
T_s	Snow temperature in degrees Fahrenheit
UCSL	Upper Columbia Snow Laboratory
W_{ao}	Initial value of the total accumulated water equivalent of the snowpack
$W_a(t)$	Water equivalent of the snowpack, at anytime t
WBSL	Willamette Basin Snow Laboratory
x	Initial water content plus added water, in percent of initial
y	Snowpack depth, in percent of initial depth
z	Snow depth, in feet or inches
α	Thermal diffusivity of the snow, in $feet^2$/ time
ρ_i	Density of the newly fallen snow
$\rho(t)$	Average pack density at a given time (t), in percent

CHAPTER I

INTRODUCTION

Demands upon available water resources have led to an increasing interest in more fundamental approaches to the science of hydrology. Accompanying these demands has been the need for better understanding of the snowmelt process. Joint investigations by the U.S. Army Corps of Engineers and the U.S. Weather Bureau (6) have contributed significantly to a more fundamental understanding of snow hydrology for project design and streamflow forecasting. These studies have focused attention upon many of the basic phenomena involved in the snowmelt process. However, a completely adequate description of the entire physical process of snowmelt under all conditions is not yet available.

The problem of synthesizing all of the various phenomena involved in the snowmelt process into a composite model to yield reliable estimates of specific snowmelt rates is difficult. The complex interrelation and variable nature of the many different phenomena occurring simultaneously further complicates the problem. In addition, many of the component parts of the process, such as the time variation of the thermal diffusivity and permeability coefficients within a snowpack, have not yet been adequately described mathematically. Thus the search for a practical and dynamic model of the snowmelt process entails formulation of relationships describing the many phenomena involved, and testing these relationships to determine the relative effects of various basic parameters upon the melting process. It is anticipated that a fundamental and systematic approach will lead to the eventual development of a standard method for synthesizing snowmelt hydrographs on the basis of commonly available hydrometeorological, physiographical, and geographical information.

Important considerations in the development of a model are the time and space increments adopted. The ultimate model would utilize continuous time and infinitesimal space increments. However, the practical limitations of this approach are obvious. The complexity of a model designed to represent a hydrologic system largely depends upon the magnitudes of the time and spatial increments utilized in the model. In particular, when large increments are applied, the scale magnitude is such that the effects of phenomena which change over relatively small increments of space and time are insignificant. For instance, on a monthly time increment, interception rates and changing snowpack temperatures are neglected. In addition, sometimes the time increment chosen coincides with the period of cyclic changes in certain hydrologic phenomena. In this event net changes in these phenomena during the time interval are usually negligible. For example, on an annual basis, storage changes within a hydrologic system are often insignificant, whereas on a monthly basis the magnitudes of these changes are frequently appreciable and need to be considered. As time and spatial increments decrease, improved definition of the hydrologic processes is required. No longer can short-term transient effects or appreciable variations in space be neglected, and the mathematical model becomes increasingly complex, with an accompanying increase in the requirements of computer capacity and capability.

The snow model is a part of the overall hydrologic model of a watershed or river basin. The air temperature can be used to indicate whether precipitation will be snow or rain. When precipitation occurs as snow, the model stores it as a snowpack of the same water equivalent. If the air temperature indicates snowmelt, the model will melt the snow and subtract the amount melted from the water equivalent of the pack. The melt appears as runoff from the snow and becomes an input to the hydrologic model

in which

Q_i = the gain or loss of latent heat caused by freezing or melting in the surface layer

Q_e = the heat transferred to or from this layer by conduction within the snowpack

Q_w = the heat transferred to the snow by precipitation

The components of the energy balance can be evaluated and tested as explained by Anderson (2). The energy balance can be applied at a point source or integrated over an entire basin by using certain empirical relationships to relate point measurements to the complete watershed.

Characteristics of the Snowpack

Several references are available which place emphasis on particular characteristics of the snowpack. Examples of some of these characteristics are density (5, 16, 20), free water holding capacity (22, 28), transmission of liquid water through the snow (16, 28), heat exchange by conduction, radiation and convection (6, 12, 43), snow evaporation and condensation (4, 26, 27, 28, 33, 39), and instrumentation and measurement of parameters (7, 16, 20).

Riley (30) investigated and modeled many of the individual components or characteristics of the snowpack, such as liquid water holding capacity, compaction, albedo of the surface, and others.

Density

Density is an important factor in snow accumulation and melt simulation. Density variations are related to new snow density, depth of snow, time after snow, and form of precipitation. As the snow compacts, the density increases until it reaches a maximum value. An average maximum density for snow in a well-settled pack is approximately 50 to 60 percent (5). Using this information, Riley (30) derived an expression for the settlement of a snowpack as

$$\frac{d[D_a(t)]}{dt} + k_{sc} D_a(t) = \frac{P_{rg}}{\rho_i} + \frac{k_{sc}}{0.6}\left[W_{ao} + \int_o^t P_{rg}\,dt\right] \quad . \quad . \quad . \quad . \quad (2.3)$$

in which

$D_a(t)$ = apparent depth of pack

P_{rg} = precipitation reaching the ground

W_{ao} = initial value of the total accumulated water equivalent of the snowpack

ρ_i = initial density of newly fallen snow

k_{sc} = a settlement time constant

The average pack density is then calculated by dividing the apparent depth into the accumulated precipitation.

Amorocho and Espildora (1) used a compaction equation proposed by Yosida (44). The equation gives the variation of density with time due to the overlying weight of newly fallen snow. The equation is

$$(1/RO_o)\, dRO_o/dt = W/[E_o \exp(kRO_o)] \quad . \quad (2.4)$$

in which

RO_o = the initial density

k = a constant equal to 21 cm^3/gr

E_o = different values according to the position of the snow layer under consideration

They calculated the new density every hour for each layer.

Bertel (5) experimentally determined a relationship between the amount of rain and the depth of the snow after settlement due to the rain. This relationship is given by the following equation,

$$Y = 147.4 - 0.47x \quad . \quad . \quad . \quad . \quad . \quad (2.5)$$

in which

y = snowpack depth in percent of initial depth

x = initial water content plus added water in percent of initial content

The density variation in a snowpack was investigated by Gray (18) by taking samples at different depths of the pack. He also investigated densities of different types of snow. At the Willamette Basin Snow Laboratory (WBSL) the densities for newly fallen snow varied from 0.08 g/cc to 0.38 g/cc. Density changes within the pack began as soon as the snow was deposited and continued through the accumulation period and into the melt period. Changes in crystal form and displacement in the snowpack are caused by several physical processes (6): (i) percolation of melt or rain water which freezes within the pack; (ii) plastic deformation of the snow matrix from weight of overlying snow causing reduction in voids; and (iii) transport of water vapor due to temperature and vapor pressure gradients and convection of air within the snowpack.

The density of newly fallen snow varies with the shape, size, and type of snow crystals, as well as temperature, humidity, and velocity of the wind. The two most important factors affecting new snow density are temperature and wind velocity. Diamond and Lowry (13) correlated new snow density to surface air temperature and found an average increase in density of 0.0036 g/cc per degree F increase at the time of deposition. Rikhter (29) reported densities of new-fallen snow varying with surface wind from 0.06 for calm conditions to 0.34 for snow deposited during gale winds. For practical purposes a good average density to use for converting depth of snow to water equivalent (6) for a 24-hour accumulation period for new snow is 0.10 g/cc.

Albedo

The albedo or reflectivity of the snow surface varies from a maximum at the time of deposition to a minimum during the spring snowmelt season. Investigators at the Central Sierra Snow Laboratory (CSSL) (6) found that newly-fallen snow had an albedo of approximately 0.8 while coarse grained melting surface snow was as low as 0.4. The albedo of the snow surface is controlled by the last snowfall. When the new snow melts, the albedo goes back to what it was before the snow.

The snow surface acts as a black body in the long wave portion of the radiation spectrum. It acts as a perfect absorber and emitter of radiation in accordance with the Stefan-Boltzman Law because of the rough, many faceted surface of the snow. Thus, there is a net exchange of long wave radiation with the snow and its environment that can be either positive or negative.

Liquid water in the snow

Water appears in a snowpack in three forms; ice, liquid, and vapor. Water moves about in the pack in the liquid and vapor phases. The movement of the vapor phase is important in the metamorphism of the snowpack, but in magnitude it is low when compared to liquid water transport. When the liquid water holding capacity has reached its limit, the downward movement of water is dependent entirely on gravitational forces.

The conditions of liquid water in the pack vary with temperature, stage of metamorphism, and the availability of liquid water. When the temperature of snow is below $32^{\circ}F$, it is said to be dry. The wetness of snow at $32^{\circ}F$ is dependent upon the availability of water and the liquid water holding capacity. The liquid water in the pack can be measured by differences in snow compaction (39), by the use of a centrifuge, by means of calorimetric methods where the amount of heat required to melt the sample of snow is measured, and by electrical capacitance in a parallel plate condenser having snow as its dielectric (17).

The forms in which liquid water exists in the pack are (6):

1. Hygroscopic water, which is adsorbed as a thin film of water on the surfaces of the snow crystals,

and unavailable to runoff until the snow crystal melts.

2. Capillary water, which is held by surface tension in the capillary spaces around the snow particles. Capillary water moves under the influence of capillary forces, but is not available to runoff until the snow melts or the spacing between the crystals changes and frees some of the capillary water.

3. Gravitational water is in transit through the snowpack under the influence of gravity and drains from the snowpack as runoff.

The time for gravitational water required to travel through a snowpack depends upon many things. The temperature, size, shape, surface area, and spacing of the snow crystals, channelization, melt, and rainfall intensities control retention and detention of water as it moves downward through the pack. Since most of these factors are continually changing the storage by the snowpack and time of travel through the pack are not constant. Gerdel (17) found generally that as density increased, the speed of transmission also increased. The lowest rate that he found was approximately 1-inch per minute during an 18-minute test and the greatest was 24 inches per minute during 35-minute tests. This indicates a large range of velocities of water traveling through snow. In late season snow the velocities would be on the high side, and, therefore, the snowpack would cause little delay before melt at the pack surface reached the ground surface.

Model Development

A snow model was developed by Riley (30). Following is a brief summary of his work, and how it fits into this research effort. This summary appeared in a report by Riley, Chadwick, and Eggleston (32).

Large increments of time and space

Both the complex nature of snowmelt and data limitations prevent a strictly analytical approach to modeling the snowmelt process. In particular, for the computation of melt on the basis of large time increments, such as a month, a rather empirical approach seemed most suitable. Accordingly a relationship was proposed which states that the rate of melt is proportional to the available energy and the quantity of precipitation stored as snow. Expressed as a differential equation the relationship appears:

$$\frac{d[W_s(t)]}{dt} = -k_s(T_a - 35)\, W_s(t) \quad . \quad . \quad . \quad (2.6)$$

in which

k_s = a proportionality constant

$W_s(t)$ = the water equivalent of the snowpack at any time (t)

From an analysis of snow course data from various parts of Utah, the value of k_s was determined to be approximately 0.10 for mountain watersheds. For valley floor areas a somewhat higher value of k_s is applicable. The independent variables on the right side of Equation 2.1 can be expressed either as continuous functions of time or as step functions consisting of mean constant values applicable throughout a particular time increment. In this model a time increment of one month was utilized with integration being performed in steps over each successive period. Thus, the final value of $W_s(t)$ at the end of the period becomes the initial value for the integration process over the following period. A test of Equation 2.6 is illustrated by Figure 2.1 which indicates predicted and actual rates of snowmelt for a watershed in Montana.

Reducing the space increments

In the snowmelt relationship of Equation 2.6 surface air temperature is applied as an index of available energy for the melting process. On a regional basis, air temperature is a reasonably good index of available energy at particular elevations. However, even if adequate data were available, air temperature alone does not provide a fully satisfactory means of comparing the energy flux among the different facets of a landscape. For a particular

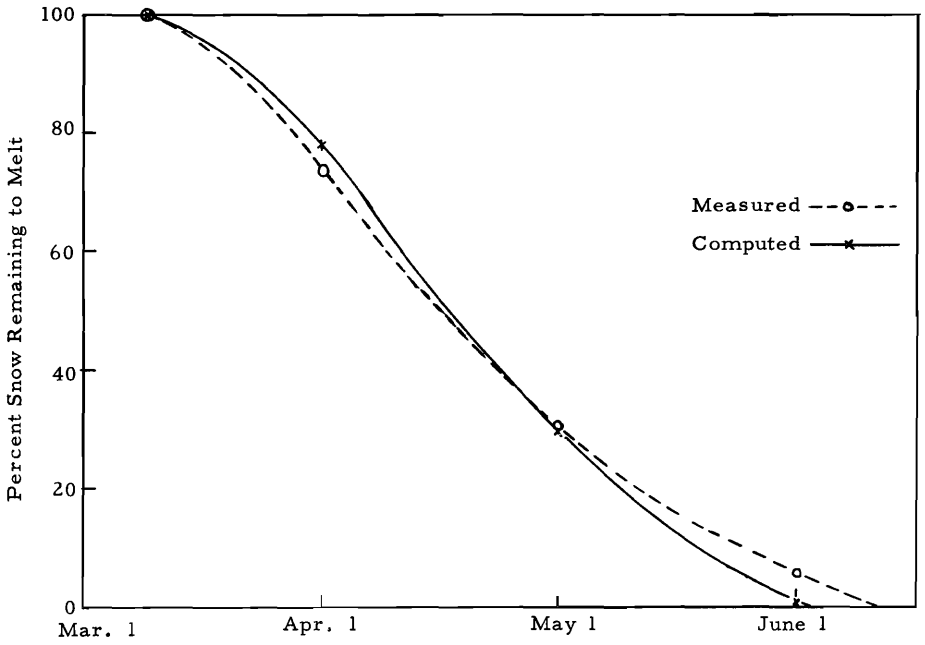

Figure 2.1. Measured and computed snowmelt rate curves for the Middle Fork Flathead River, Montana, 1947.

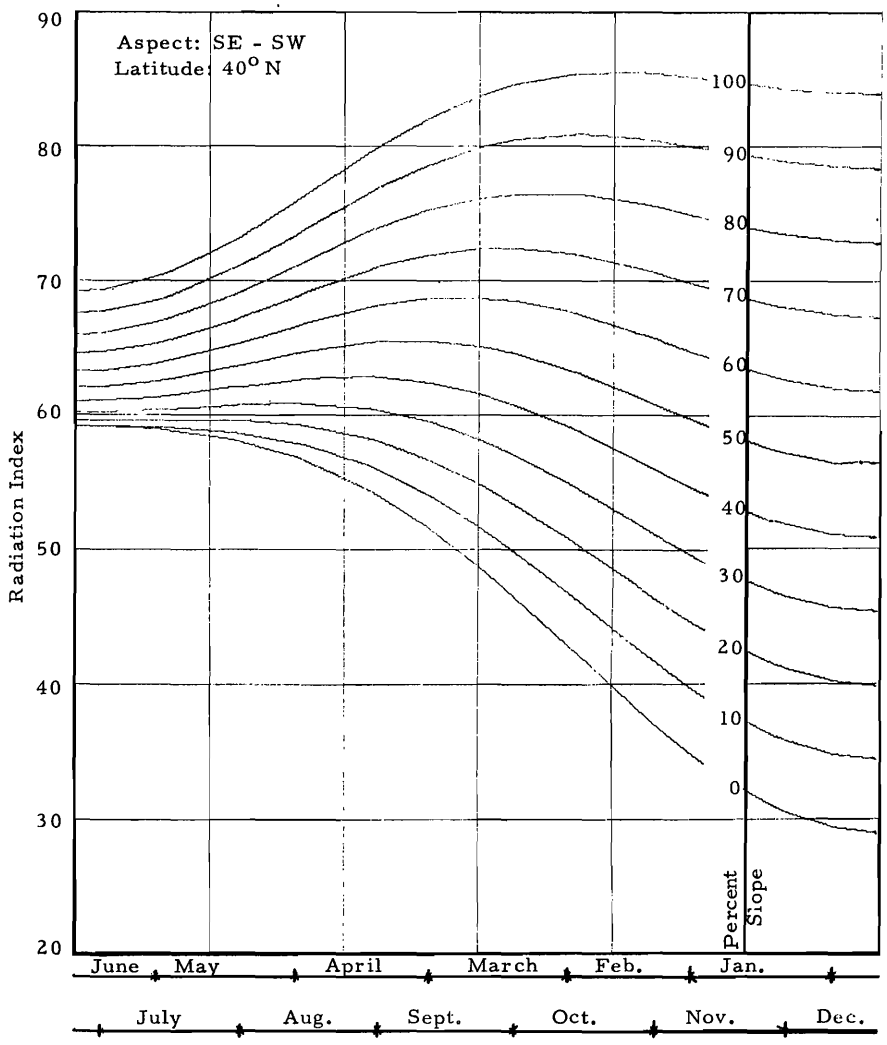

Figure 2.2. Radiation index values as a function of slope inclination and time of year.

elevation, Equation 2.6 would indicate no appreciable differences between melting rates on, for example, easterly and southerly slopes. When large units or areas are considered by a model, the effects of slope aspect differences often tend to average. However, for small zones, aspect effects are important and should be considered by a snowmelt relationship.

The potential insolation parameter has been proposed as a means of comparing the energy flux among the different facets of a landscape (14, 23, 34, 35). In the concept of potential insolation, the earth's atmosphere is ignored. Thus, irradiation of a surface by direct sunshine is considered to be only a function of the angle between the surface and the sun's rays. This angle, in turn, is a function only of the geometric relationships between the surface and the sun as expressed by latitude, degree of slope and aspect of the surface, and the declination and hour angle of the sun. For a given site the only variation in instantaneous potential insolation will be perfectly cyclical with time, depending upon the changes in hour angle and declination. Thus, the use of potential insolation as a parameter of surface energy is sufficiently simple to make feasible its wide application.

Frequently, potential insolation for a particular surface is expressed as a percentage of the maximum possible radiation rate at the outer limit of the earth's atmosphere. The resulting dimensionless quantity is termed radiation index. Figure 2.2 illustrates a digital computer plot of the radiation index calculated for a particular aspect and expressed as a function of slope inclination and solar declination. The latitude is 40°N. Because direct radiation is equal upon facets that show symmetry with respect to a north-south axis, two aspects are represented by this figure.

For this model a term for radiation index is added to Equation 2.6 and the result appears as:

$$\frac{d[W_s(t)]}{dt} = -k_s(T_a - 35)\frac{RI_s}{RI_h} W_s(t) \quad . \quad . \quad (2.7)$$

A computer plot showing snowmelt rate as computed by Equation 2.7 for the Circle Valley watershed (1962) is shown by Figure 2.3. The Circle Valley is a subbasin of the Sevier River drainage in central Utah. The plot indicates snow accumulation during the months of January, February, March, and December of that year. The points of discontinuity in the snowmelt portion of the plot result from the input to the program of mean monthly (rather than continuous) temperature values.

Small increments of time and space

For this model an attempt was made to represent the various segments of the snow ablation process in a somewhat rational manner. A thoroughly rational approach to the problem of evaluating snowmelt involves a consideration of four processes of heat transfer, namely radiation, convection, and mass transfer. The importance of each of these processes is highly variable, depending upon conditions of weather and local environment. For example, in late spring, given a clear day and fairly open terrain, radiation is the prime factor in the melting of snow. However, under conditions of heavy cloud cover or heavily forested terrain, radiation becomes less important. In the exposed areas wind is an important element in the convection process, while in heavily forested areas wind becomes a minor factor.

The sources of heat involved in the melt of snow are as follows: (i) adsorbed solar radiation, (ii) net long wave (terrestrial) radiation, (iii) convection heat transfer from the air, (iv) latent heat of water vaporization by condensation from the air, (v) conduction of heat from the ground, and (vi) heat content of rain water (28, 6).

Rational formulas based upon the various factors listed in the preceding paragraph have been developed for snowmelt at a point. However, data required for the solution of these relationships are frequently lacking. For this reason and because of the complex nature of the process, in this model much reliance is still placed upon the empirical

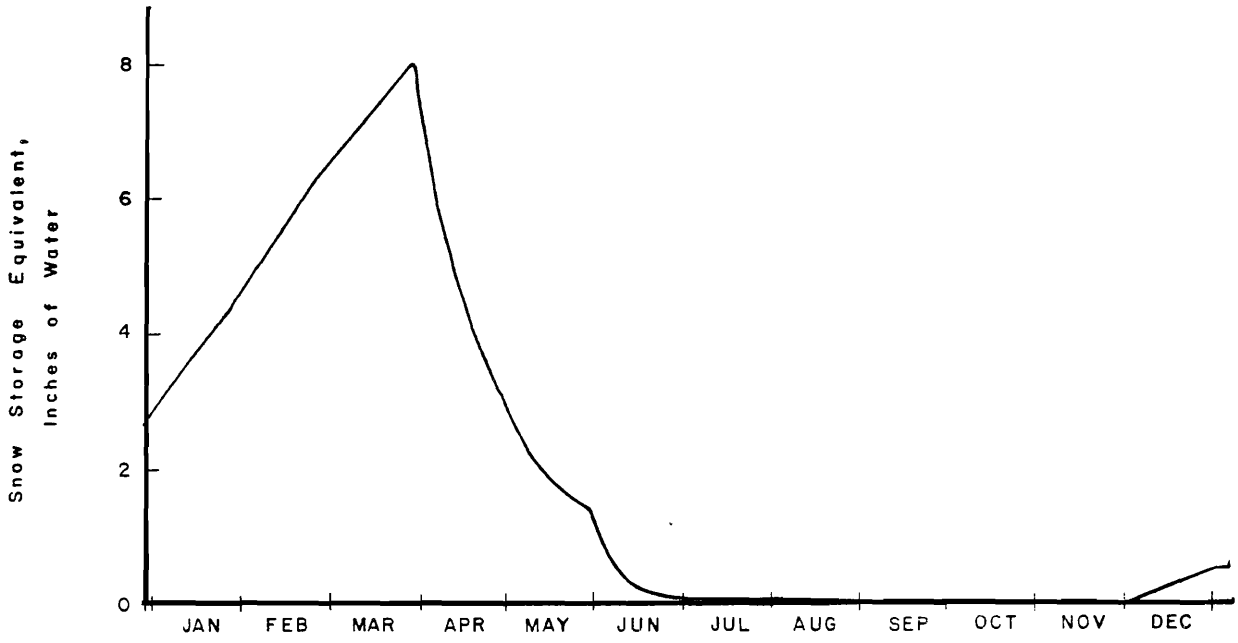

Figure 2.3. Computed accumulated snow storage equivalent on the watershed area of Circle Valley during 1962.

model of the snowmelt process, most were tested individually; and it is considered that they are sufficiently general in nature to permit their broad geographic application with perhaps appropriate adjustments in certain constants.

The two primary causes of snowpack ablation are net evaporation from the top surface of the pack and melting of the snow. Evaporation losses approach in the development of relations for predicting snowmelt. Many of the equations used in the model were developed from published charts and other available sources of information. While Riley did not test these equations in a composite from snow surfaces are estimated in the model by an empirical Equation 2.8 (31). Values of the independent variables in this equation are, of course, those which apply to the particular time increment being utilized in the model. For short-term melt estimates, such as a daily basis, it is necessary to take into account the temperature of the snowpack. Significant melt will not appear at the bottom of the pack until it has reached an isothermal temperature of 32°F, and its free water holding capacity has been satisfied (6). Thus, it is necessary to predict at any time, t, both the heat required to raise the pack to 32°F and the free

water holding capacity of the pack. Determining the required heat can be accomplished by predicting the snowpack temperature profile or by using a heat sink concept. The temperature profile was selected for this study.

A flow chart of the snow accumulation and ablation processes is shown by Figure 2.4. A brief discussion of each segment of this process is presented herein.

Evaporation. The mean daily temperature was used to calculate evaporation, snowmelt at the surface, snow surface temperature, and as an index to indicate the form of the precipitation. The equation used to calculate evaporation is a modification of the Blaney-Criddle Formula as modified by Phelen and others of the Soil Conservation Service (36, 37, 30)

$$E_{cr} = K_c K_t \frac{TP}{100} \quad . \quad . \quad . \quad . \quad . \quad . \quad (2.8)$$

in which

K_c = a function mainly of the physiology and stage of growth of the crop

K_c = 1.0 for water surfaces and 0.25 for snow surfaces or bare ground

K_t = a function of temperature, ^{o}F, and is equal to (0.0173T - 0.314)

T = temperature in ^{o}F

P = the percent of annual daylight hours per time period

A lumped evaluation of K_c for snow would indicate that evaporation values are net. Greater evaporation actually occurs but is offset by condensation.

Equation 2.8 can be further modified to include an elevation correction factor. The elevation influence is multiplied by the crop coefficient parameter, K_c. Thus, Equation 2.8 becomes:

$$Et_{cr} = K_c\left(K_t \frac{T_a P}{100} + C_c(E_s - E_v)\right) \quad . \quad . \quad (2.9)$$

in which

C_c = the elevation correction factor applicable

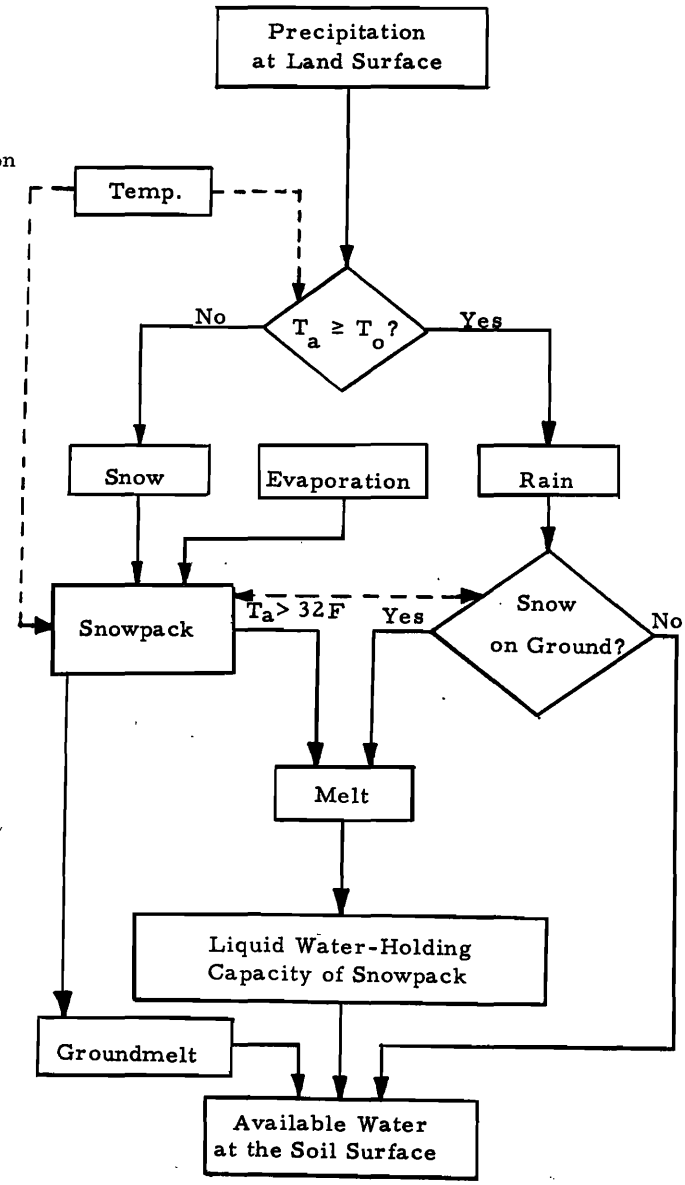

Figure 2.4. A flow chart of the snow accumulation and ablation process.

to the particular time increment

E_s = the mean elevation of the watershed zone in thousands of feet

E_v = the mean elevation of the valley floor in thousands of feet

In a study by Riley (30) the average annual elevation correction factor of 0.0027 inches per day per thousand feet was applied.

The two parameters of temperature and daylight hours are indicators of total energy available to surfaces subject to the evapotranspiration process. These indicators integrate total energy received over a regional horizontal area. To account for sloping land surfaces, such as occur on a watershed, the potential insolation parameter was introduced into Equation 2.9 by Riley (30), which becomes:

$$Et_{cr} = \frac{RI_s}{RI_h} K_c \left(K_t \frac{T_a P}{100} + C_c (E_s - E_v)\right) \quad . \quad (2.10)$$

in which all parameters, whether continuously variable or finite mean values, are applicable to the same time increment, and

RI_s = the radiation index for a particular watershed zone possessing a known degree and aspect of slope

RI_h = the radiation index for a horizontal surface at the same latitude as the particular watershed under study

In this study Equation 2.10 was applied at a point and the elevation correction was not needed. The equation becomes:

$$Et_{cr} = \frac{RI_s}{RI_h} K_c K_t \frac{T_a P}{100} \quad . \quad . \quad . \quad . \quad . \quad (2.11)$$

Free water holding capacity. The free water holding capacity of snow is the amount of water held against gravity within the pack. This capacity is a function of pack density and several other factors. Since these other factors are difficult to evaluate, it is common to use a relationship which is a function of average snowpack density alone. After the free water holding capacity has been filled, additional surface melt will move to the bottom of the pack. Figure 2.5(a) indicates an approximation to a relationship developed by the U.S. Corps of Engineers (6). The following two equations express the relationship shown by this figure.

$$L_c(t) = 0.05\, W_s(t), \quad (\rho(t) \leq 0.40) \quad . \quad . \quad (2.12)$$

$$L_c(t) = [0.1\, \rho(t) + 0.01]\, W_s(t), \quad (0.40 < \rho(t) \leq 0.60) \quad . \quad . \quad . \quad . \quad . \quad (2.13)$$

in which

$L_c(t)$ = the liquid water holding capacity in inches at a given time (t)

$\rho(t)$ = the average pack density for a given time (t)

Snowpack density. The density of a snowpack is influenced mainly by the density of new snow and the compaction of existing snow. Studies at the Central Sierra Snow Laboratory (CSSL) (6) have shown that the density of new snow varies approximately with the surface air temperature.

The average density of a pack may, of course, be obtained at any time by taking the ratio of the water equivalent to the pack depth at time, t. Changes in snowpack depth are caused by melt, evaporation, snowfall, and settlement. However, it can be assumed with some degree of approximation that evaporation and melt do not cause changes in the average density of the pack. This parameter is then computed by the equation:

$$\rho(t) = \frac{W_a(t)}{D_a(t)} \quad . \quad . \quad . \quad . \quad . \quad . \quad . \quad . \quad (2.14)$$

in which the value of W_a at any time, t, is given by summing an initial value of W_a (expressed as $W_a(0)$) and the accumulated precipitation over the time interval, t. Thus:

$$W_a(t) = W_a(0) + \int P_{rg}\, dt \quad . \quad . \quad . \quad . \quad (2.15)$$

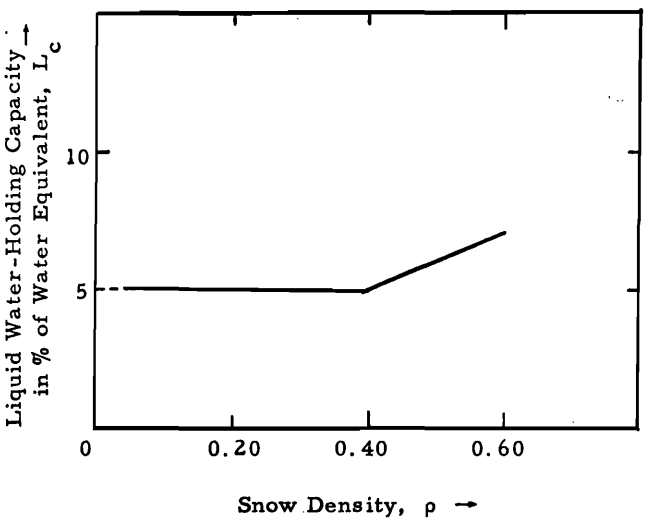

Figure 2.5(a). Liquid water-holding capacity of snow as a function of snow density.

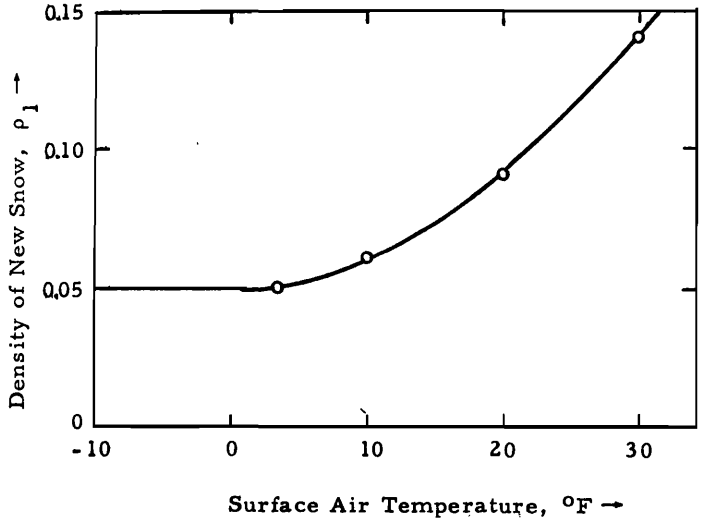

Figure 2.5(b). Density of new snow as a function of surface air temperature.

For a given initial snow depth, the value of $D_a(t)$ is increased by subsequent snowfalls and decreased by settlement of the pack. Observations (6) indicate that the settlement rate of a snowpack can be expressed as a function of the difference between the average pack density and the maximum pack density at any time. An average maximum density for snow in a well-settled pack is between 50 to 60 percent (6).

On the basis of this assumption and by applying a settlement time constant, k_{sc}, the following equation was developed for computing the value of D_a at any time, t:

$$\frac{d[D_a(t)]}{dt} + k_{sc} D_a(t) = \frac{P_{rg}}{\rho_i} + \frac{k_{sc}}{0.6} [D_a(0) + \int_o^t P_{rg} dt] \quad . \quad . \quad . \quad . \quad . \quad . \quad (2.16)$$

The solution of Equation 2.16 yields the value of $D_a(t)$ required in Equation 2.14 for estimating the average density of the snowpack. If a study is begun before the accumulation of any snow, $D_a(0)$ is equal to zero.

A test of Equation 2.16 is illustrated by Figure 2.6, which indicates both predicted and actual depths of a snowpack. The equation was applied on the basis of a daily time increment and k_{sc} was considered equal to 0.10 for a digital computer solution of Equation 2.16. Evaporation and melt losses were assumed negligible during this test period.

Snowpack temperatures. A procedure for predicting the temperature profile within a snowpack should take into account the conduction of heat through the snow crystals, and the heat transferred into the pack from both rain and surface melt. First, the development of an expression to describe temperature conditions within the snowpack for given boundary values as a function of both depth and time should be considered. Assuming that lateral or horizontal

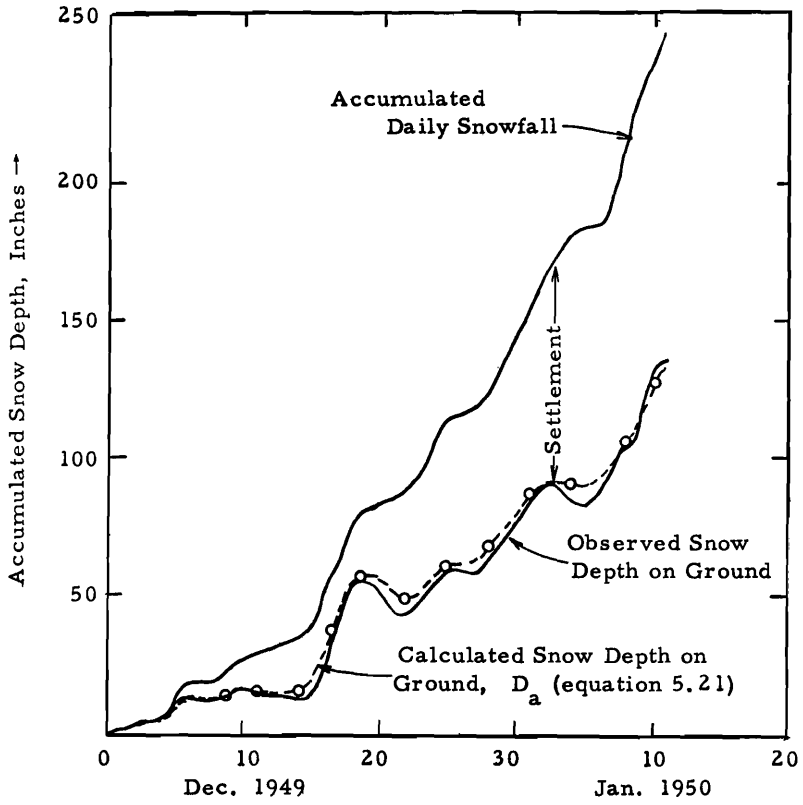

Note: Observations made at the Willamette Basin Snow Laboratory (reference 49)

Figure 2.6. Comparison between observed and calculated settled snow depths.

heat transfer within the pack is negligible, and that the snow surface temperature is equal to the air temperature, T_a, for $T_a < 32^{\circ}F$, a column of snow of finite diameter is governed by the conditions illustrated in Figure 2.7(a). For $T_a \geq 32^{\circ}F$, the snow surface temperature is assumed to be $32^{\circ}F$. As with most assumptions, this assumption may deviate from actual conditions, but is used to simplify the problem. Description of the snow surface temperature as it actually occurs would require continuous simulation in time of the snow-air interface and continuous simulation in space and time of the snowpack. Data necessary for this type of simulation are not available; therefore, the assumption which was made seems desirable. Several studies have indicated that the temperature at the bottom of the pack is usually maintained at approximately $32^{\circ}F$ by heat flow from the ground (15, 6). In its simplest form the problem then is characterized by one-dimensional heat flow in an assumed homogeneous column of snow with depth, D(t), and insulated sides. The value of D(t) is given by

$$D(t) = \frac{W_s(t)}{\rho(t)} \quad . \quad . \quad . \quad . \quad . \quad . \quad . \quad (2.17)$$

in which $\rho(t)$ is given by Equation 2.14 and the value of $W_s(t)$ is given by subtracting evaporation and melt losses from the precipitation reaching the ground as snow.

The heat flow equation applicable to this problem is expressed in partial derivative form as follows (18):

$$\frac{\partial^2 T_s}{\partial Z^2} = \frac{1}{\alpha_v} \frac{\partial T_s}{\partial t} \quad . \quad . \quad . \quad . \quad . \quad . \quad (2.18)$$

in which

Z = snow depth, in feet

T_s = the snow temperature, in $^{\circ}F$

α_v = the thermal diffusivity of the snow, in feet^2/time

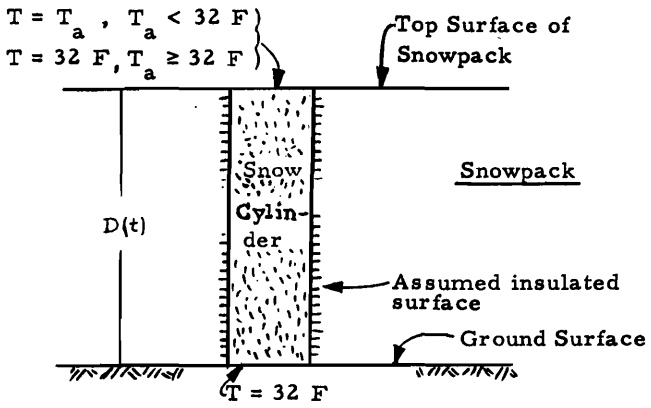

Figure 2.7(a). An assumed snow cylinder showing boundary temperature.

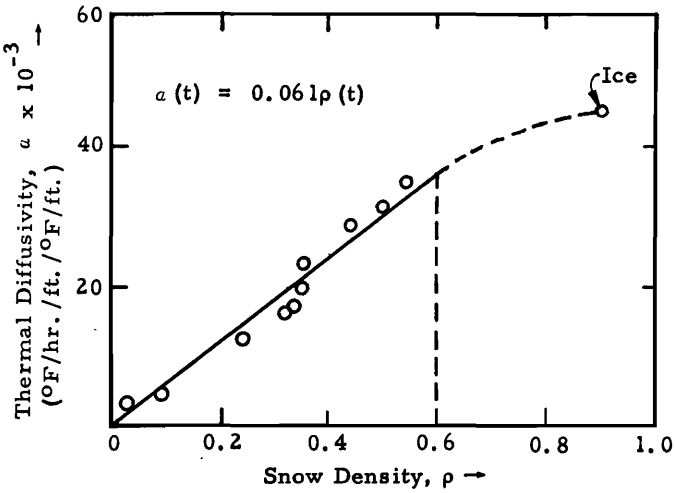

Figure 2.7(b). Thermal diffusivity of snow as a function of density.

The ever-changing thermal and physical properties of the snowpack make the theory of heat flow in snow much more complicated than is the case for a homogeneous solid. Thus, the factors which affect the thermal diffusivity of snow are its structural and crystalline character, the degree of compaction, the extent of ice planes, the degree of wetness, and the temperature of the snow (6). However, experimental work has shown that density is generally a satisfactory index of the thermal properties of the snowpack. Figure 2.7(b) illustrates the following empirical relationship between density and thermal diffusivity of snow (6).

$$\alpha(t) = 0.061\,\rho(t), \quad (0 < \rho \leq 0.60) \quad . \quad . \quad (2.19)$$

There is an appreciable variation in snow density with depth, and a more accurate approach to this problem would be to divide the snowpack into finite depth increments and to consider the entire melt process in each zone. This procedure would, however, considerably complicate the model, and it is anticipated that the results of the more approximate method will be sufficiently precise to permit an evaluation of the overall approach adopted.

The solution of Equation 2.18 will predict both transient and steady-state temperatures with independent variables of depth and time for given values α_v, the thermal diffusivity. However, the analog computer has only one dependent variable, voltage, and one independent variable, time. Therefore, the standard procedure for solving a partial differential equation such as Equation 2.18 is to fix one of its independent variables, say distance, and to then solve the resulting ordinary differential equation. The point at which the depth Z is fixed is called a "node." By taking a sufficient number of nodes of the variable in the interval of interest, a set of curves is obtained which represents the solution of the partial differential equation. Thus, in this case,

the partial derivatives with respect to Z are approximated by finite depth differences. With the finite depth differences, Equation 2.18 can be simplified and rearranged in its finite difference form for solution on the analog computer:

$$\frac{dT_j}{dt} = \frac{a(t)}{[\Delta Z(t)]^2} [T_{j+1} + T_{j-1} - 2T_j] \quad . \quad . \quad (2.20)$$

An example of finite depth increments within the snowpack is shown in Figure 2.8. In this case, the snowpack has been divided into three equal depth zones. T_1 and T_4 each represent one-sixth of the total pack depth, while T_2 and T_3 each represent temperatures in one-third of the pack. The model then computes on a continuous basis the changing values of T_2 and T_3. A sample temperature profile within the snowpack for a particular time is shown in Figure 2.8.

As previously indicated, temperature changes within a snowpack result not only from conduction, as expressed by Equation 2.18, but also from the freezing within the pack of both rainwater and melt from the snow surface. Thus, the temperature increase due to this effect within the j-th depth zone of the pack is given by

$$\frac{dT_{sj}}{dt} = \frac{144}{W_s(t)/m} [M_{rs}(t) + P_{rg}(t)] \quad . \quad . \quad (2.21)$$

in which

m = the number of depth zones into which the pack is divided

In the case of rain falling on snow, the temperature of the rain is assumed to be equal to that of the surface air. For air temperatures in excess of $32^{\circ}F$ there might be some question that the heat given up by the rain in cooling to $32^{\circ}F$ should be included in the above equation. However, this heat contributes to surface melt, and is included in the melt equation. In the event that the snowpack is not yet isothermal at $32^{\circ}F$, the precipitation and melt (now both at a temperature of $32^{\circ}F$) move downward through the pack until freezing occurs. If at any time during a finite period of integration, the temperature at one level reaches $32^{\circ}F$, heat given up by freezing water within the pack immediately begins to influence the temperature at the adjacent lower level. Similarly, as soon as the pack is brought to the isothermal state, any further water present in the pack does not freeze but rather enters the free water storage capacity of the snow as estimated by the relationship of Figure 2.5(a). When this capacity is satisfied, free water (in addition to groundmelt) appears at the bottom of the pack.

Snowpack melt. Basically the calculation of melt is based on a degree-day factor. The base temperature selected for this computation is $32^{\circ}F$. Thus, the rate of melt before any adjustments are made is given by (6, 37):

$$M_{rs} = F(T_a - 32) \quad . \quad . \quad . \quad . \quad . \quad . \quad (2.22)$$

in which

F = a rate factor expressed as inches per unit of time per degree F above $32^{\circ}F$

As in the case of the evapotranspiration equation, the air temperature parameter is an index of the total insolation received on a regional basis, and the value of F in Equation 2.22 will therefore vary with the degree of slope and aspect of the land surface. To provide an adjustment of this variation, the radiation index parameter was again utilized so that

$$F = k_m \left(\frac{RI_s}{RI_h}\right) \quad . \quad . \quad . \quad . \quad . \quad . \quad (2.23)$$

in which

k_m = a constant of proportionality

In the northern hemisphere, the ratio RI_s/RI_h decreases on northerly slopes with decreases in solar declination, while for southerly slopes the ratio increases with decreasing declination. Thus, on northerly slopes Equation 2.23 will yield less melt per degree of temperature above $32^{\circ}F$ in the winter months than in the spring months. The reverse of this situation will apply for south-facing slopes.

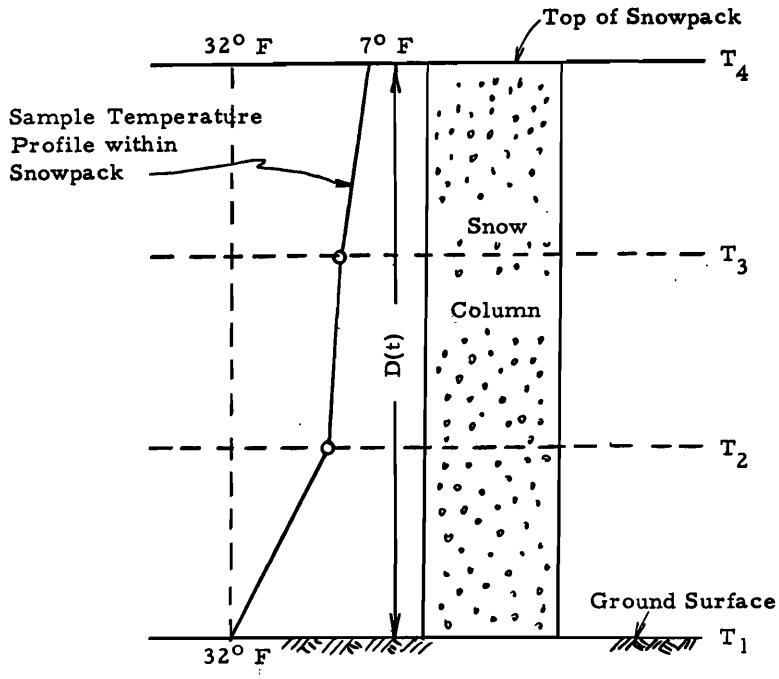

Notes: 1. Number of depth zones, m = 3.
2. Boundary conditions:
$T_4 = T_a$, $T_a < 32$ F
$T_4 = 32$ F , $T_a \geq 32$ F
$T_1 = 32$ F

Figure 2.8. An example of finite depth increments within the snowpack.

These results are in agreement with actual observations (3, 6).

Now, by combining Equations 2.22 and 2.23 the melt equation becomes

$$M_{rs} = k_m \left(\frac{RI_s}{RI_h}\right) (T_a - 32) \quad . \quad . \quad . \quad . \quad (2.24)$$

The effect of vegetative cover on snowmelt can be represented by the use of a solar radiation transmission coefficient for vegetation. Studies by the Corps of Engineers (31, 6, 37) indicate a relationship between the effective or weighted cover coefficient, C_v and the vegetation transmission coefficient, k_v, to be of the form:

$$k_v = \exp(-4C_v) \quad . \quad . \quad . \quad . \quad . \quad . \quad (2.25)$$

in which

C_v = the vegetation canopy density

The melt equation is now written:

$$M_{rs} = k_m k_v \left(\frac{RI_s}{RI_h}\right) (T_a - 32) \quad . \quad . \quad . \quad (2.26)$$

The albedo, or reflectivity, of the snowpack is important in estimating the amount of solar radiation absorbed by the pack. Albedo is expressed as the ratio of reflected shortwave to incident radiation on the snow surface. Values range from about 0.80 for newly fallen snow to as little as 0.40 for melting, late-season snow (28, 6, 37). This decrease in albedo may be expressed as a function of time in the differential form

$$\frac{dA}{dt} = -k_a[A(t) - 0.04] \text{ , } [0.40 \leq 0.80]$$

$$. \quad . \quad . \quad (2.27)$$

The integrated form of this equation is as follows:

$$A(t) = 0.40(1 + e^{-k_a t}) \quad . \quad . \quad . \quad . \quad . \quad (2.28)$$

The value of the time constant, k_a, is about 0.20. Both Equations 2.21 and 2.28 are subject to the conditions that a fall of new snow returns the value of A(t) to 0.80, and the occurrence of rain drives the value of A(t) to 0.40. The latter condition might introduce a question as to the rate at which rain "ages" the surface of a snowpack, but the simplifying assumption is made here that surface melt under most conditions of rainfall quickly exposes lower and previously aged snow surfaces. A comparison of Equation 2.28 with an experimentally determined curve (12) is shown by Figure 2.9.

The effect of albedo is now included by modifying Equation 2.26 as follows:

$$M_{rs} = k_m k_v \left(\frac{RI_s}{RI_h}\right) (T_a - 32)(1 - A) \quad . \quad . \quad (2.29)$$

Finally, as previously indicated, the adjustment of this equation to include the effect of rain falling on a snowpack is accomplished by assuming the temperature of the rain to be equal to that of the air. Thus,

$$M_{rp} = (T_a - 32)\frac{P_{rg}}{144} \quad . \quad . \quad . \quad . \quad . \quad (2.30)$$

The equation for surface melt then becomes

$$M_{rs} = k_m k_v \left(\frac{RI_s}{RI_h}\right) (T_a - 32)(1 - A) + (T_a - 32)\frac{P_{rg}}{144} \quad . \quad . \quad . \quad . \quad . \quad (2.31)$$

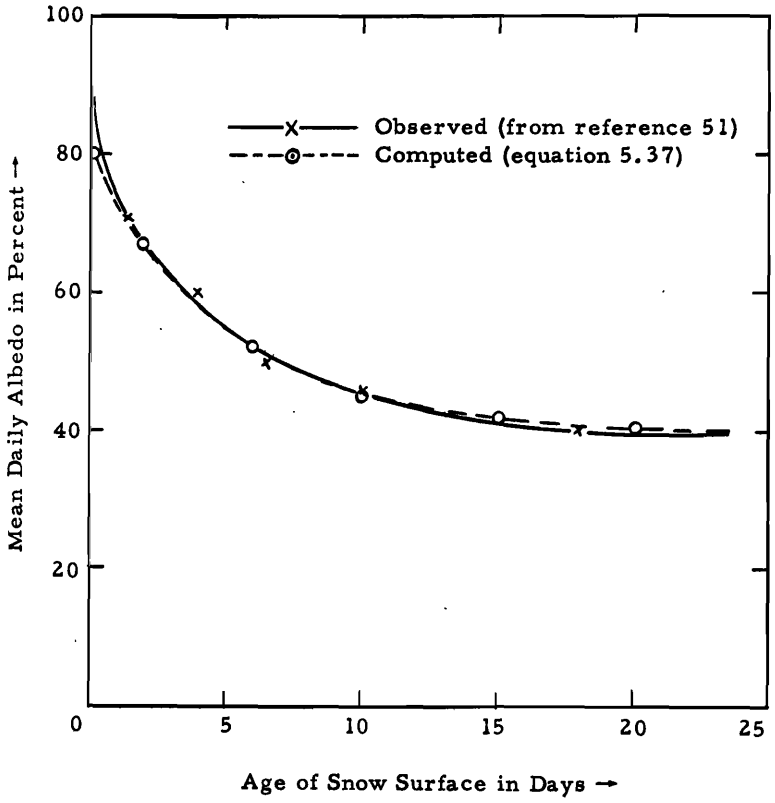

Figure 2.9. A comparison between observed and computed snow surface albedo.

For each watershed zone a uniform depth of snowpack is assumed to exist over the entire area throughout the entire winter and snowmelt season. No adjustment is made for partial snow cover over a zone.

A preliminary estimate of the value of the constant k_m in the preceding equations was obtained by applying Equation 2.29 to the watershed of the Central Sierra Snow Laboratory (6, 37). This watershed is situated at a latitude of $39^{o}22'$ north, has a mean elevation of approximately 7,500 feet, an average aspect of about 11 degrees west of due south, and an average slope of approximately 13 percent. An average value of F (Equation 2.22) for melt at a point under no forest cover during the snowmelt period has been determined as 0.106 inch per degree day, based on mean daily temperatures. The average declination of the sun during the snowmelt period was 10 degrees. From this information values of RI_s and RI_h were established as being equal to 57 and 55 respectively. The vegetation transmission coefficient, k_v, applicable to the snow courses, was estimated to be 0.43 and the value of the albedo during the melt period was assumed at 0.40.

Now substituting in Equation 2.29, $0.106 = k_m [0.43 \frac{0.57}{0.55} (1) (1 - 0.40)]$ from which $k_m \simeq 0.40$.

The value of k_m computed by the same procedure for the Willamette Basin Snow Laboratory (WBSL) also approximately equalled this figure.

A uniform groundmelt rate, M_{rg}, of 0.02 inch per day is assumed to occur (3, 28, 36) and this quantity is added to the portion of the surface melt appearing at the bottom of the pack. Thus, total melt, M_r, is given by

$$M_r = M_{rs} + M_{rg} \quad . \quad . \quad . \quad . \quad . \quad . \quad . \quad (2.32)$$

From this point both snowmelt water and rain falling directly on bare ground enter the soil at an infiltration rate characteristic of the soil, with any surplus water forming surface runoff. The surface runoff component first must satisfy an estimated depression storage requirement for the zone. Additional surface runoff beyond this requirement is then routed off the watershed.

CHAPTER III
PROCEDURE AND IMPROVEMENTS

Procedure

The model used in this study was based on previous work of Riley (30). The equations used to formulate the model are included in Chapter II beginning with Equation 2.1 and ending with Equation 2.32. The model was initially programmed for verification on the analog computer, but was later reprogrammed for the new hybrid computer. The modeling accomplished on the analog computer will be discussed first.

The model was time scaled so that one second of machine time represented one day in real time. The input data were assembled on a mean daily basis for parameters like temperature and a total daily basis for parameters like precipitation. The digital data were input to the analog computer through a system of stepping potentiometers which could transfer one month of data in one run.

Each succeeding month was modeled after setting the input data on the stepping potentiometers, adjusting the model coefficients as necessary, and placing the initial conditions on the integrators where applicable. Initial conditions for each month were the final values for the same parameter from the preceding month. This procedure was repeated through the snow storage and snowmelt seasons until the snowpack was completely melted.

One year of data was used to verify the model and the verification was tested by using other years of data. This testing revealed weaknesses in the model that were corrected by using the procedure shown by the flow diagram in Figure 3.1.

The available information was collected, a mathematical model for snow accumulation and melt was formulated, and a model for the analog computer was constructed utilizing existing techniques. Constraints and limitations were imposed upon the model which helped to explain the basic hydrologic relationships. The improved relationships were incorporated into the synthesized systems model.

The systems model was improved until it qualified for use in management and sensitivity studies. The sensitivity analysis was used to determine which parts and which coefficients of the model would produce the largest change in snowmelt as a result of reasonable variation. This would indicate which parts would need to be studied further and which parts could be neglected or simplified.

The early work with the model revealed that the relationships of snowmelt routing through the pack, liquid water released from the pack by melting snow, and heat given up from freezing liquid water in the pack during periods of below freezing temperatures were not adequately considered or defined by the model. The relationships between routing, release of liquid water during melt, and latent heat transfer were derived and incorporated into the analog model so that the processes which take place during snow accumulation and melt were simulated more closely. These components are described in the following sections.

Improvements

Surface melt routing

The surface melt and rain on snow must be routed through the snowpack to satisfy certain conditions before water can appear at the bottom of the snowpack. First, the pack must become isothermal at 32°F. This is accomplished by heat being conducted into the snow and water from the surface

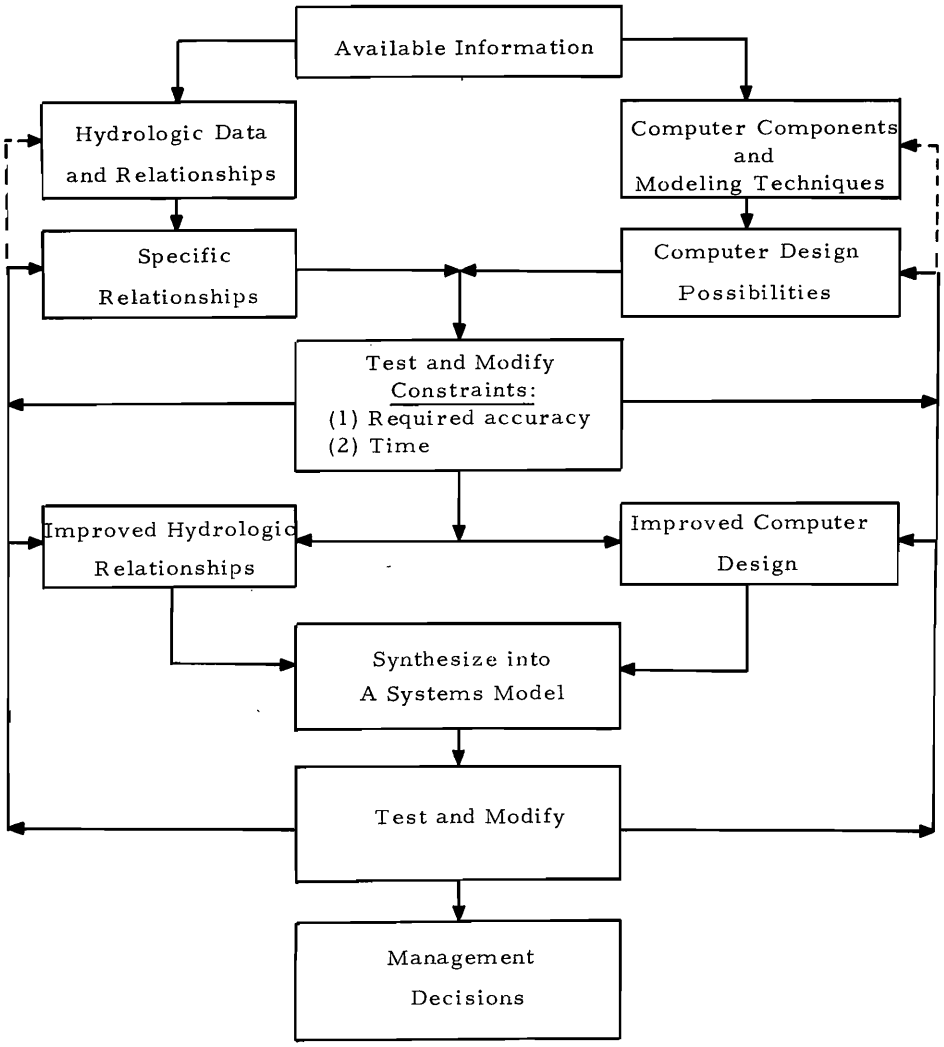

Figure 3.1. Development process of a hydrologic model.

melt or rain freezing in the snowpack and giving off its heat of fusion which warms the pack to 32°F. Second, the liquid water holding capacity of the snow must be satisfied by surface melt or rain.

When these conditions are satisfied, any additional melt or rain at the snow surface is acted upon by the force of gravity and will appear at the bottom of the pack as water for runoff or infiltration into the soil. Determination of snow permeability is a complicated form of porous media flow which has been investigated by Kuroiwa (21) who used cooled kerosene as a fluid. Permeability changed from the first and second tests on a low density snow sample. Later tests had greater permeability and were repeatable.

For samples of snow with high and medium densities the first tests did not vary significantly from the latter ones. The initial permeability for the first snowmelt would probably be low and hard to predict. Later periods of runoff or continued melt would see a higher permeability and would take less time to appear at the bottom of the snowpack. The permeability would continue to increase as the pack becomes more dense and more channeled and snowgrains become larger as explored by Gerdel (17).

The routing of the water through the pack was accomplished by assuming that the snow acted as a storage reservoir and delayed the snowmelt from the surface. It would also reduce the peak and give the hydrograph at the bottom of the pack a recession portion much like a stream hydrograph. The change in storage of the gravity water as it travels through the snowpack is a function of depth of snow, density of the pack, and channelization that has taken place. A differential equation that describes this routing procedure as a function of storage coefficient, k_s, is:

$$\frac{ds}{dt} = -k_s S + f(i) \quad . \quad . \quad . \quad . \quad . \quad . \quad (3.1)$$

in which

S = amount of gravity water in storage

k_s = discharge coefficient as a function of depth

$f(i)$ = surface melt input rate

The discharge coefficient, k_s, would vary from a minimum value at a full pack depth to a maximum of 1.0 at zero pack depth. In Equation 3.1 k_s could be described as:

$$k_s = 1.0 - 0.0025D \quad . \quad . \quad . \quad . \quad . \quad (3.2)$$

in which

D = depth of snow

k_s = 1.0 when $D = 0$, and

k_s = 0.5 when $D = 200$ inches

Liquid water

Liquid water is held in the pack by capillary and hygroscopic forces until the water holding capacity of the snow is satisfied. The liquid water holding capacity of the snow is reduced as the snow melts from the pack. As the snow melts, liquid water, equivalent to the reduction in capacity, is released and combines with snowmelt to be routed through the pack and become runoff. A differential equation that describes this condition is:

$$\frac{dQ_{f(t)}}{dt} = \left[\frac{Q_{f(t-1)} - L_{c(t)}}{\Delta t}\right] \quad . \quad . \quad . \quad . \quad (3.3)$$

in which

$Q_{f(t)}$ = liquid water content at end of time, t

$Q_{f(t-1)}$ = liquid water content at beginning of period, t

$L_{c(t)}$ = liquid water capacity at end of time, t

In the first model the liquid water released from the pack as the snow melted was not added to the runoff from the pack and created a situation requiring from 5 to 7 percent excess melt to reduce the pack to zero. This was because the runoff represented a loss to the snowpack and was subtracted from the water equivalent. For a snowpack with a 40 inch water equivalent, the amount of excess melt required would be from 2.0 to 2.8 inches and the snow would last from one to two days longer depending on the mean daily temperature at the end of the melt season. Incorporating Equation 3.2 into the analog model corrected this situation.

The other problem involved with the liquid water is the heat of fusion that is released when it freezes. This occurs after a period of melt and part or all of the pack is isothermal with its water holding capacity satisfied, and the mean daily air temperature falls below 32°F.

If the air temperature falls below the freezing point, heat contributions from Equation 2.14 cease. The pack temperature is computed by Equation 2.12 plus the heat given off by freezing liquid water. This heat contribution is calculated by a relationship similar to Equation 2.14, namely:

$$\frac{dT_{sj}}{dt} = \frac{144}{W_s(t)/m}\left[Q_{fr}(t)\right] \quad . \quad . \quad . \quad . \quad (3.4)$$

in which

T_{sj} = temperature of snow at point j

$W_s(t)$ = water equivalent of snowpack at time t

$Q_{fr}(t)$ = freezing rate of liquid water in the pack

m = number of layers into which the pack is divided

Equation 3.4 will contribute heat to the snow until all of the liquid water has been frozen in each layer working from the top down or until melt again appears at the surface and begins to heat the snowpack.

The rate at which liquid water freezes in the pack is a function of air temperature and time. Air temperature is related to the freezing rate by the thermal diffusivity of the snow and the total amount of water frozen is dependent on air temperature degree days below 32°F. A relationship with time that is expressed as a differential equation is:

$$\frac{d[Q_{fr}(t)]}{dt} = k_f L_w \quad . \quad . \quad . \quad . \quad . \quad . \quad . \quad (3.5)$$

in which

k_f = a coefficient which regulates the rate of liquid water freezing and is a function of time

L_w = total liquid water in the snow

$\frac{d[Q_{fr}(t)]}{dt}$ = rate at which liquid water is freezing in inches/day

Equation 3.5 gives a decay type relationship for the freezing of liquid water in the pack. This describes the behavior of the freezing liquid water in the pack, since it freezes rapidly near the surface of the snow and slower farther from the surface or deeper in the pack.

For a many layered snowpack, the coefficient could be set so the liquid water freezes slower in each layer successively deeper in the pack. In the many layered situation, the liquid water of each layer would have to be frozen before the water in the next layer would start to freeze. If the cold period lasted long enough, the entire pack would eventually reach a temperature below 32°F.

CHAPTER IV
SIMULATION MODEL

The simulation model was initially programmed on a tube type analog computer. The model was later improved and reprogrammed on a solid-state digital-analog hybrid computer. The model application was at a point and represents the conditions that take place at a particular location and not the average conditions for the watershed. Data from the Central Sierra Snow Laboratory (CSSL) were used to varify and test the model.

Central Sierra Snow Laboratory

A laboratory basin map is shown in Figure 4.1 with the hydrologic stations marked. Data used in this study were obtained at station 1 which is the headquarters station located on Castle Creek where it leaves the 3.96 square mile drainage basin. The basin is located at the crest of the Central Sierra Range near Donner Pass, California. The basin

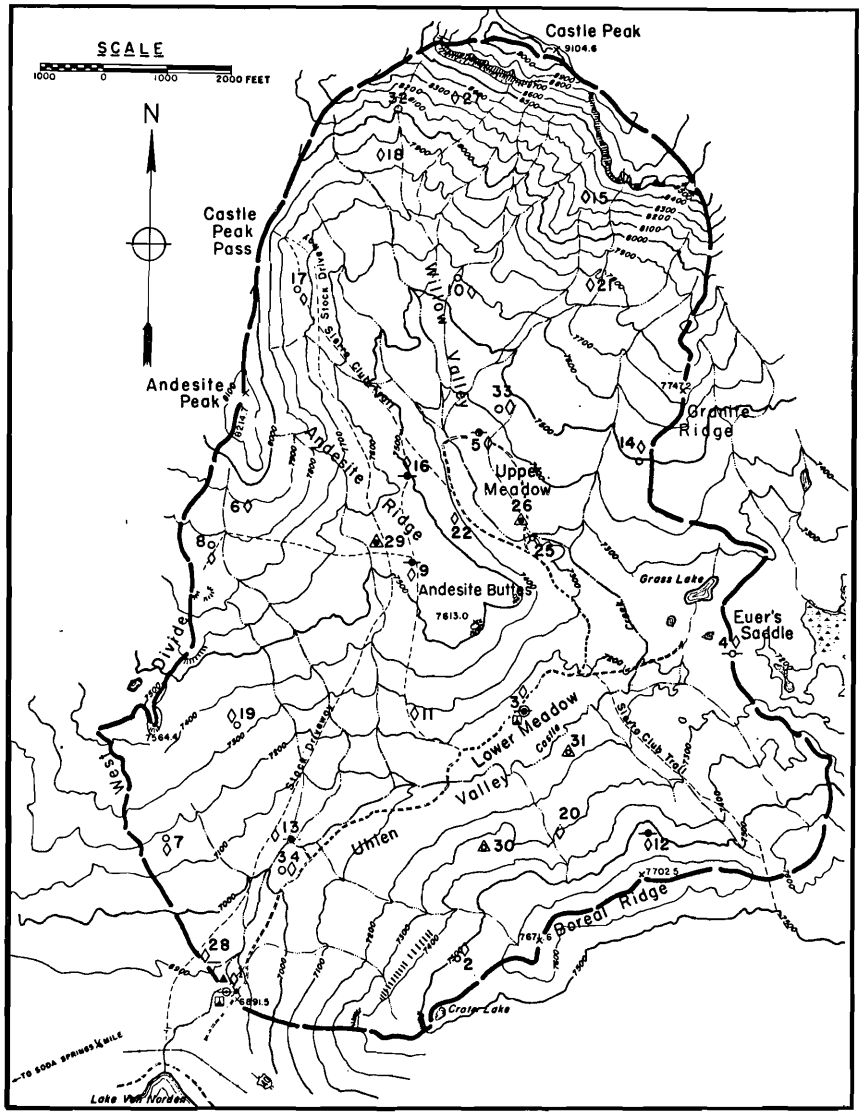

Figure 4.1. Map of Central Sierra Snow Laboratory Basin.

orientation is in a southwest facing direction. The eastern edge of the basin forms a segment of the Sierra Nevada divide.

The northern end of the basin is bounded by Castle Peak (elevation 9105 feet) which forms a sharp escarpment with steep slopes, almost vertical in places, and rises about 1500 feet above the valley floor. On the west, the divide is formed in part by Andesite Peak (maximum elevation 8215 feet). Andesite Ridge extends into the basin and effectively divides the western part of the basin into two parts. Castle Creek is the only major drainage channel within the basin. It heads on the slopes of Castle Peak, and flows southeastward through the upper meadow and swings in around Andesite Ridge, from where it flows southwestward to the basin outlet. The channel slopes average about 200 feet per mile except in the lower meadow where the slope averages 70 feet per mile. The area elevation curve is shown in Figure 4.2(a) and area slope curve in Figure 4.2(b).

The soil is relatively thin and of the sandy loam type. About 35 percent of the basin area is exposed granite rock, mostly weathered, 55 percent overlying volcanic rock, and 10 percent made up of glacial moraines and alluvial deposits. The forest cover is primarily second-growth lodgepole pine. The forest is relatively light and open with about 40 percent of the basin forested and only 20 percent of the forested area directly beneath the tree crowns. Various bushes cover about 15 percent of the basin, and grass covers about 6 percent of the basin, while 40 percent of the basin has no vegetation cover.

The average April 1 snowpack water accumulation is about 32 inches. The snowmelt generates about 75 percent of the total annual runoff during the months of April, May, and June. Castle Creek normally becomes dry near the first of August. The winter flow is proportional to the amount of snowmelt and winter rain. The winter flow volume is relatively low.

Hybrid Model

Hybrid computer

An EAI 590 hybrid computer was obtained by the Utah Water Research Laboratory during the summer of 1969. The hybrid computer consists of a digital and an analog computer linked together to form a system which possesses the advantages of both computers. The hybrid computer is shown in Figure 4.3.

Hybrid computing systems have many advantages for simulation purposes. The hybrid is especially adept at providing adequate simulation fidelity in fast-time and real-time studies. The programmer has at his disposal the advantages of direct integration, memory, and logic. Since its initial development, computer hybridization has undergone steady improvement. The increase in speed, band width, and dynamic accuracy of the analog components, along with the development of high-speed switching devices (both analog and digital) has allowed the application of new programming techniques. Accurate, high-speed repetitive and iterative computations are now possible. In addition, high-speed digital-to-analog and analog-to-digital converters permit fast multichannel function storage and playback, and make possible simulation where functions of two or three variables are required, or where digital solution of dynamic equations (in order to obtain high accuracy) must be accomplished. The modern hybrid computing system thus represents a high level of efficiency in organization and design, combined with speed and dynamic accuracy.

Hybrid adaptation

The computer program used on the vacuum tube analog was modified and changed to be used with the hybrid system. This modification involved putting the snowmelt and evaporation parts on the digital computer. The flow chart for this digital program is shown in Figure 4.4 while the actual

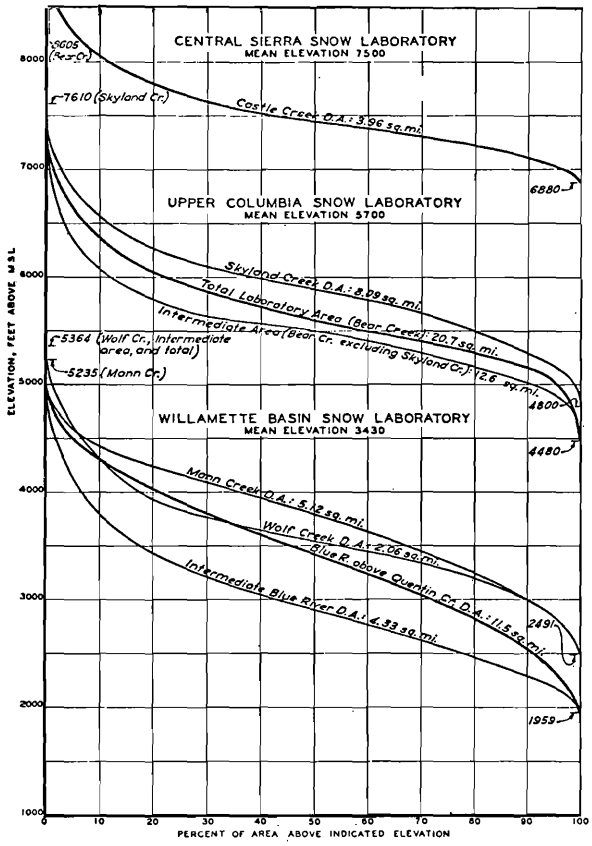

Figure 4.2(a). Area-elevation curves.

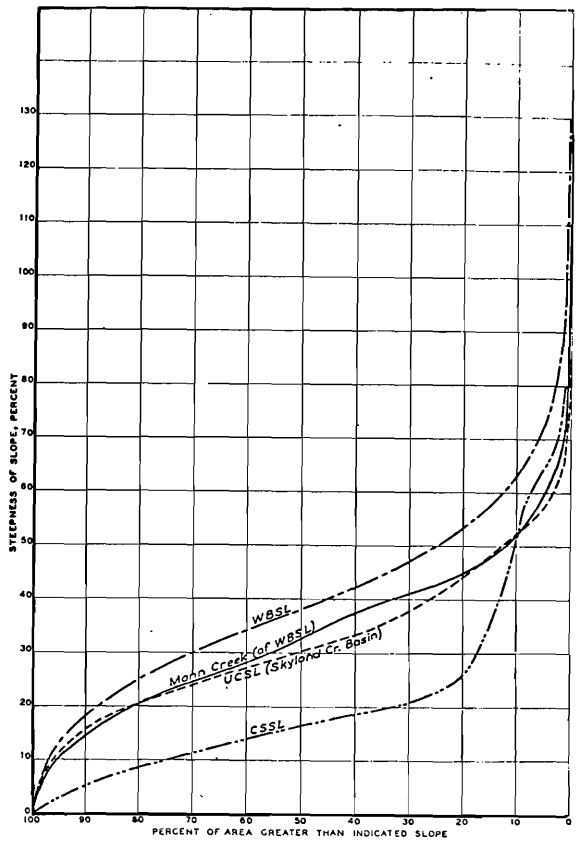

Figure 4.2(b). Area-slope curves.

program is contained in Appendix A. The digital program uses the 1-albedo decay curve calculated from Figure 2.9, k_v, k_m, RI_s, RI_h, the number of days in each month, and daily percent of daylight hours. With this information the computer is ready to read the data tape which contains air temperature, precipitation, and new snow density correlated to air temperature as shown in Figure 2.5(b).

The computer accepts the data and tests the temperature to see if it is above 32°F. The degree day (DECD) factor and snow surface temperature (TEMSS) are calculated and the temperature (T_a) is again tested to see if it is equal to or greater than 35°F. If it is, any precipitation (PRG) that falls is in the form of rain. If T_a is less than 35°F the PRG is assumed to fall as snow and the depth of the new snow is calculated by dividing the density (DIN)

into PRG. The percent of energy absorbed (ALBI) by the snow is then calculated by setting it to its minimum value of 0.2 if PRG fell as snow. The maximum value for ALBI of 0.6 occurs after 25 days have elapsed from the end of the last snow storm. Initially ALBI was set to 0.6 when rain fell on snow but it was found that this created too much melt. ALBI was allowed to continue to increase as time passed after the last snow until it reached a maximum of 0.6. With this information the program was ready to calculate the data to be used by the hybrid program.

The snowmelt at the surface of the snowpack was calculated and the PRG that fell as rain was added to the M_{rs} to form the total water available from the surface (HOS2). Evaporation, EVAP, was calculated as a function of T_a, percent of daylight hours, and Radiation Indexes. Below the temperature of $18^{o}F$ the equation added water to the snowpack by condensation. It was identified by a negative sign on EVAP. All of the variables to be used in the hybrid program were scaled to be input to the analog computer directly from the output tape. The variables output are evaporation (EVAP), snow surface temperature (TEMSS), new snow depth (SNAC), water available at snow surface (HOS2), and daily precipitation (PRG).

Synchronization of the digital and analog computers

The synchronization of the digital and analog computers presented a problem in adapting the snowmelt model to the hybrid computer. Synchronization was accomplished by using the digital counter which outputs a logic "one" at a given interval on the counter dial. Figure 4.5 shows the logic program used for this purpose and the output from the circuit. This output was interrogated each time the digital computer cycled through the digital program do loop. When the signal changes from logic "one" to "zero" or from logic "zero" to "one," the digital transfers simultaneously to the analog all of the data that have been prepared for input.

Digital program for the hybrid model

The digital program is shown in Appendix A, and a flow chart for the program is shown in Figure 4.6. The digital program reads a set of data from the data tape to be input to the analog. The data are for one day and are loaded by the digital to the interface system, then transferred to the analog upon call from the logic program. The digital checks the density calculated by the analog by means of an analog to digital channel, tests to determine if the density is greater than 0.4, and sets control line 1 to a logic 1. If the density is less than 0.4, control line 0 is set to a logic 1. Next the digital tests NCO to see if it is negative or positive. NCO is a parameter which tells the digital what path to follow in the digital program. If NCO is positive, the sense lines are tested until sense line 1 is high; NCO is set negative and the computer reads a new set of data. When NCO is negative the digital tests sense line 0 until it becomes high, sets NCO positive, and reads a new set of data.

After the digital reads more data it returns to the position where the data are transferred to the analog. The digital transfers new data at the beginning of each second of machine time, which represents one day in actual time. The digital cycles through this loop until all of the data have been read and transferred to the analog. At this point the analog is placed in the hold mode allowing the final values to be read from the digital voltmeter on the analog console.

Analog program for the hybrid model

The analog program was changed for the hybrid computer system by replacing some of the active computing parts with a digital program. These parts were integrators, summers, multipliers, diodes, and comparators involved in the snowmelt and evaporation parts of the program. The analog diagram is shown in Figure 4.7. This program is based on the equations of Chapter II and Chapter III.

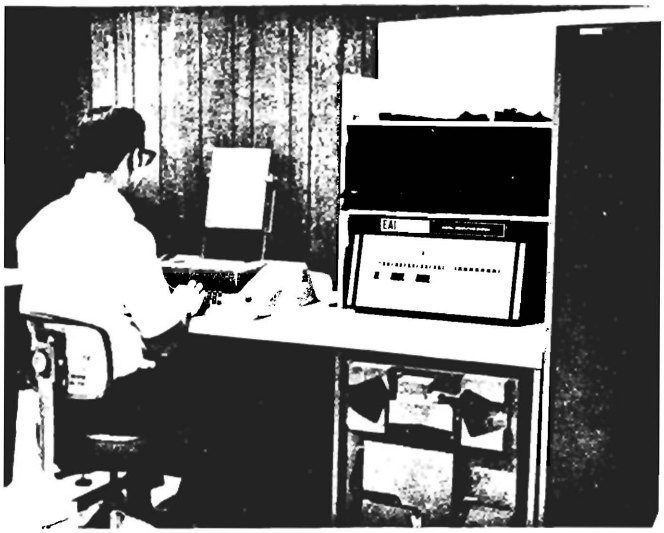

The console of the digital unit.

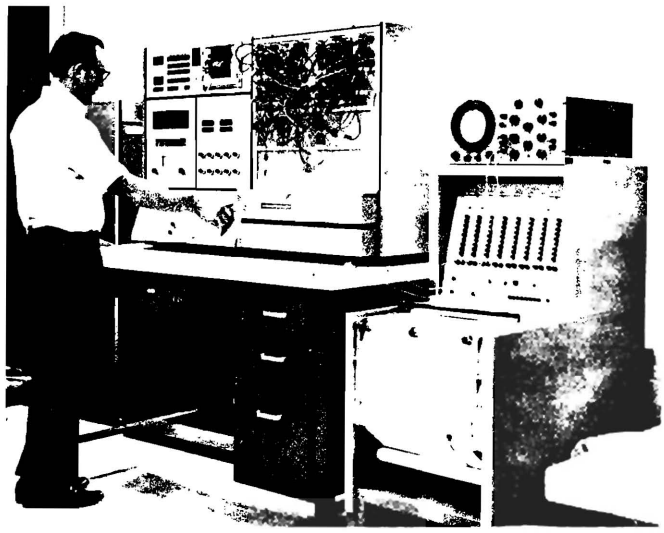

A view of the analog unit showing the servo-set pots, digital voltmeter, program board, and output devices.

Figure 4.3. Hybrid computer at Utah Water Research Laboratory.

The program calculates the average density, ρ, of the snowpack shown in Figure 4.8 by dividing $D_a(t)$ (Figure 4.9) into the accumulated precipitation of Figure 4.10. The compaction coefficient, k_{sc}, of Equation 2.16 which is used to calculate $D_a(t)$ was found to be equal to 0.05 for the Central Sierra Snow Laboratory data.

The density, ρ, was then used to compute other parameters of the snowpack. Snow depth, D, was calculated by dividing ρ into the water equivalent, $W_a(t)$, of the snowpack, which is shown in Figure 4.11. The liquid water holding capacity, L_c, is a function of snow density and is calculated according to Figure 2.5(a) and is shown in Figure 4.12, while thermal diffusivity is calculated from density by Equation 2.19 and used to determine the change in snowpack temperature as a function of snow depth squared. The iterative procedure of Chapter II is used to calculate the temperature of the snow at a point within the pack.

The program divides the pack into two parts of equal depths in calculating the temperature of the snow at the middle of the pack as shown in Figure 4.13. The snow surface temperature is assumed to be equal to the air temperature if the air temperature is equal to or less than 32°F. If air temperature is above 32°F the snow surface temperature is 32°F. The temperature of the snow at the ground and snow interface is assumed equal to 32°F. The calculated temperature in the pack, air temperature, and surface temperature are shown in Figure 4.13 for comparison. Surface temperature is represented by the air temperature when it is below 32°F and 32°F when air temperature is above freezing. When the air temperature decreases and is less than the temperature at the center, the center temperature decreases. Also when the surface temperature is greater, the center temperature will increase. In Figure 4.13 the center of the pack temperature shows rapid fluctuation early in December when the snow depth

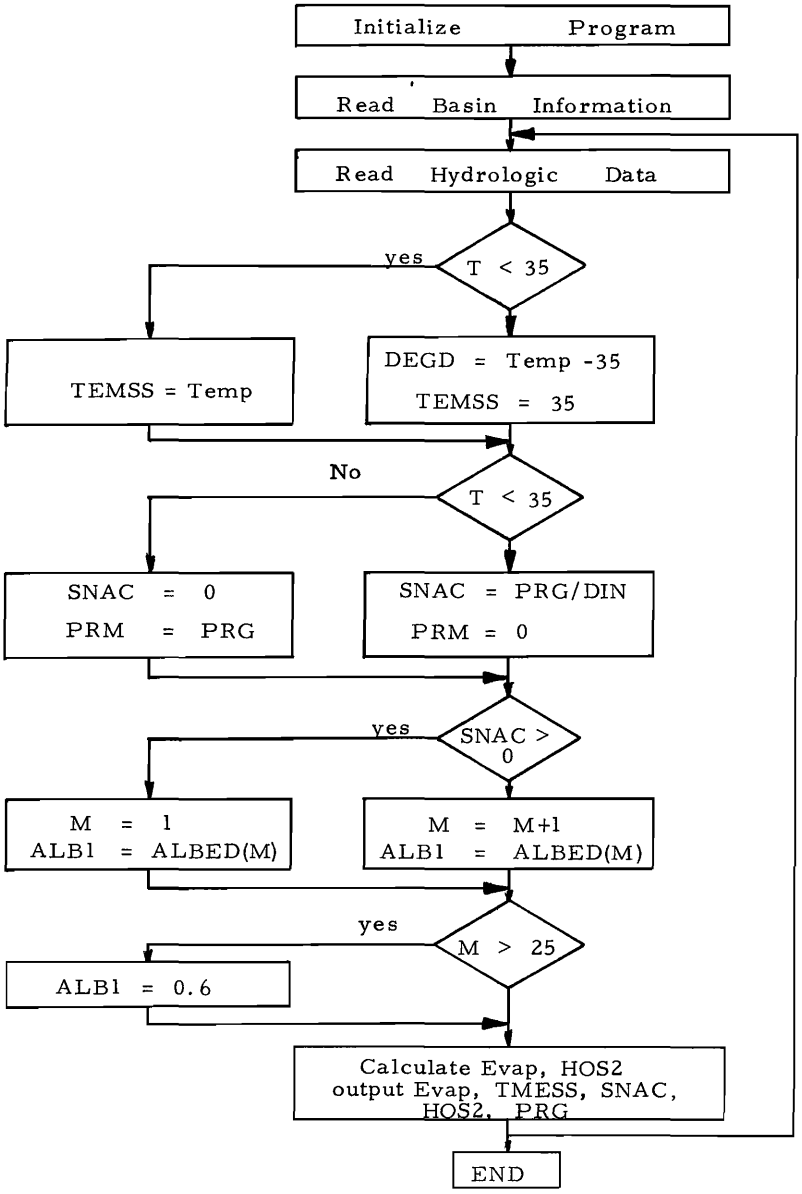

Figure 4.4. Flow chart of digital program to produce tape for hybrid computer program.

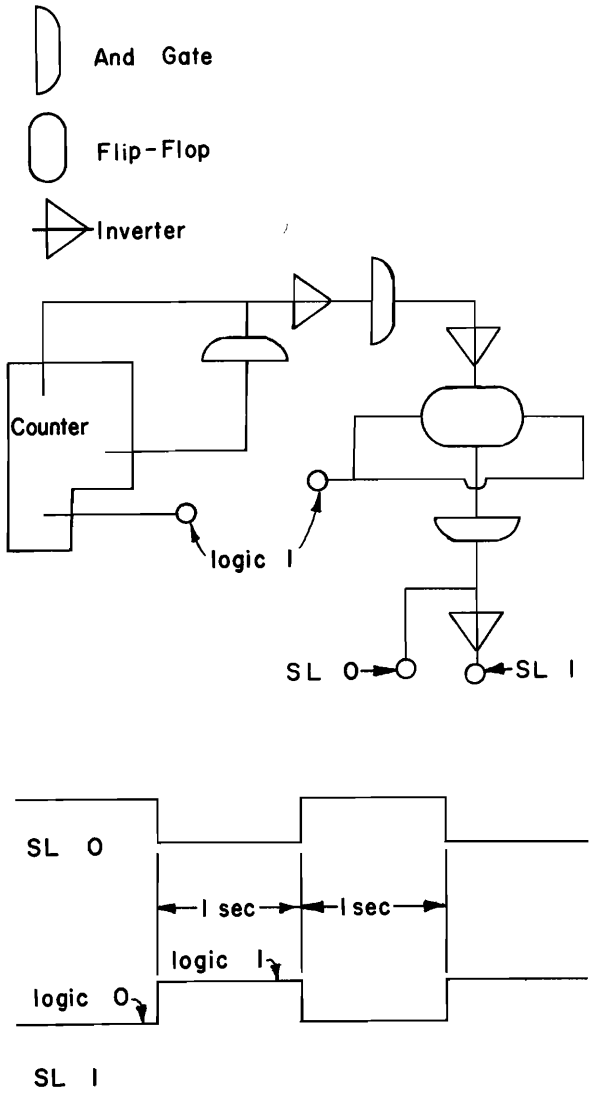

Figure 4.5. Logic diagram and output of sense lines 0 to 1 to control digital computer.

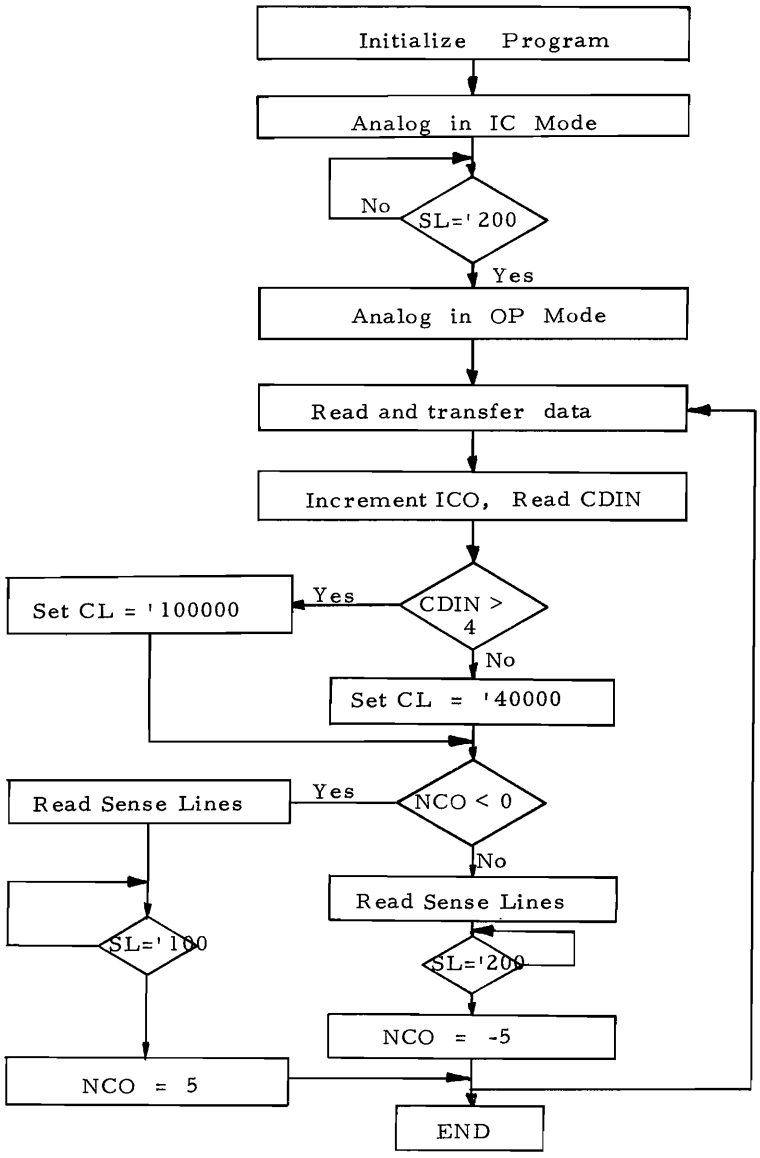

Figure 4.6. Flow chart of hybrid computer program.

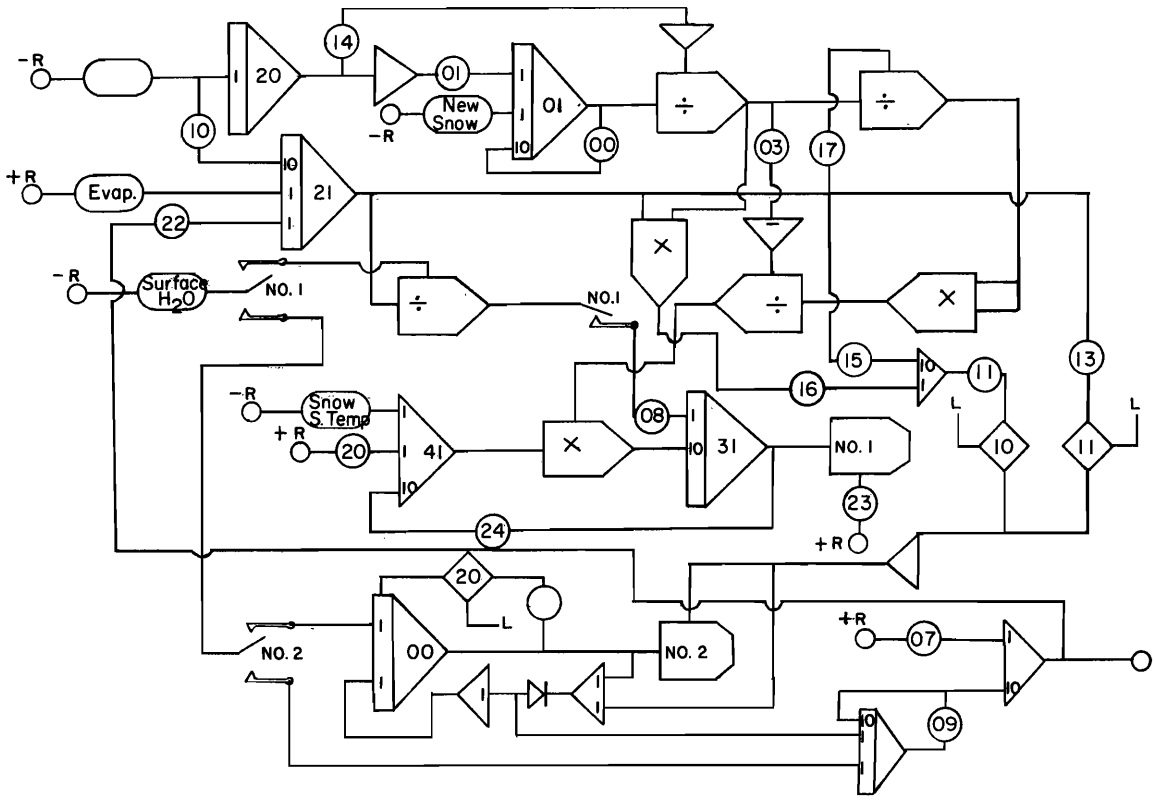

Figure 4.7. Diagram of analog program used with the hybrid computer system.

is shallow and little variation when the pack is deep during the months of January, February, and March. The reason for this can be seen in Figure 4.14 which is a plot of $\alpha/10Z^2$ versus time for 1949-50. This value is sensitive to surface temperature changes when the snow is shallow.

In Figure 4.13 the points of rapid temperature increase, as shown on January 15, are due to surface melt freezing in the pack and giving up its heat of fusion to bring the pack to isothermal conditions. The heat of fusion is a major source of the heat in raising the pack temperature to 32°F. When the pack is isothermal at 32°F, the surface melt must satisfy the liquid water holding capacity of the snow before runoff can occur.

Liquid water in the pack and liquid water holding capacity are shown in Figure 4.15 for the snow season of 1949-50. The rapid increases in the liquid water contents indicate surface melt filling up the liquid water holding capacity of the pack. The flat horizontal peaks show that the L_c is either full or there is no water available to satisfy this condition. The periodic drop in the liquid water of Figure 4.15 indicates periods of time when the temperature is below 32°F, which causes the liquid water contained in the snow to freeze from the surface down until another period of above 32°F temperature occurs. When another period of melt is encountered, some of the melt is used to warm the pack until it is isothermal, and to satisfy the liquid water holding capacity before more runoff can appear at the bottom of the pack.

With the pack isothermal at 32°F and the liquid water holding capacity satisfied, any melt at the snow surface will eventually appear at the bottom of the pack as runoff. This runoff will either enter the soil mantle by infiltration or flow along the soil surface. The surface melt is routed through the pack

to form an outflow hydrograph as shown in Figure 4.13. Melt runoff is shown with air temperature to indicate the relationship between these variables.

Verification of the model

To verify the model and test its reliability, data from the Central Sierra Snow Laboratory were used (7, 8, 11). The data represented the three years of 1946-47, 1949-50, and 1950-51, and included surface air temperature and precipitation with initial conditions of accumulated precipitation. Initial values required for the model were snow water equivalent, snow temperature, and apparent depth as determined from observations. The year of 1949-50 was used to verify the model while the years of 1946-47 and 1950-51 were used to test the reliability of the verified model. The verified coefficients are shown in Table 4.1.

Figures 4.8, 4.16, and 4.17 show plots of simulated average density versus field measurements for the years indicated in the plots. The water equivalent of the snowpack with the simulated and measured values is shown in Figures 4.18, 4.19, and 4.20 for the years of 1946-47, 1949-50, and 1950-51, respectively. The points placed on the figures are field measured values and are subject to field error. However, field measurements were assumed to be correct and were used to check the accuracy of the model.

In Figures 4.19 and 4.20 the water equivalents are equal to zero at the end of the simulation period. The days when the snow was completely melted are June 5 for 1949-50 and May 8 for 1950-51. Figure 4.19 shows that for the year 1949-50 the simulation model melted all of the snow by June 4 which is one day earlier than the records show. Figure 4.20 shows that the year of 1950-51 was as good and that the snow was gone on May 18, one day before it was actually gone in the records. In Figure 4.18 the water equivalent reduced to zero on May 5, but the records show that the snow was gone by April 25.

The years of 1946-47 and 1950-51 are similar in total precipitation falling during the winter season, but the records show that the snow was melted 23 days earlier in 1946-47. The snowmelt runoff for each of the two years is shown in Figure 4.21 for comparison. The runoff is about the same until the first of April after which time the year of 1950-51 had more melt.

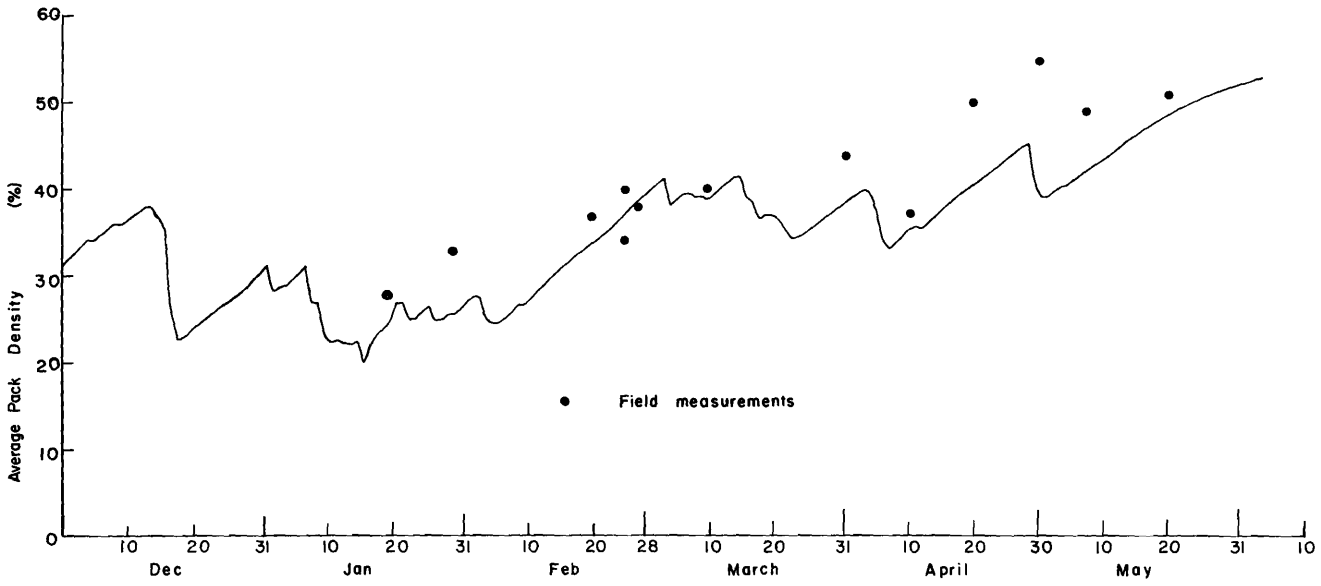

Figure 4.8. Calculated density, ρ, of the snowpack versus time for the year 1949-50, CSSL.

Adaptability to other basins

The simulation model was applied to two other regions: the Upper Columbia Snow Laboratory (UCSL) shown in Figure 4.22 and the Willamette Basin Snow Laboratory (WBSL) shown in Figure 4.23. These basins are quite different from the Central Sierra Snow Laboratory area.

The Upper Columbia Snow Laboratory is located at a latitude of 48.3° north, with an average altitude of 5700 feet above mean sea level in Northwestern Montana, and is typically cold, with low annual precipitation. The drainage area is 20.7 square miles with 8.09 square miles located on Skyland Creek. The mean daily temperature between December 1 and March 31 is frequently below zero. The annual precipitation is near 50 inches, with a majority of the precipitation falling during the winter snow. The snowmelt generally starts in April and all of the snow is usually melted by July 1. Little streamflow runoff is generated by winter snowmelt and the basin is heavily forested with coniferous trees.

Data used from this laboratory were for the winter of 1948-49 (9). Figure 4.24 shows the computer output for water equivalent. The points on the plot are from actual data. The records show that for this year and location the snow was gone by May 20 and Figure 4.24 shows that there was 0.4 inches of water left on the 20th for the plot without ground melt contributions to runoff. With ground melt included in the simulation, the snow was melted by May 15 which is 5 days early. Because of the extreme cold as shown in Figure 4.25, it is assumed that no ground melt would apply. The plots of water equivalent in Figure 4.24 also point this out. The plot without ground melt fits the data better than the one with ground melt.

Figure 4.26 shows a plot of computed runoff from the pack. The first runoff begins on April 10 and continues without stopping until all the snow is gone. The records of discharge from Skyland Creek (9) show that streamflow started to increase slightly on April 4 with a discharge increasing from 8 cfs to 27 cfs by April 10. On the 11th the discharge jumped to 41 cfs and continued to increase with short periods of decreases to a maximum of 258 cfs on May 16. The calculated peak runoff rate appears on May 15 from the pack, which for the small drainage basin could delay the peak flow one day. The recorded increase in runoff appearing before April 10 could be from steeper south facing slopes which would have been earlier and increased melt because of their slope and aspect.

Figure 4.27 shows the calculated average density for the snowpack as compared to the measured values. It shows that the calculated density has good correlation to the field measurements. Figure 4.28 shows the actual snow depth given by the average density and water equivalent.

The Willamette Basin Snow Laboratory is located in Northwestern Oregon, with a latitude of 44.2° north with a mean elevation of 3430 feet. The annual average precipitation is about 120 inches but may reach as high as 150 inches. The precipitation falls in the winter as either rain or snow. Often the runoff from winter rain and melt is greater than during the spring runoff season. The basin is covered with a heavy stand of coniferous trees. The data used for the Willamette Basin were for the year 1949-50 (10).

The calculated average density of the snowpack is shown in Figure 4.29. The values are close to the field measured values and vary from being more to less dense than the field measurements. The maximum error is 13.6 percent of the measured value. The snow temperature at the center of the pack is shown in Figure 4.30 and shows that it is 32°F most of the time that snow is on the ground. This agrees with the Corps of Engineers' findings in their cooperative studies (10) which contain no field data for comparison with the calculated values.

Because of climate conditions resulting from the low elevation of the Willamette Basin, it was necessary to adjust certain parameters in the model. For example, it was necessary to lower the temperature criterion for the form of precipitation from 35°F to

29°F. This adjustment increased the proportion of the total precipitation which occurred in the model in the form of rain, and provided good correlation with field measured values. Computed snowmelt rates for the Willamette Basin Snow Laboratory during the 1949-50 winter season are shown by Figure 4.31. Comparisons for this same period between observed and computed values of the snow water equivalent and total depth are shown by Figures 4.32 and 4.33, respectively.

The coefficients involved in the simulation, verification, and testing of the model for the CSSL and the adaptation to the WBSL and UCSL regions are shown in Table 4.1. The table shows that for the CSSL all of the coefficients were left the same for the different years. The year that the model gave the poorest results was 1946-47. This could have been improved by increasing k_m, decreasing k_f, or changing both. For the UCSL, the vegetation transmission coefficient was reduced due to the more dense vegetation, the ground melt was removed and the maximum density of the snow was reduced to 0.50 due to the extreme cold during the year 1948-49. In the WBSL simulation and test, the temperature boundary between snow and rain had to be lowered to 29°F, the vegetation transmission coefficient was reduced due to the increased vegetation density, and the compaction coefficient was reduced to 0.03. The monthly radiation index values were changed to fit the conditions at each basin for each month of the snow season. Table 4.1 shows the value for the month of April used at each of the snow laboratories. The indexes are a function of latitude, slope, and aspect of the basin. The simulated output shows that the model is quite general and can be adapted to other areas by making minor adjustments in the model.

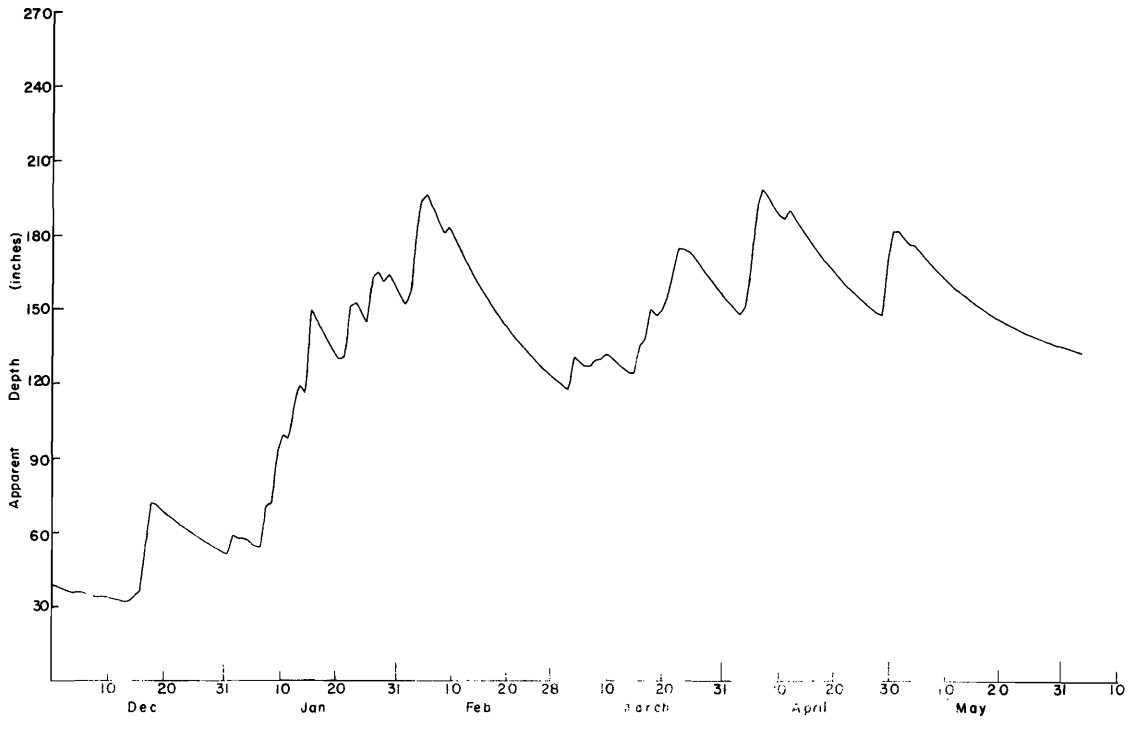

Figure 4.9. Calculated apparent depth of snowpack versus time for the year 1949-50, CSSL.

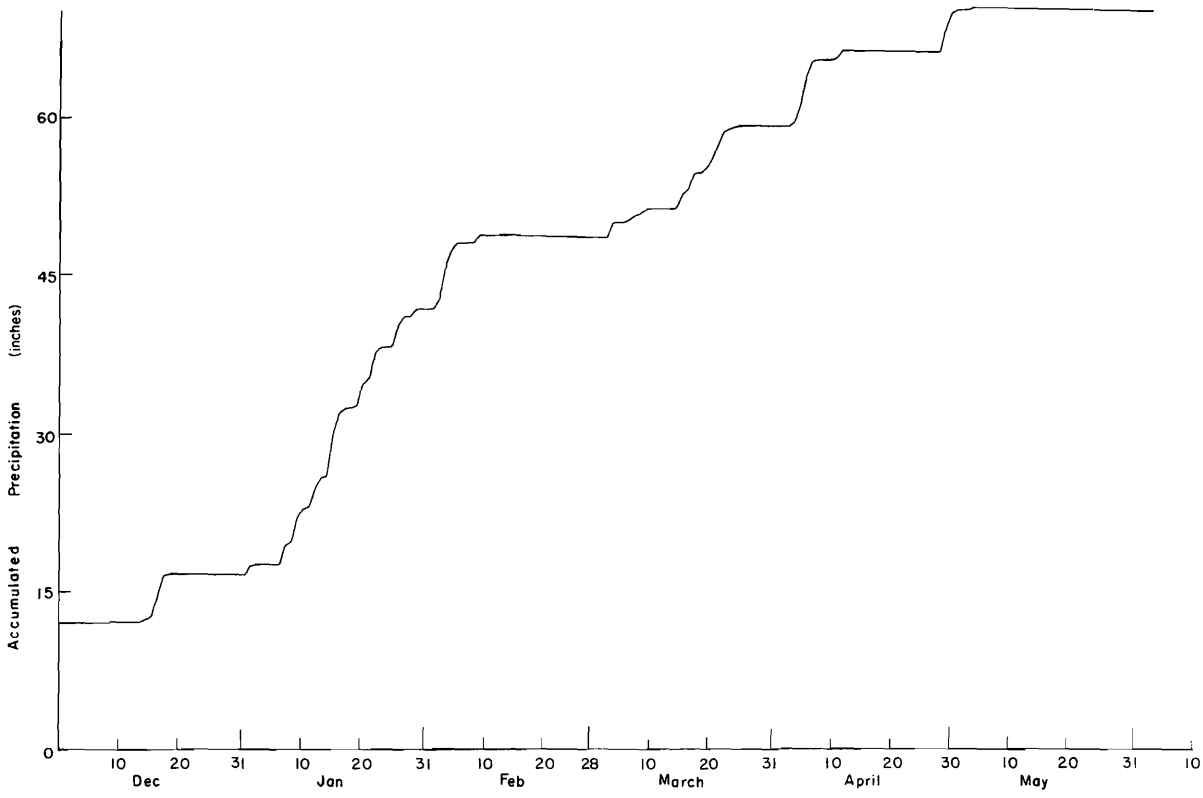

Figure 4.10. Accumulated precipitation versus time since beginning of snow accumulation for the year 1949-50, CSSL.

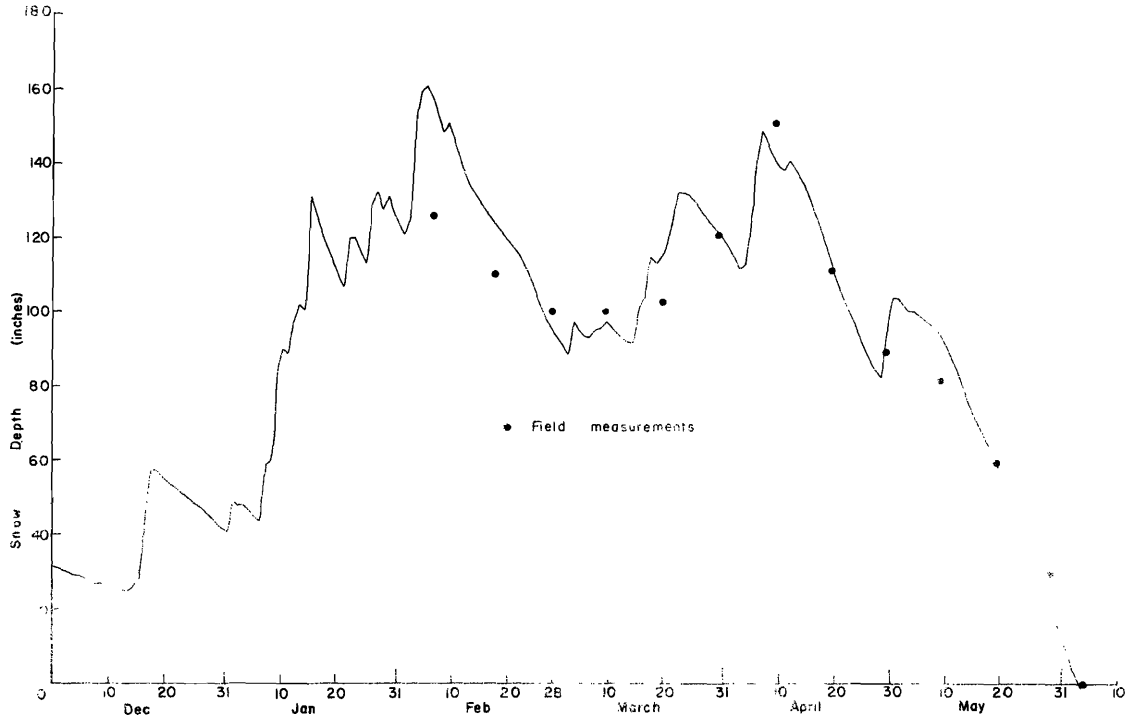

Figure 4.11. Calculated actual depth of snow versus time for the year 1949-50, CSSL.

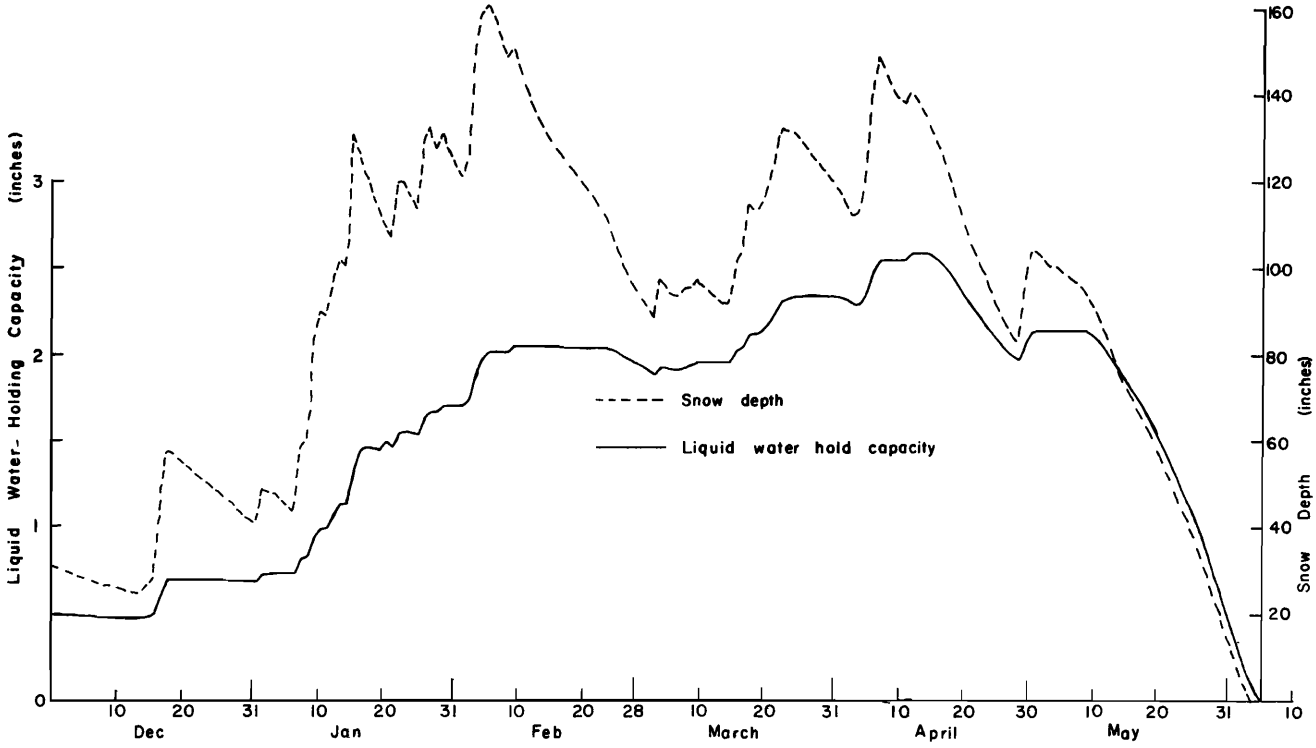

Figure 4.12. Calculated liquid water holding capacity of the snow as a function of average density of the snowpack for the year 1949-50.

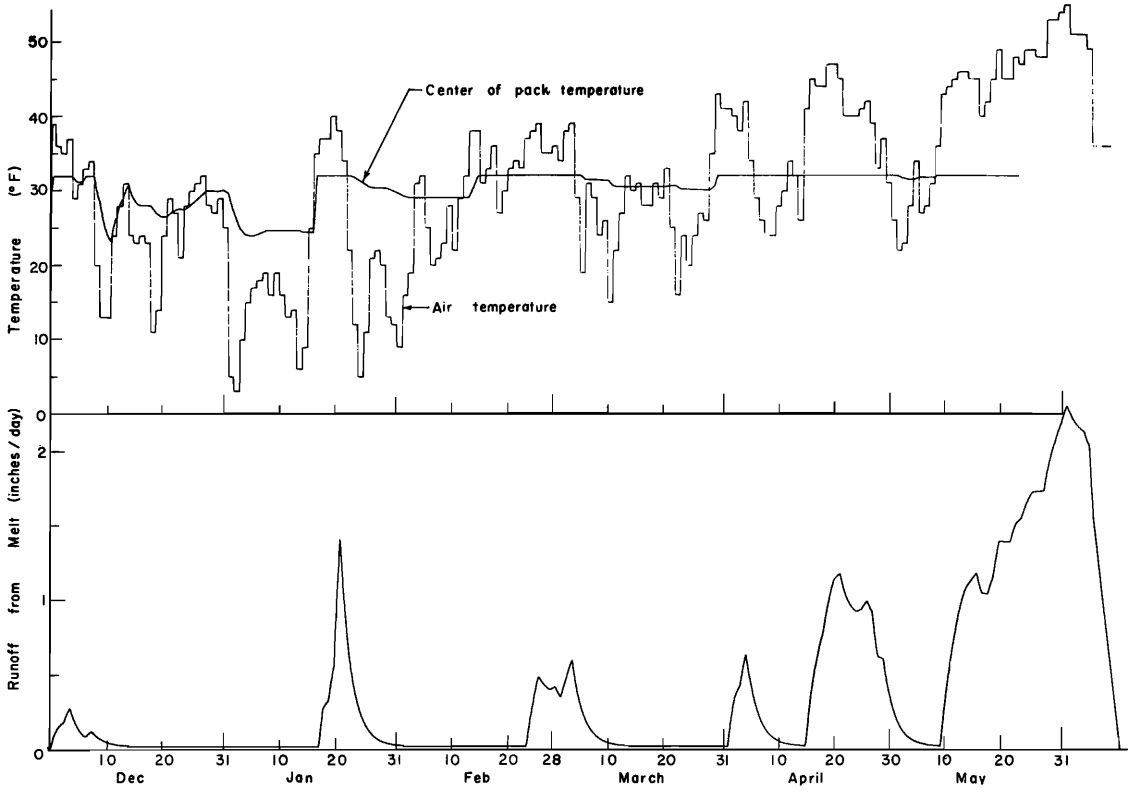

Figure 4.13. Calculated center of the snowpack and air temperature, ^{o}F and runoff due to snowmelt versus time for the year 1949-50, CSSL.

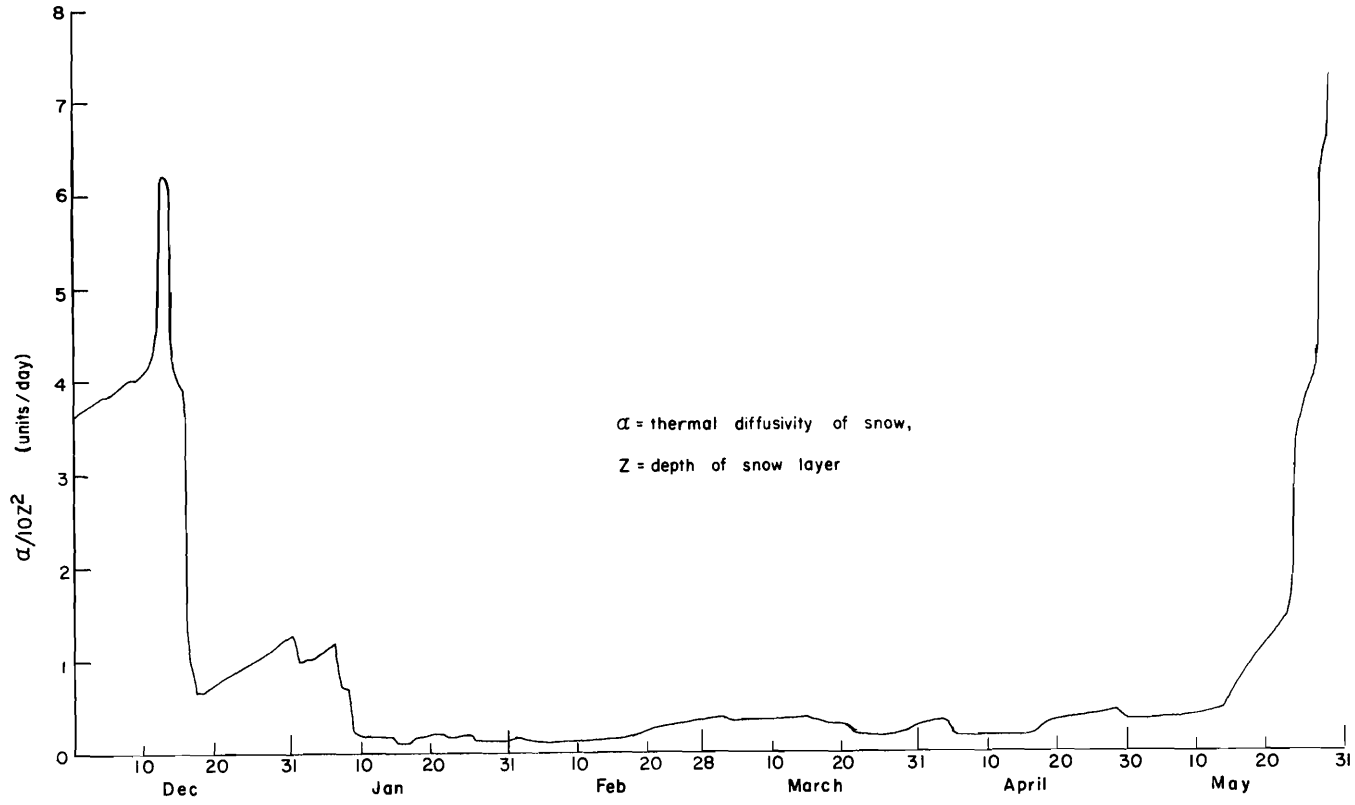

Figure 4.14. Plot of $\alpha/10t^2$ versus time for the year 1949-50, CSSL.

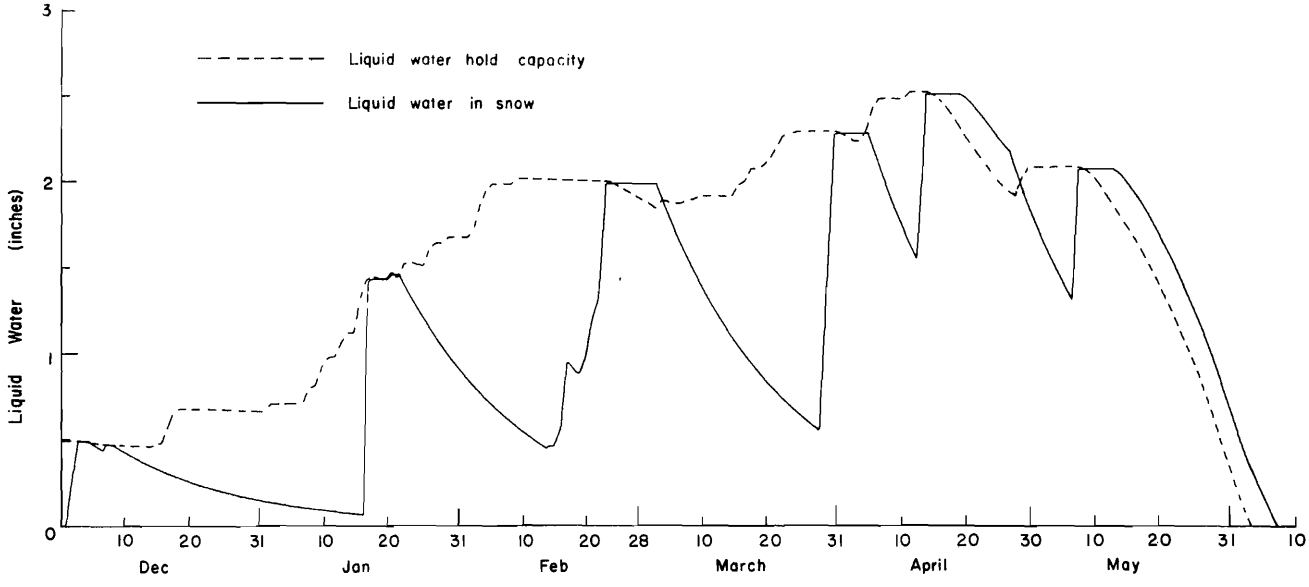

Figure 4.15. Calculated plot of liquid water holding capacity and liquid water in the snow versus time for the year 1949-50, CSSL.

Table 4.1. Summary of coefficient values used in simulation study for each basin.

Basin	Year	k_m	k_v	k_s	k_f	k_{sc}	Temperature for Rain	Ground melt "/day	April RI_s	April RI_h	P_i	P_{max}
CSSL	1946-47	0.40	0.43	0.5	0.05	0.05	35°F	0.02	0.57	0.55	0.10	0.6
	1949-50	0.40	0.43	0.5	0.05	0.05	35°F	0.02	0.57	0.55		
	1950-51	0.40	0.43	0.5	0.05	0.05	35°F	0.02	0.57	0.55		
UCSL	1948-49	0.40	0.25	0.5	0.05	0.05	35°F	0.00			Air Temp. Correlated	0.5
WBSL	1949-50	0.40	0.25	0.5	0.00	0.03	29°F	0.02			0.10	0.6

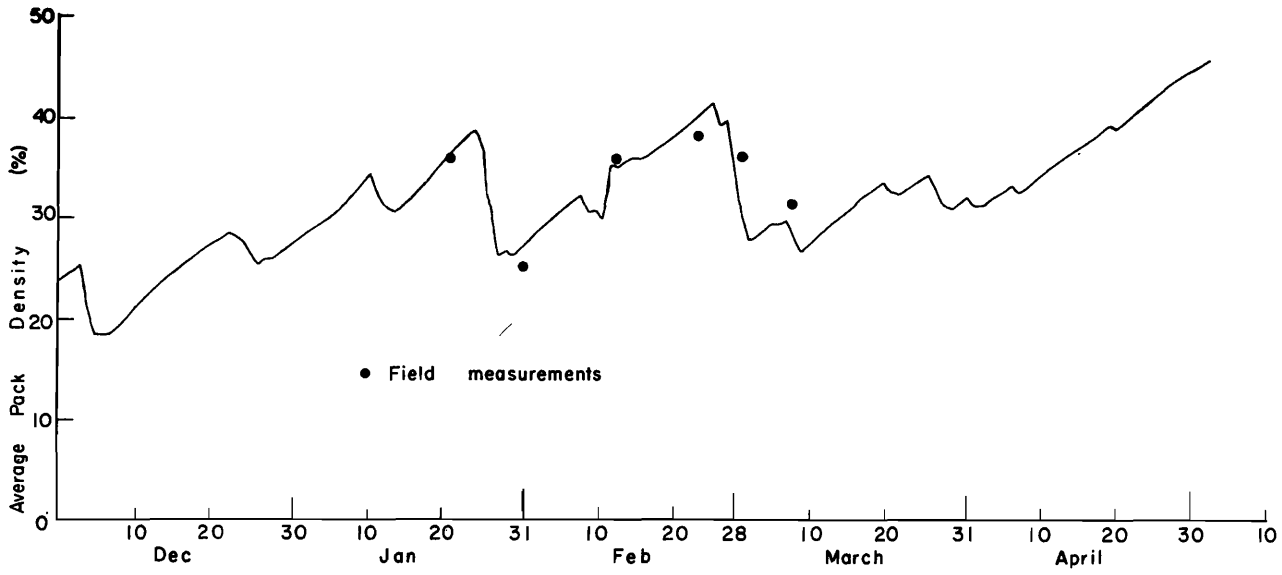

Figure 4.16. Calculated average density of snowpack for the year 1946-47, CSSL.

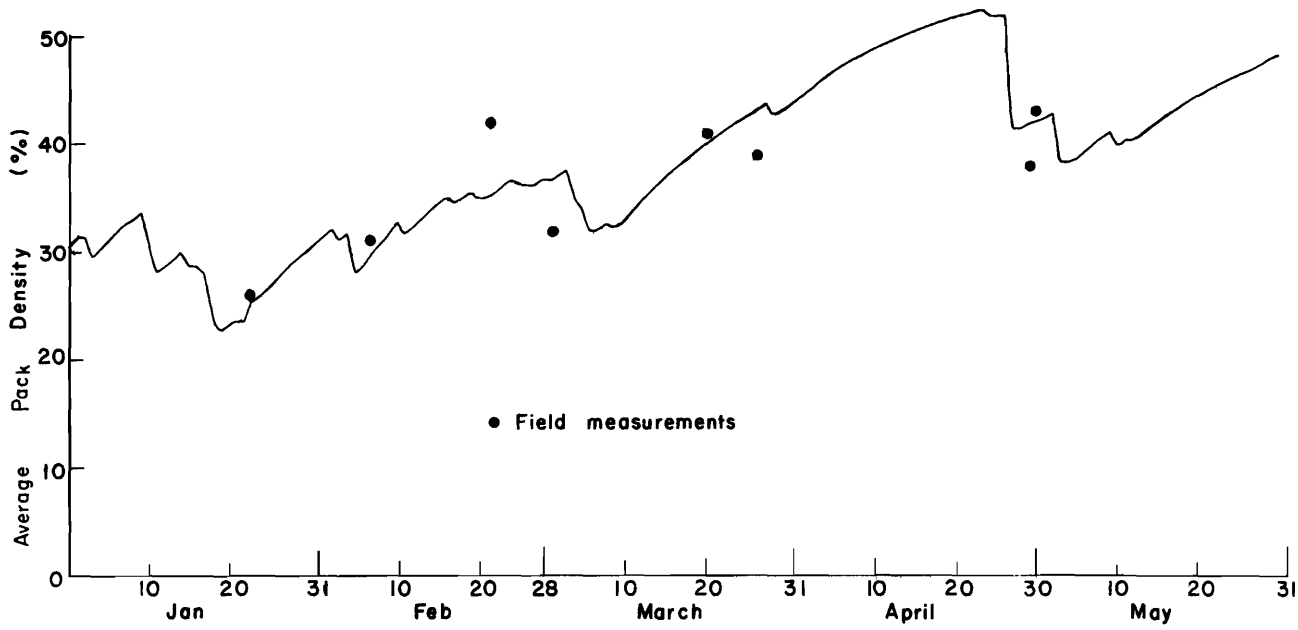

Figure 4.17. Calculated average density of snowpack for the year 1950-51, CSSL.

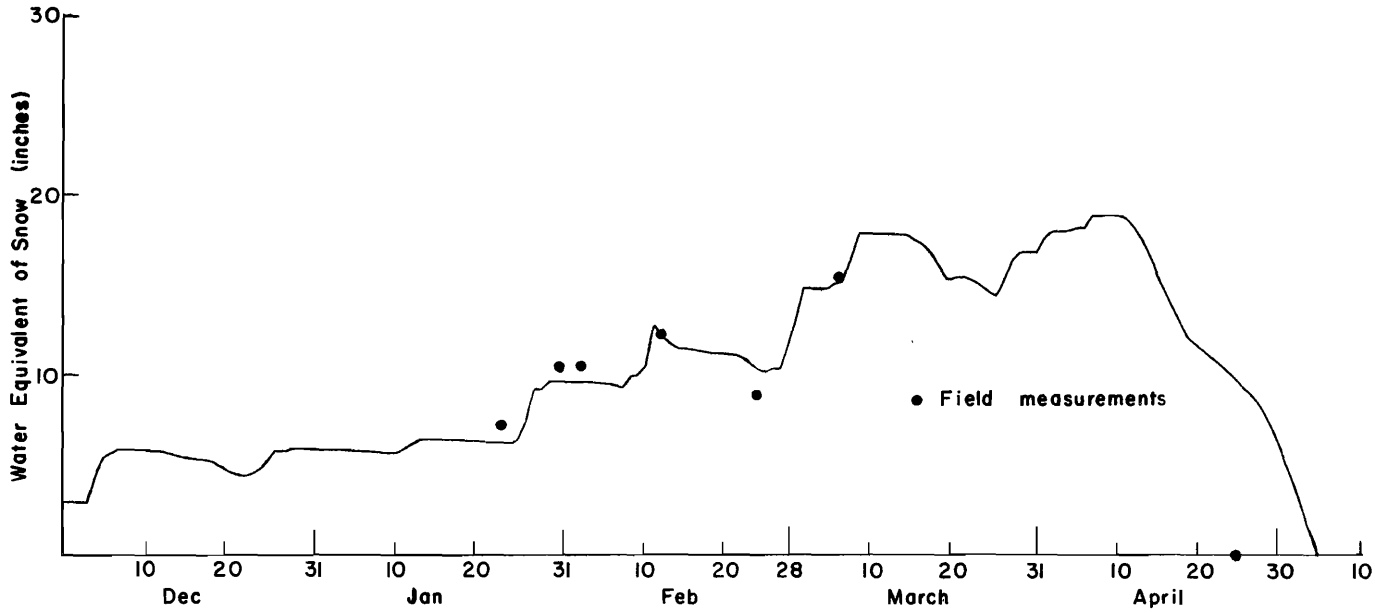

Figure 4.18. Calculated water equivalent of the snowpack for the year 1946-47, CSSL.

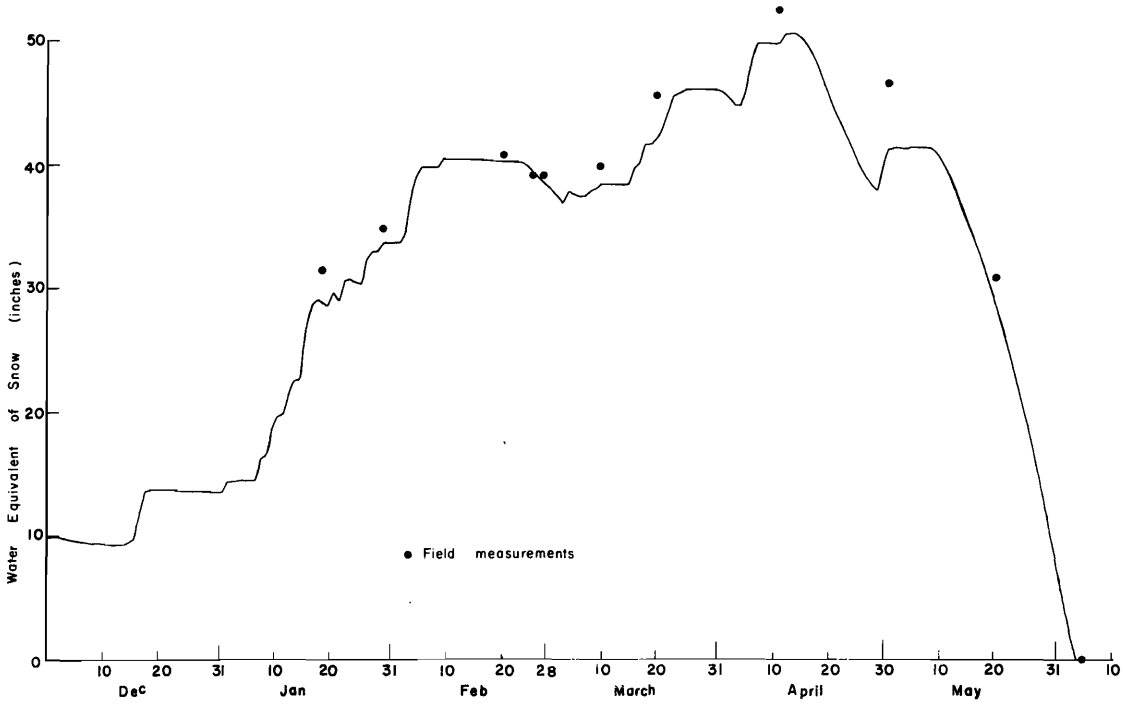

Figure 4.19. Calculated water equivalent of the snowpack for the year 1949-50, CSSL.

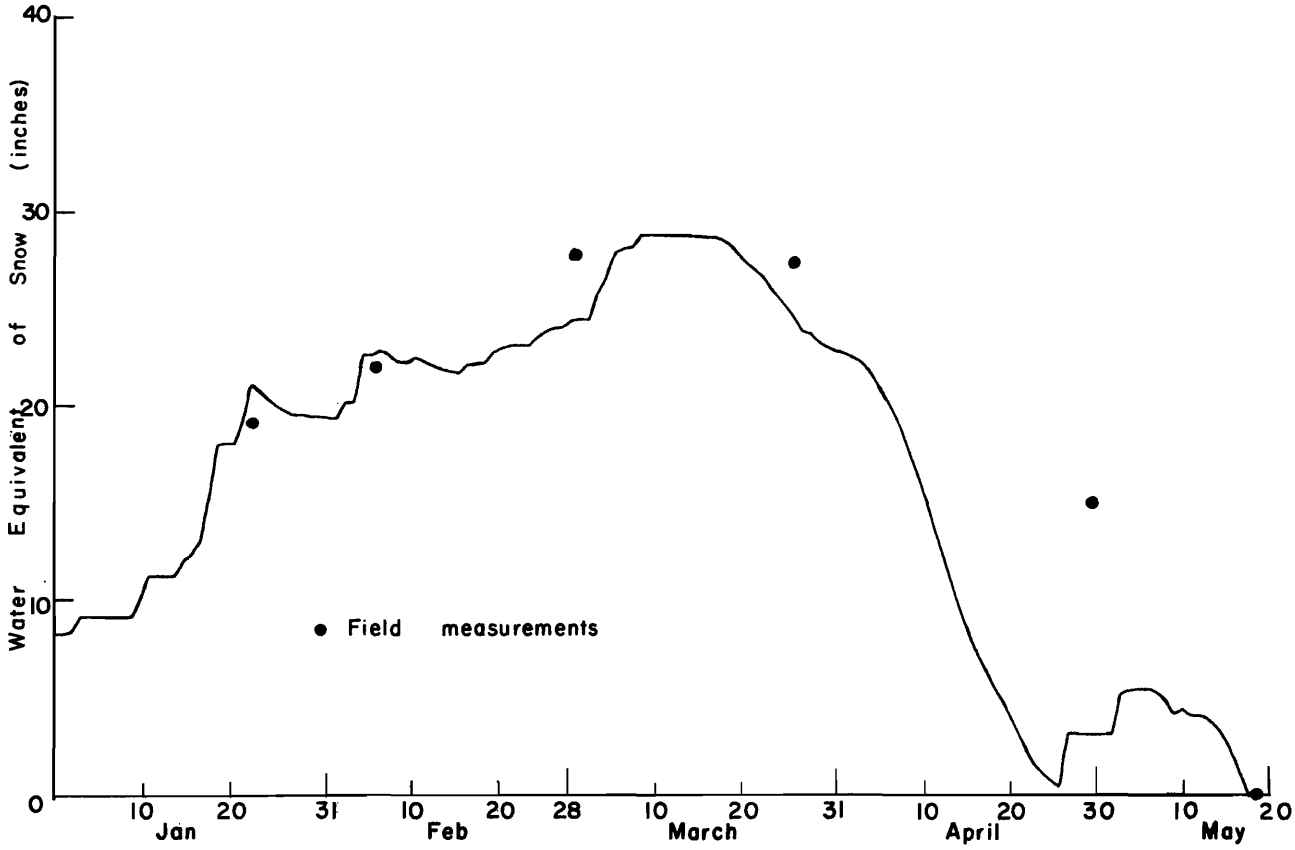

Figure 4.20. Calculated water equivalent of the snowpack for the year 1950-51, CSSL.

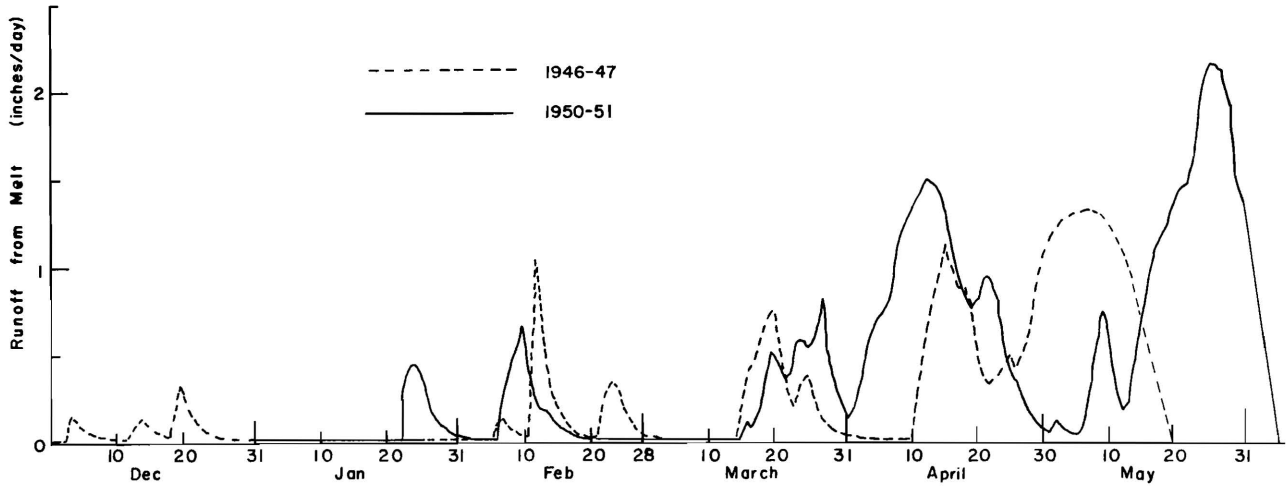

Figure 4.21. Computed runoff at the bottom of the pack due to snowmelt for the years of 1946-47 and 1950-51, CSSL.

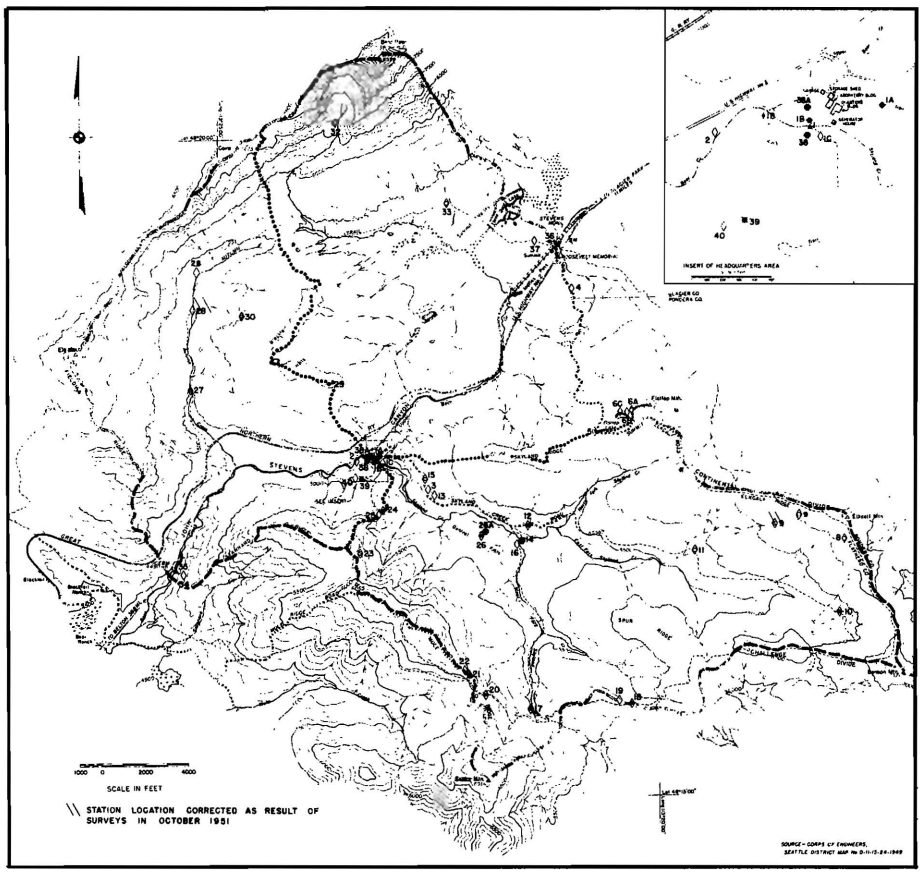

Figure 4.22. Map of the Upper Columbia Snow Laboratory drainage and meteorologic stations.

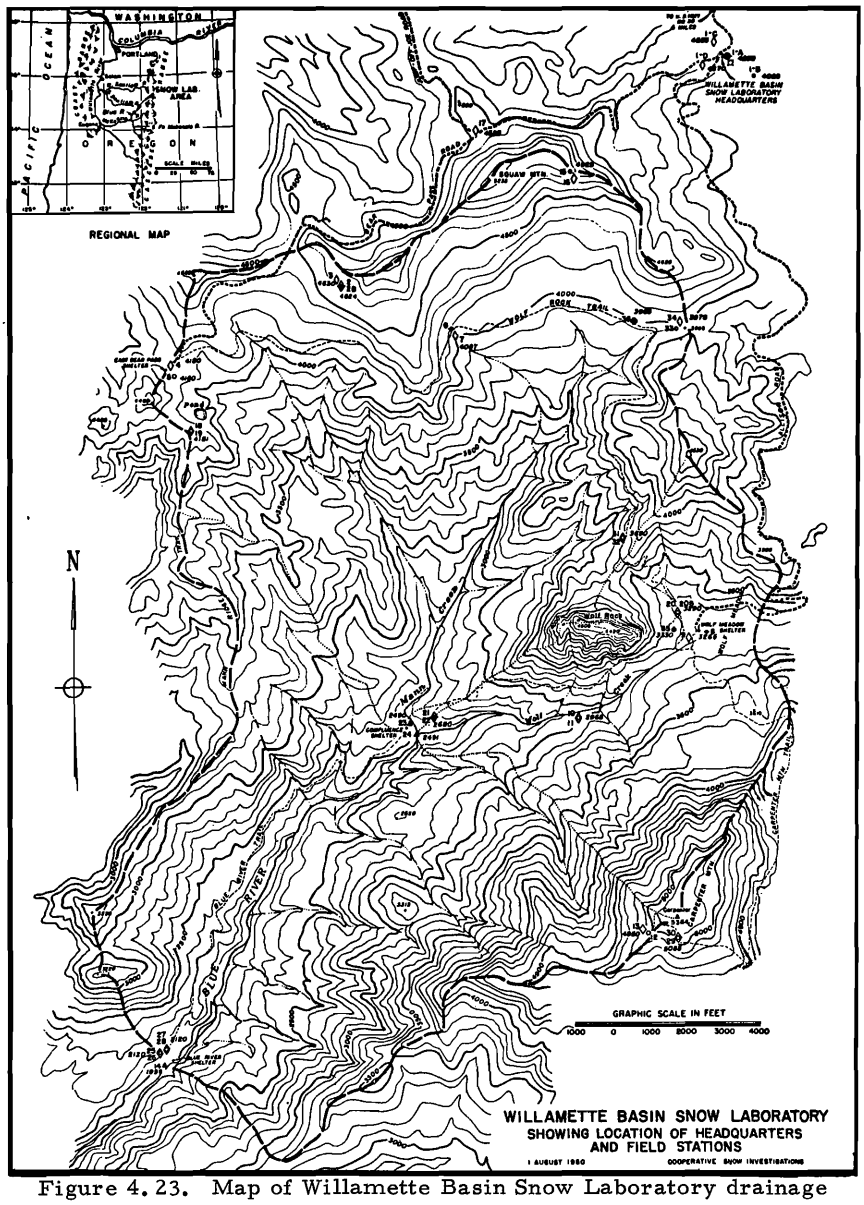

Figure 4.23. Map of Willamette Basin Snow Laboratory drainage area and meteorlogic stations.

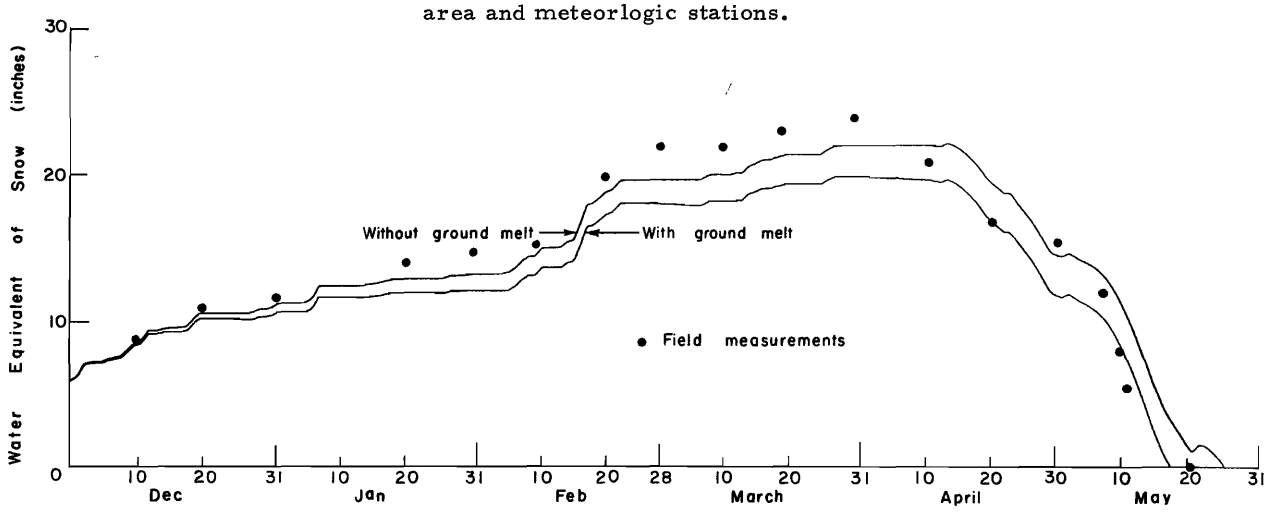

Figure 4.24. Calculated water equivalent of the snowpack for the year 1948-49, UCSL.

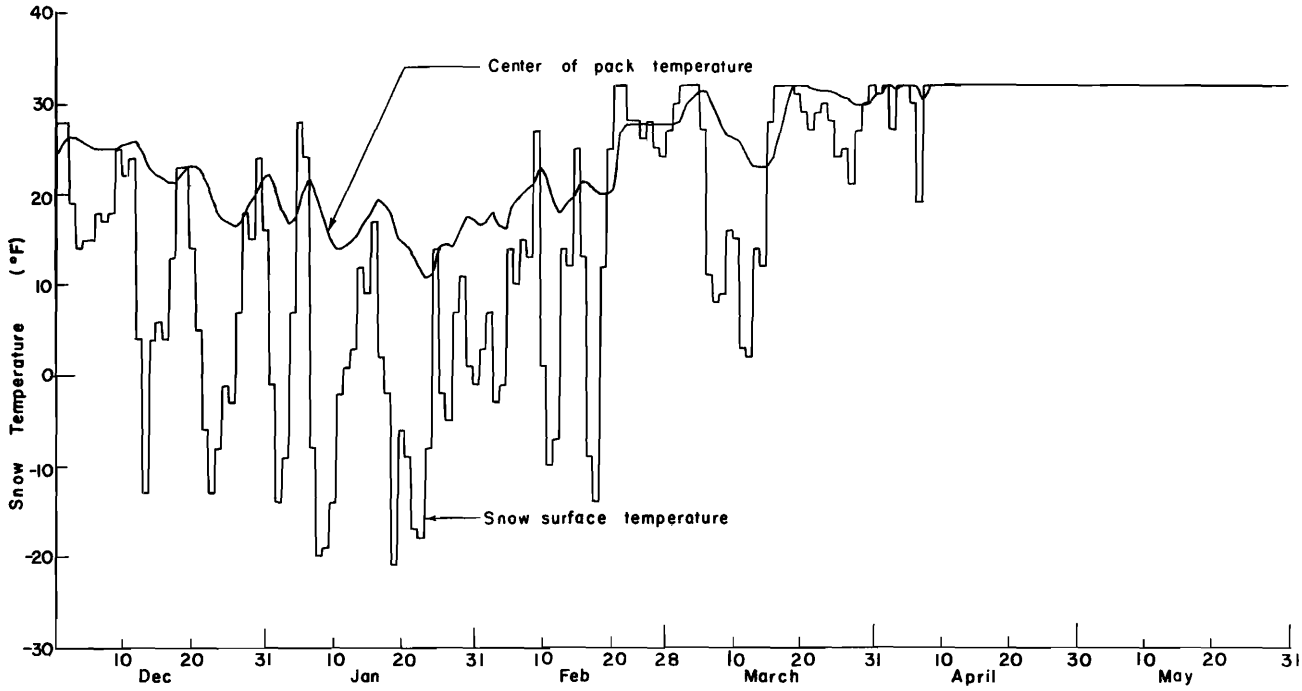

Figure 4.25. Calculated snow surface and center of snowpack temperatures versus time for the year 1948-49, UCSL.

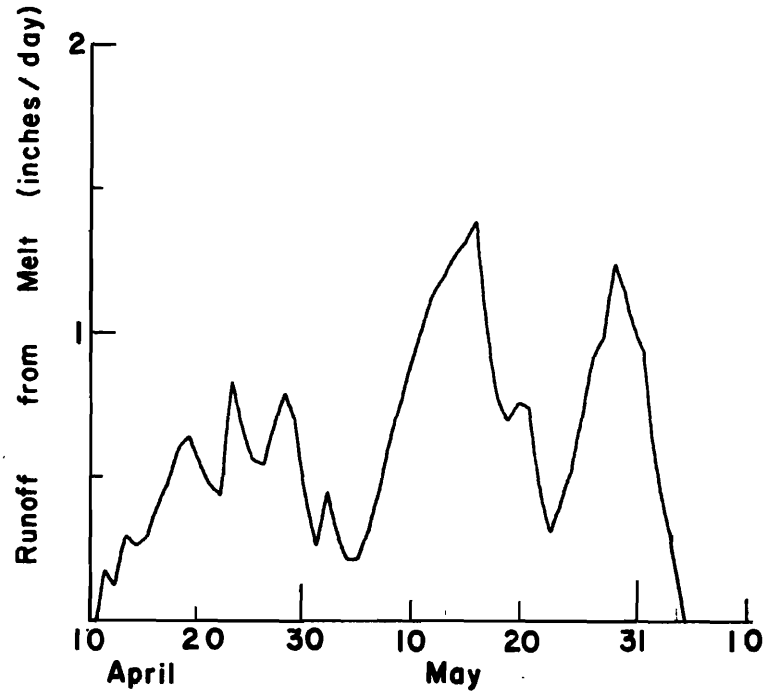

Figure 4.26. Calculated runoff due to snowmelt versus time for the year 1948-49, UCSL.

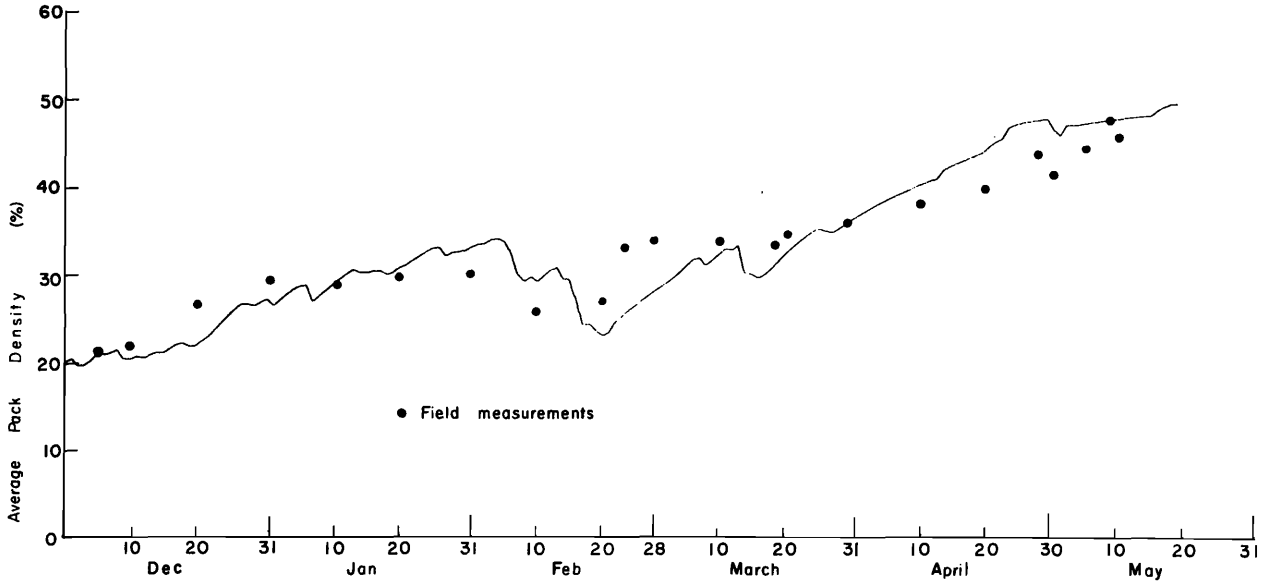

Figure 4.27. Calculated average density of the snowpack for the year 1948-49, UCSL.

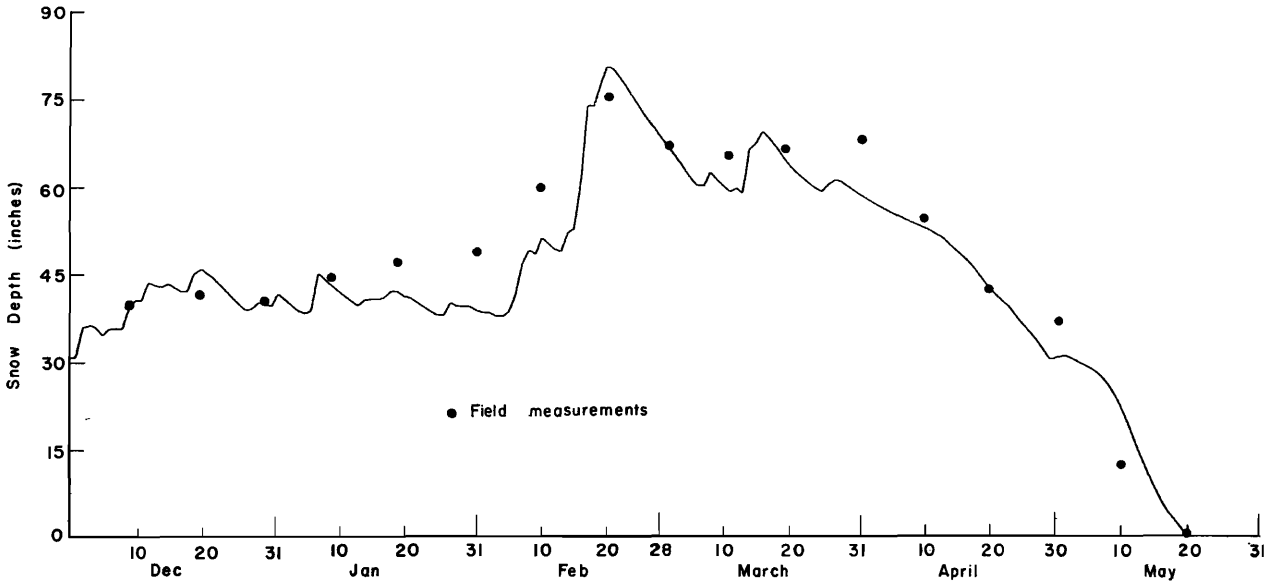

Figure 4.28. Calculated depth of snow for the year 1948-49, UCSL.

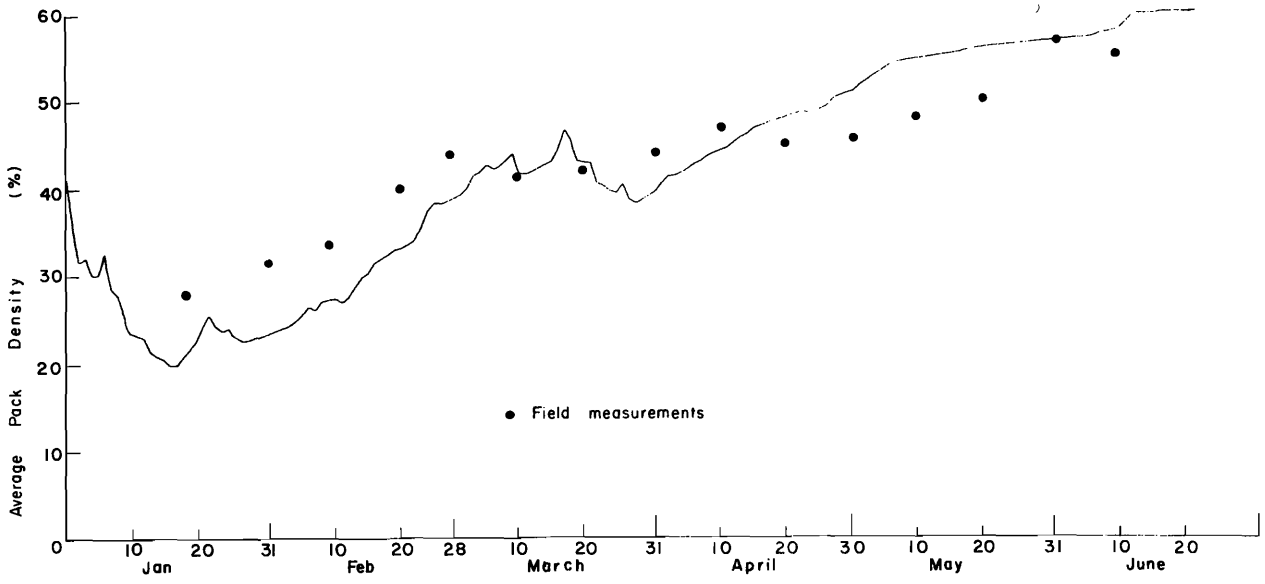

Figure 4.29. Calculated average density of the snowpack for the year 1949-50, WBSL.

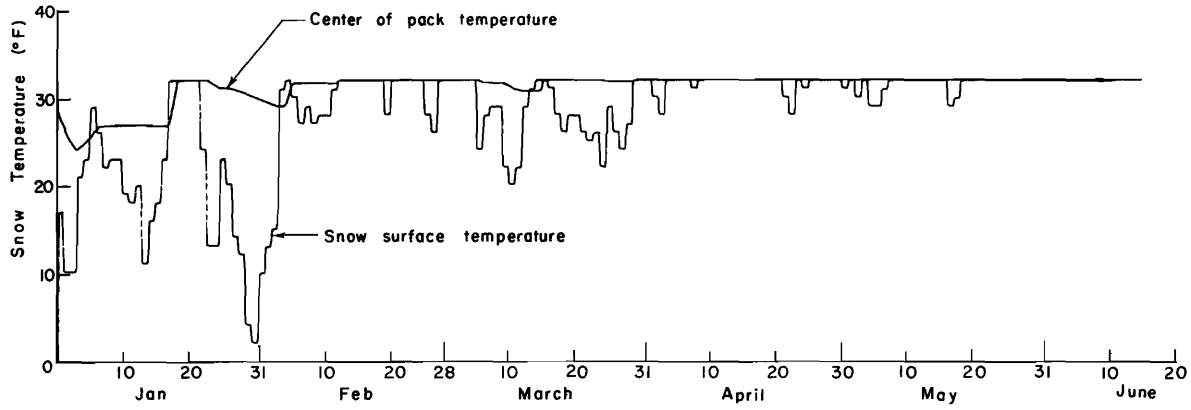

Figure 4.30. Calculated surface and center of the pack temperature for the year 1949-50, WBSL.

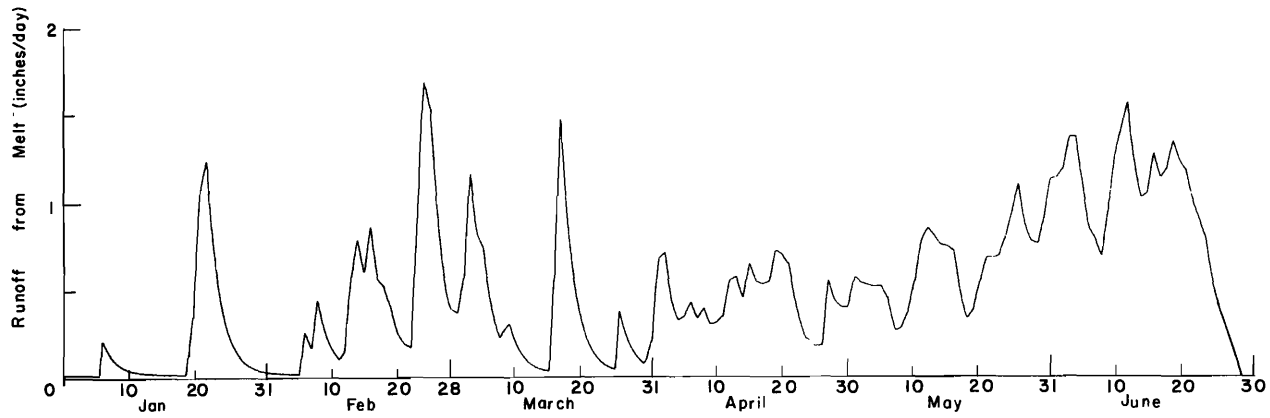

Figure 4.31. Calculated runoff due to snowmelt for the year 1949-50, WBSL.

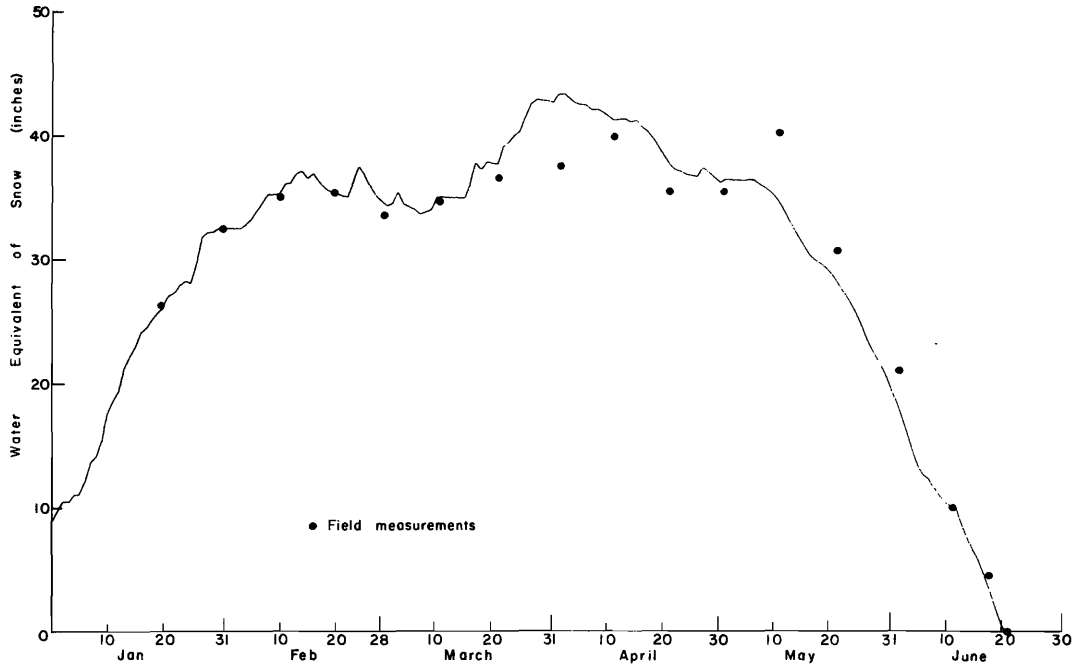

Figure 4.32. Calculated water equivalent of the snow for the year 1949-50, WBSL.

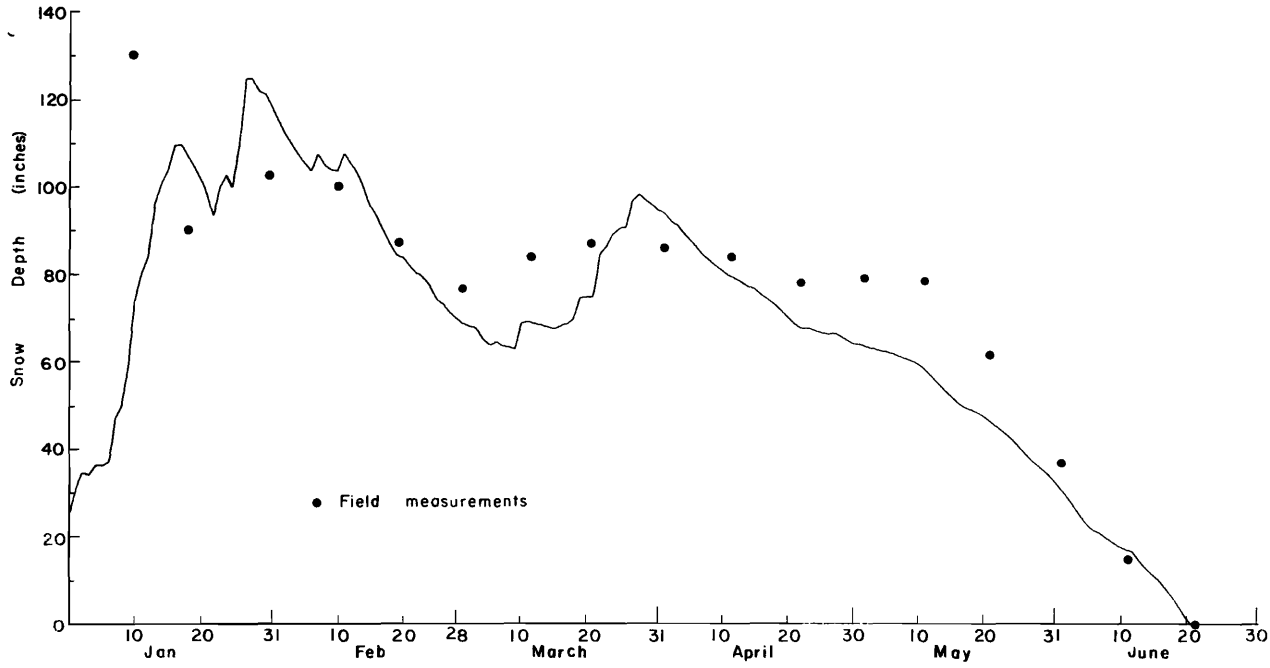

Figure 4.33. Calculated actual snow depth for the year 1949-50, WBSL.

CHAPTER V
SENSITIVITY ANALYSIS

The variable parameters, initial conditions, and coefficients were investigated as to their effect on the simulation reliability. The coefficients were varied and the output plotted to see how the simulation results were changed.

Initial Conditions

The initial conditions varied were those for the apparent depth, the accumulated precipitation, and the temperature of snow at the center of the pack. These conditions are usually not defined by data and so must be assumed or estimated by the judgment of the investigator.

Of the initial conditions, the apparent depth has the most effect on the average snowpack density. The apparent depth is divided into the accumulated precipitation to determine the density as shown by Equation 2.14. Figure 5.1 shows the results of varying the apparent depth from 15 to 32 inches for a given water equivalent of 6 inches. This caused a variation in the inital density from 0.4 to 0.19, of which 0.31 gave the best fit for the average pack density. However, as shown by Figure 5.1, within approximately 15 days, the average pack densities are essentially the same for each initial condition used. The initial condition on the apparent depth, therefore, is not significant after a relatively short period of time. For short term simulation, however, it would be important to have the proper value. Apparent depth initial conditions can be determined if density and accumulated precipitation are both known.

The initial condition of the accumulated precipitation was increased to check the effect that it would have on the average density of the snowpack, which is shown in Figure 5.2. Increased accumulated precipitation increases the average density for a short period of time. By the end of two months the density is essentially the same and the difference is small (5 percent) after 15 days. This is because the increase of 1.1 inches of precipitation is no longer significant compared to the total amount that has accumulated since the beginning of snow accumulation. If the period of time simulated started when most of the snow had accumulated, an error of 1 or 2 inches in estimating the initial condition for accumulated precipitation would not significantly affect the average density of the pack. The accumulated precipitation should be determined with as small a percentage of error as possible from the precipitation data available.

The other initial condition investigated was the temperature at the center of the snowpack. In Figure 5.3 three initial conditions are shown with their effect on center pack temperature and snowmelt runoff. The assumed temperature to start the simulation was $32^{\circ}F$ with isothermal conditions. The highest runoff before December 10 is shown in Figure 5.3 with this initial condition of $32^{\circ}F$. The initial condition was reduced to $25^{\circ}F$ and the runoff from the pack was reduced as shown by the dashed line. Part of the runoff was frozen and the heat given off was used to heat the pack to isothermal conditions. When the initial condition was reduced to $0^{\circ}F$, the surface melt was completely used in heating up the pack and produced no runoff as shown by the dotted line. By December 10 the temperature at the center of the pack was the same and the temperature and liquid water of the pack were no longer affected by the initial temperature chosen for the center of the pack.

This information shows that initial conditions on the center pack temperature have little effect early in the season when the pack depths are shallow. The amount of snowmelt frozen by the pack within the $0^{\circ}F$ initial condition was 0.8 inches. In a basin with little winter melt, the appearance of runoff could be affected by choosing a bad initial temperature if the pack was deep at the beginning of the simulation period.

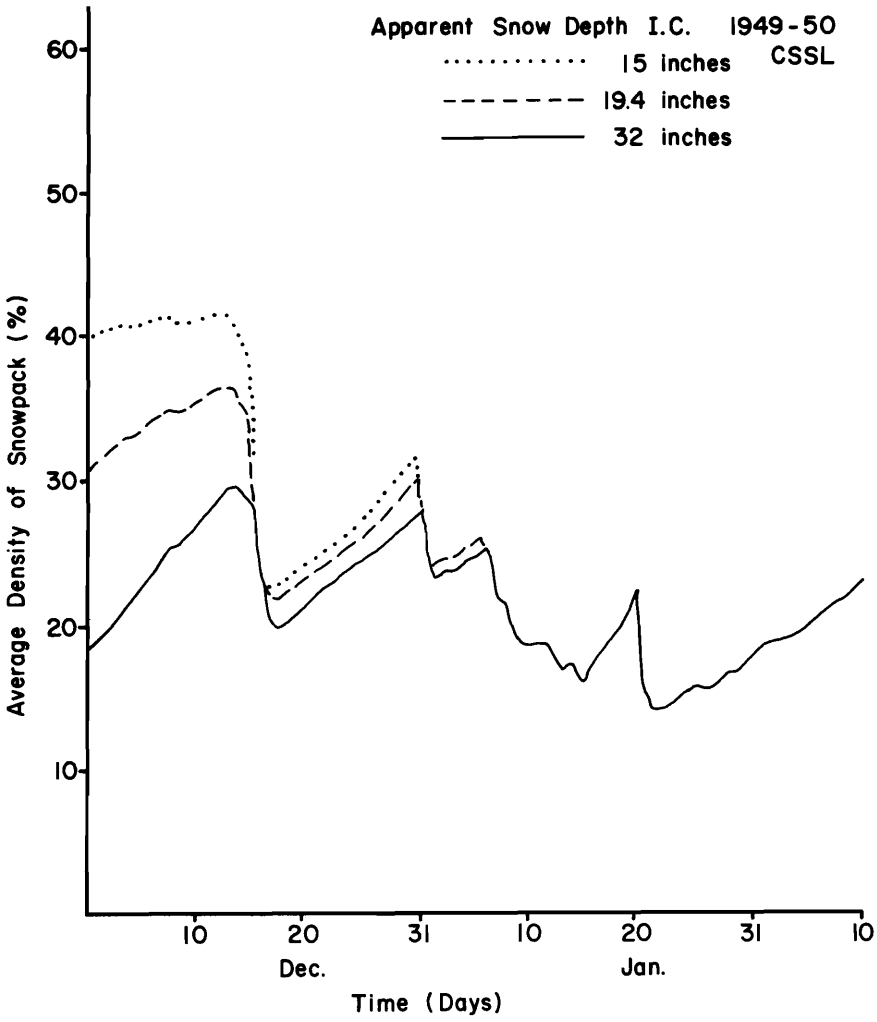

Figure 5.1. Average snowpack density as a function of time and initial conditions of apparent depth.

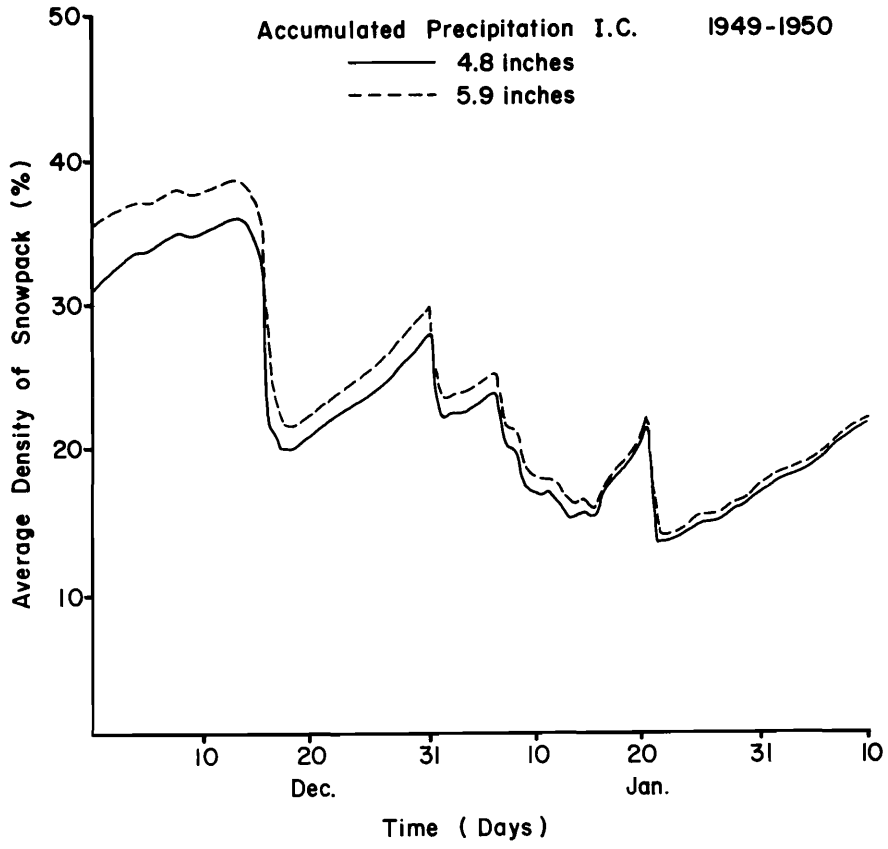

Figure 5.2. Plot of average snowpack density as a function of accumulated precipitation initial values.

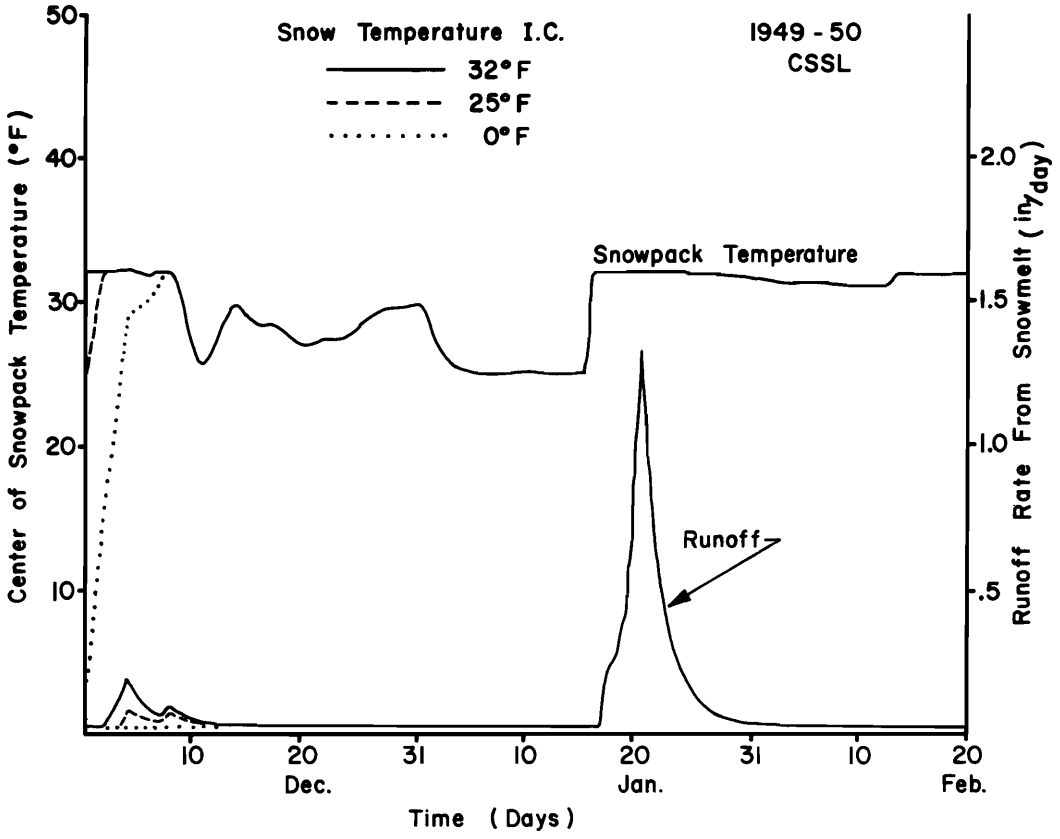

Figure 5.3. The initial snowpack temperature at center as it affects center of pack temperature and runoff.

Coefficients

The proportionality constant, k_m, of Equation 2.31 is used to determine the snowmelt rate. The constant, k_m, was estimated to be approximately equal to 0.40 for the Central Sierra Snow Laboratory and to check the effect of k_m, holding other things constant, the data of 1949-50 were used. The constant, k_m, was varied from 0.40 to 0.60; and the effect is shown in Figure 5.4.

Figure 5.4 is a plot of runoff versus time. It shows that the runoff was increased approximately half by increasing k_m by half. The time of appearance of the runoff at the bottom of the pack for a k_m of 0.60 was earlier than for a k_m of 0.40 because the increased melt brought the pack to "ripe" conditions earlier. With k_m reduced below 0.40, the appearance of runoff would be delayed because a greater percent of the surface melt would be used in ripening the pack. Increasing k_m reduced the water equivalent of the pack because of the increased surface melt, and the snow was gone earlier than it should have been. This test shows that the model is quite sensitive to k_m, which should be determined as accurately as possible.

Figure 5.4 is a sensitivity test and assumes that the extra runoff is available in the snowpack. The upper curve does not represent actual conditions so far as the snowpack is concerned.

The surface melt routing factor, k_s, was used in the simulation program to reproduce the delay between surface snowmelt and runoff and was assumed to be constant for all depths of snow. Figure 5.5 is a plot of water equivalent versus time as a function of k_s. For k_s, equal to 1.0 or no routing, the water equivalent was gone two days earlier than for a k_s of 0.5. The routing factor is a function of depth of the snowpack, density, and channeling that has taken place in the pack. If k_s cannot be varied according to the depth of snow, it would be better to use a k_s that would delay the surface melt less than one day. The reason for this is shown in Figure 5.5, which indicates that the disappearance of the snow is delayed at the end of the melt season by two days which is unrealistic since the snow is almost gone and there should be no delay of the surface melt for a shallow pack. For floods caused by rain on snow with a deep snowpack, the routing factor would be important in predicting the flood peak. The reason is shown in Figure 5.6 which shows routing values of 0.5 and 0.9. The 0.9 value has the highest peak and a shorter recession curve. It takes five more days for the 0.5 value than the 0.9 value to stop contributing snowmelt to the runoff. However, only two days of this time is contributing significantly greater amounts of melt. The main effect would be felt in the peak flow amounts. For a large watershed the amount and duration of melt would be important rather than the peak outflow from the snow due to the three or four day lag in time of concentration.

The liquid water in the snow must be refrozen as the surface temperature of the pack goes below 32°F. The liquid water starts to freeze at the surface and continues to freeze down into the pack, depending on the value and duration of minimum temperature. Figure 5.7 shows various assumptions as to how the liquid water is refrozen. As the center temperature goes below 32°F, a coefficient k_f is switched into the program and starts the liquid water freezing as a function of time. Values of 0.05, 0.1, and 0.0 were tested as shown in Figure 5.7. The effect of k_f on snowmelt runoff is shown in Figure 5.8. The runoff from the pack is increased and appears earlier because less of the surface melt is required to satisfy the liquid water holding capacity of the pack. Because of this, the snow is melted a day earlier. The increased runoff is also shown in Figure 5.8 by the decrease in the water equivalent of the snow. In Figure 5.7 the reduction of the high peaks in the liquid water held in the snow is because the lower values of k_f allow more runoff from

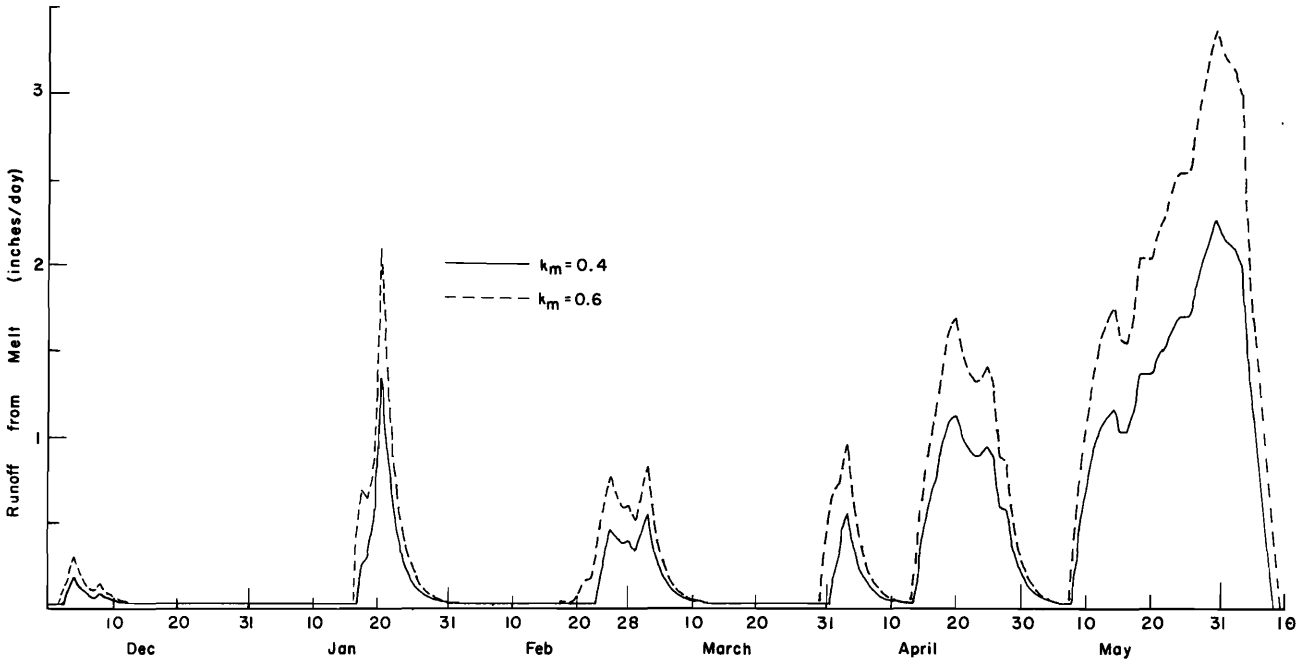

Figure 5.4. Runoff hydrograph from CSSL, 1949-50, for two values of the proportionality constant, k_m.

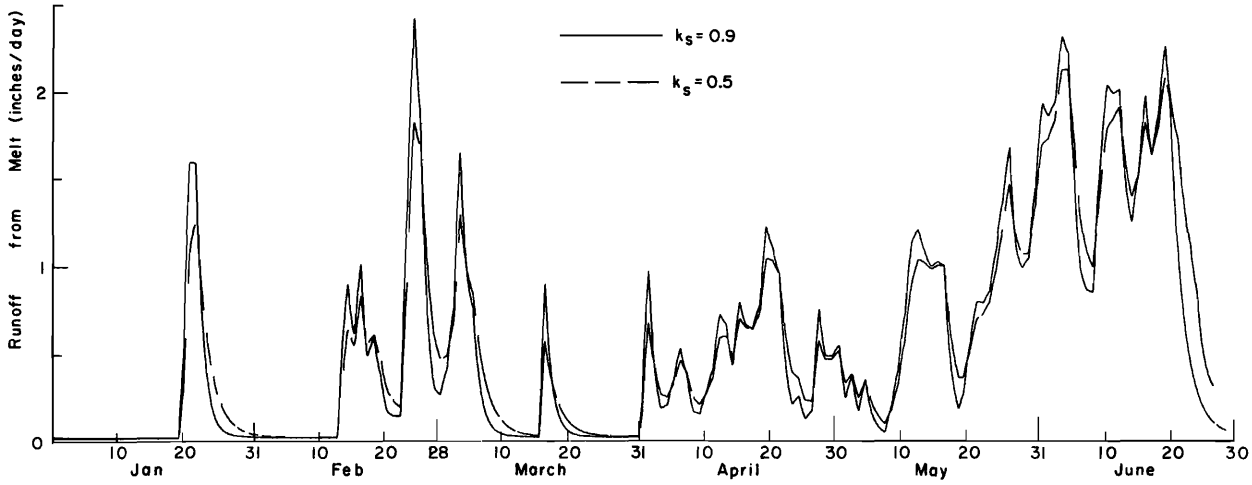

Figure 5.5. Runoff hydrograph for two snowmelt routing coefficients, k_s.

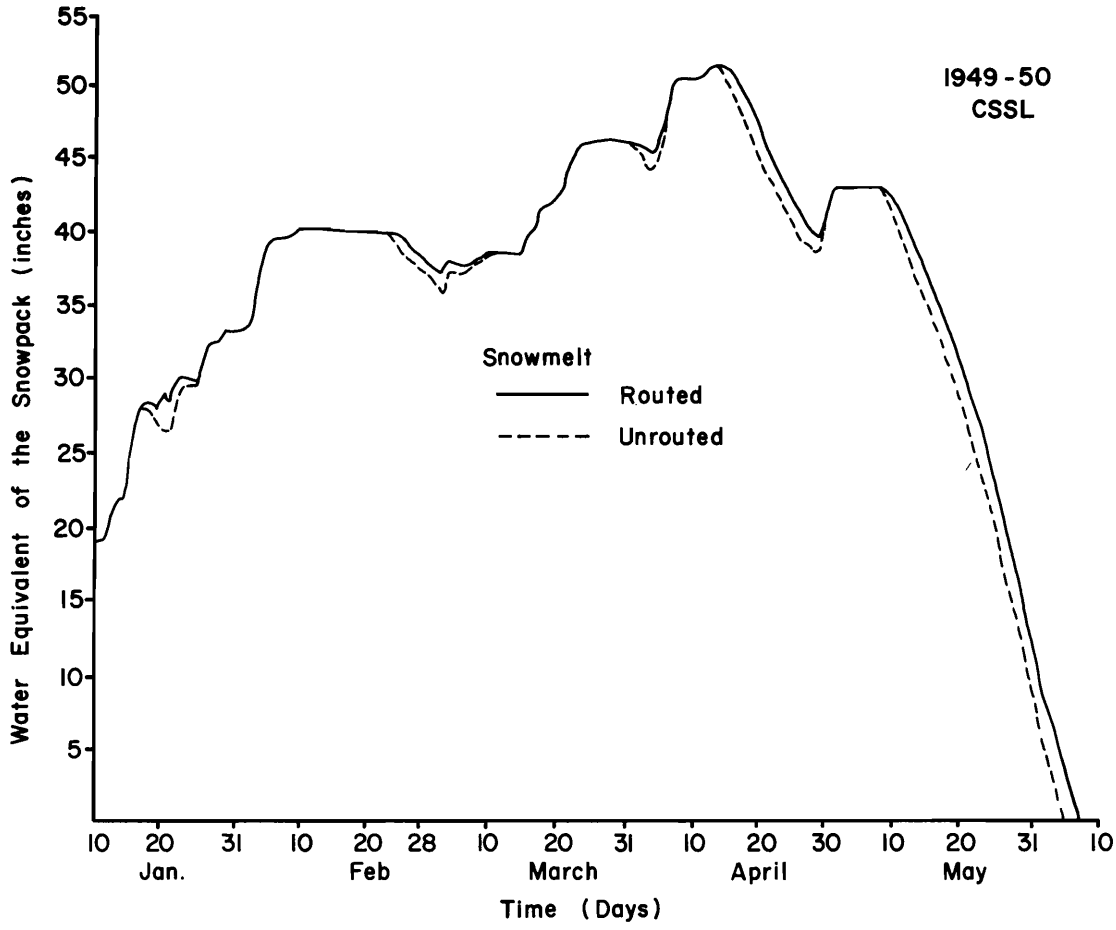

Figure 5.6. Water equivalent of the pack as a function of snowmelt routing coefficient, k_s.

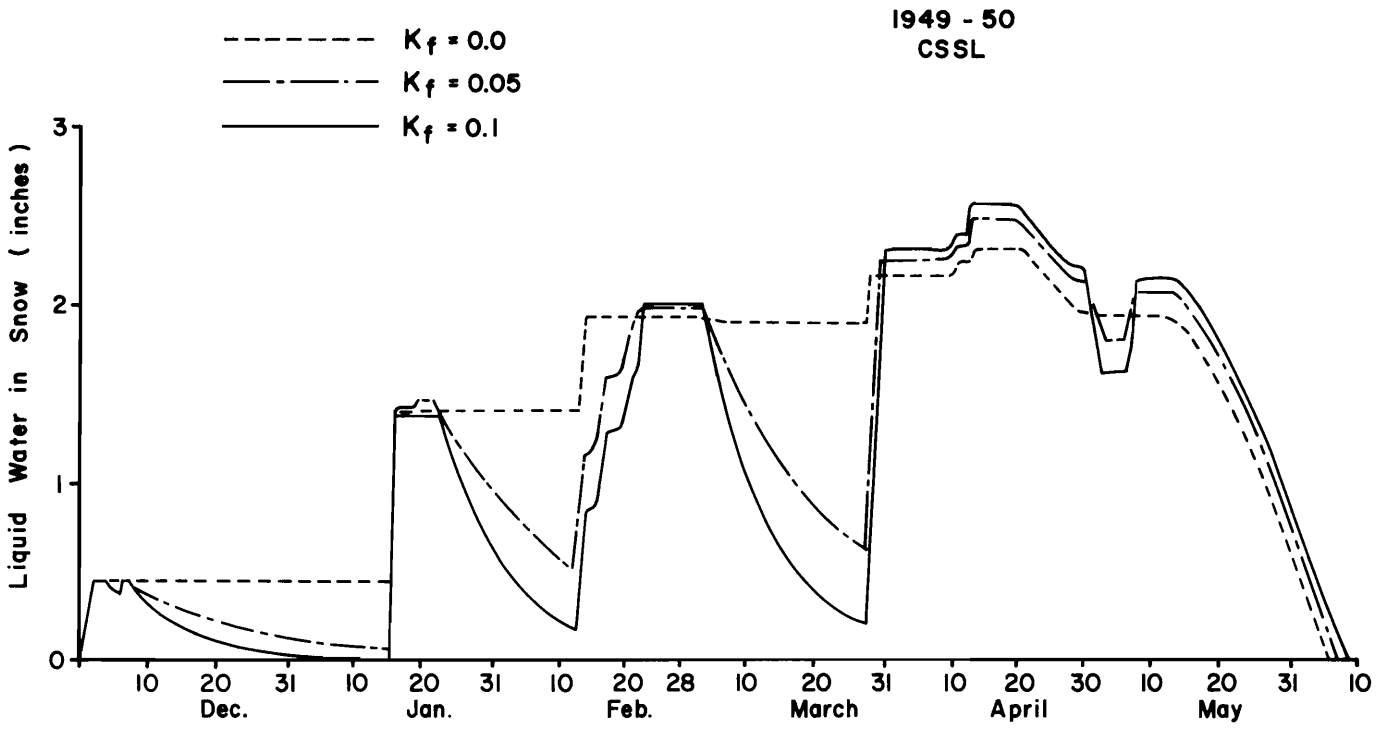

Figure 5.7. Liquid water in the pack as affected by coefficient, k_f, which controls the rate of freezing when center of pack temperature goes below 32°F.

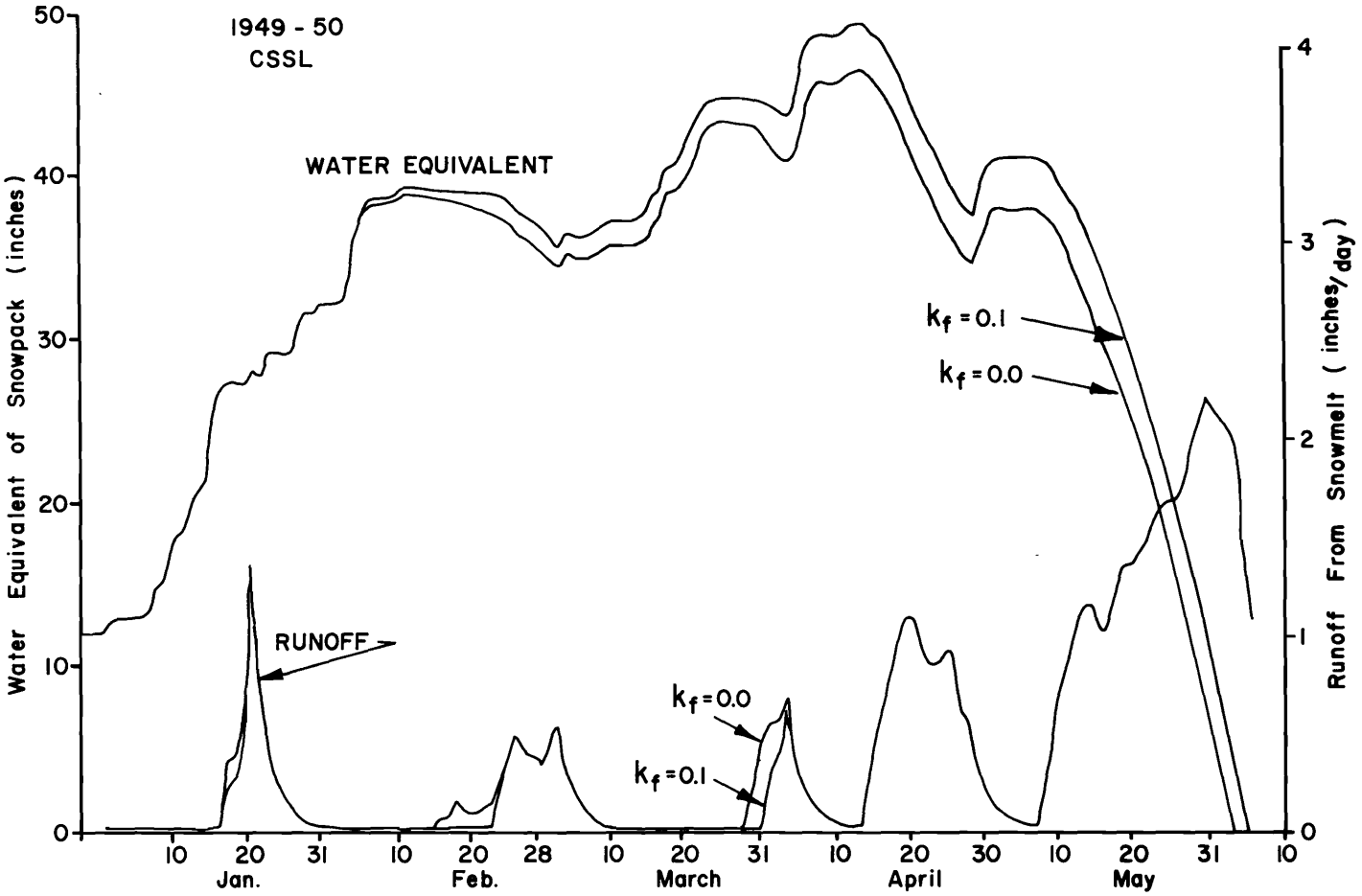

Figure 5.8. Snowmelt runoff from the snowpack and water equivalent as affected by k_f.

snowmelt and reduce the water equivalent of the snowpack.

The effect of thermal diffusivity, α, on the center of the pack temperature was evaluated. This was done by varying the coefficient α, of Equation 2.18 by a factor of ten. The results are shown in Figure 5.9. As the coefficient is increased, the center temperature becomes more sensitive to changes in the snow surface temperature, because, when α is increased, the thermal conductivity of the snowpack is increased. The temperature gradient within the pack would be steeper and reflect more nearly the average between the snow surface temperature and the ground temperature of 32^{o}F. Equation 2.18 in its finite difference form is:

$$\frac{dT_j}{dt} = \frac{\alpha(t)}{[z(t)]^2} [T_{j+1} + T_{j-1} - 2T_j] \quad . \ . \ . \ . \ . \quad 6.1$$

with boundary conditions:

For $T_a < 32^{o}$F

$T_1 = 32^{o}$F, assumed ground temperature

$T_{m+1} = T_a(t)$, air temperature

For $T_a \geq 32^{o}$F

$T_1 = T_{m+1} = 32^{o}$F

in which

T_1 = the snow temperature at the ground

T_{m+1} = the snow surface temperature

T_j = intermediate temperatures within the snowpack

The term $[\Delta x(t)]^2$ can be written as $[D/m]^2$ in which D is the snow depth and m is the number of sublayers in the snowpack. As the snow depth increases, the term $\alpha / [\Delta z]^2$ decreases and a change in temperature at one of the points T_{j+1} or T_{j-1} has less effect on the temperature at point T_j. The effect of increasing snow depth can be seen in Figure 4.24 which is a plot of $\alpha / [10z^2]$ versus time for the year 1949-50 of the Central Sierra Snow Laboratory data. The decreased value of $\alpha / [10z^2]$ means that a given temperature change at the surface would have less effect on the center of the pack temperature. Equation 2.19 shows α as a function of density.

The average density of the snowpack is affected by the compaction coefficient, k_{sc}. The effect of two values of k_{sc}, 0.05 and 0.1, is shown in Figure 5.10. The value of 0.1 has a more dense snowpack and at the end of the year has an average density of 58.5 percent, which is almost at the assumed maximum density for the pack. The points on Figure 5.10 are from actual field measurements for comparison with the calculated average density. This shows that for 1949-50, CSSL data, a value for k_{sc} between 0.1 and 0.05 would give better results than either 0.05 or 0.1. The value of 0.05 used in the three years simulation gives the best composite fit for all of the years. A k_{sc} of 0.05 was also good for the Upper Columbia Snow Laboratory, while a value of 0.03 was used for the Willamette Basin.

Input Variations

New snow density

The density of the new snow was varied as shown in Figure 5.11. Figure 5.12 shows a plot of average density versus time for the three new snow density relationships. As the density of the new snow was increased, the average pack density was also increased. The average density was affected the most during the period of high snow accumulation and less during the snowmelt season. During a long period of time without new snow the average pack density would approach the same value for the three new snow density relationships used. This can be seen at the end of the plot in Figure 5.12 as the three density curves are getting closer together. The three curves would be one at the point of maximum density for the pack.

Density and snow depth measurements were not taken at the exact time the new snow was deposited. These measurements were taken daily at the snow

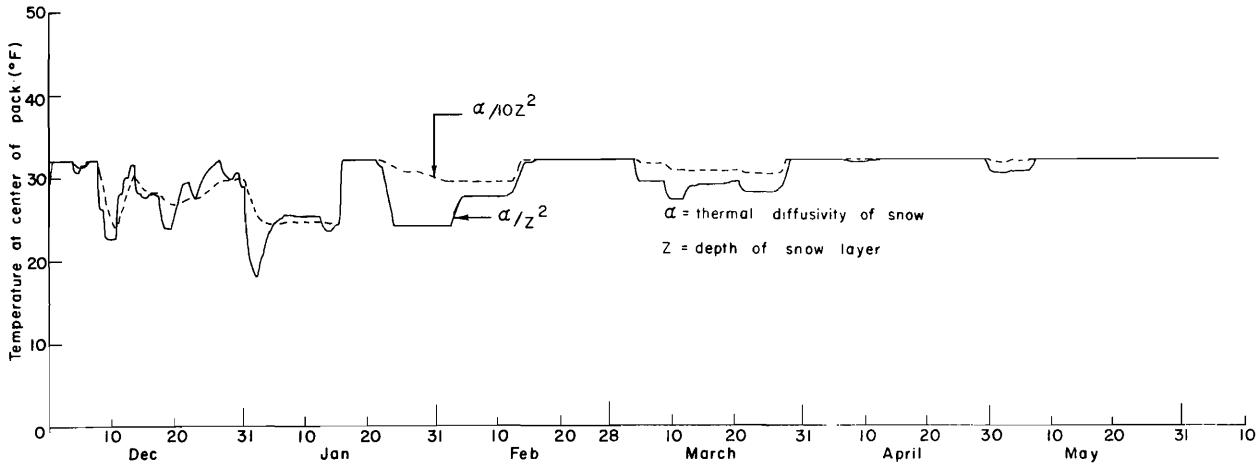

Figure 5.9. Center of the pack temperature as a function of thermal diffusivity, α.

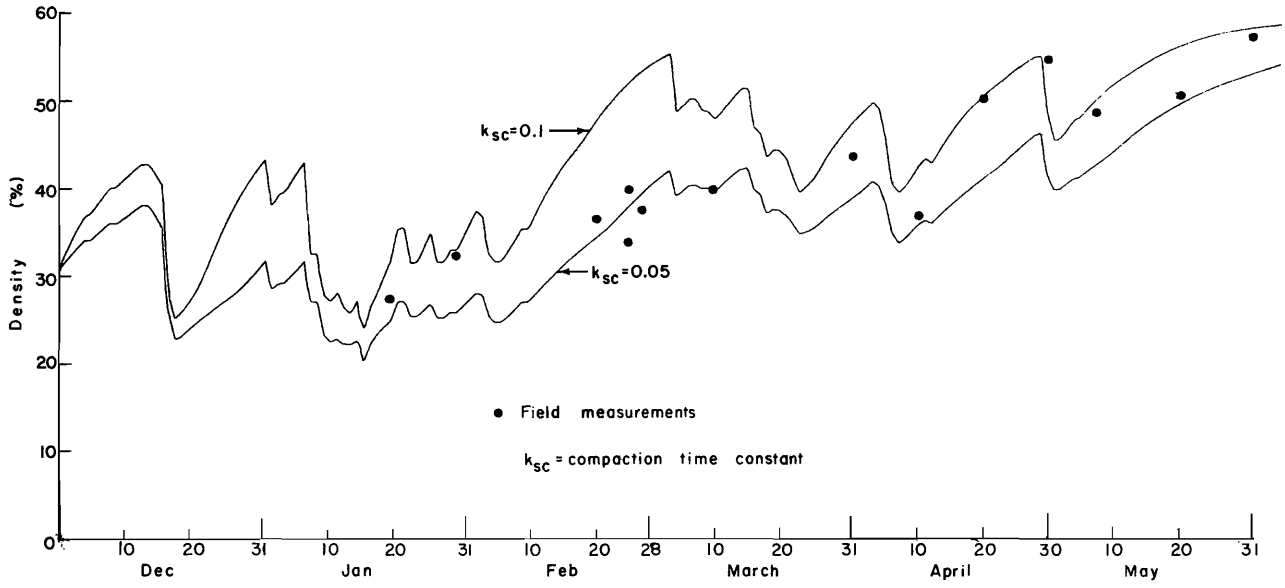

Figure 5.10. Average snowpack density as a function of compaction coefficient, k_{sc}.

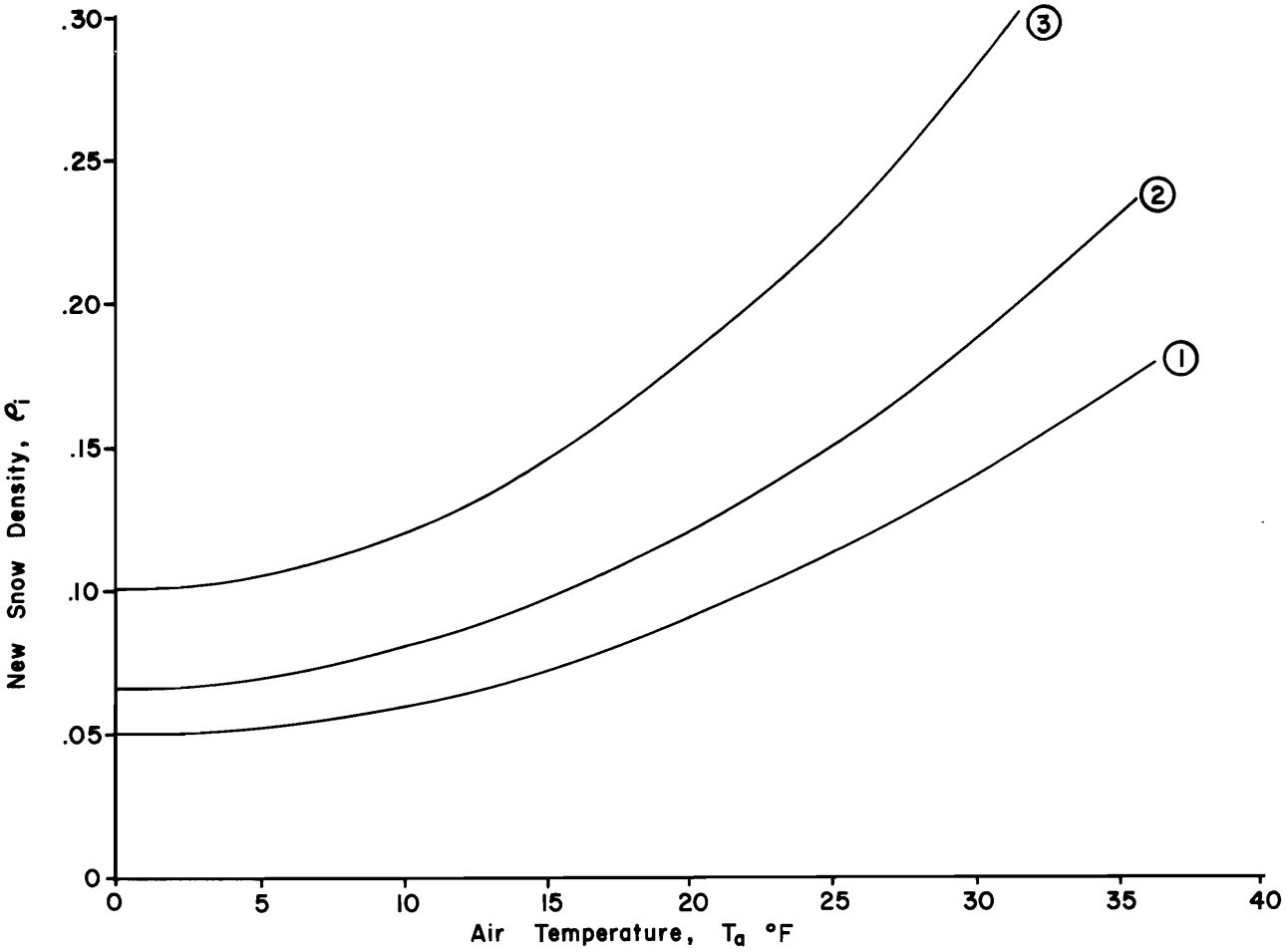

Figure 5.11. Plot of three new snow density relationships used to test affect on average snowpack density.

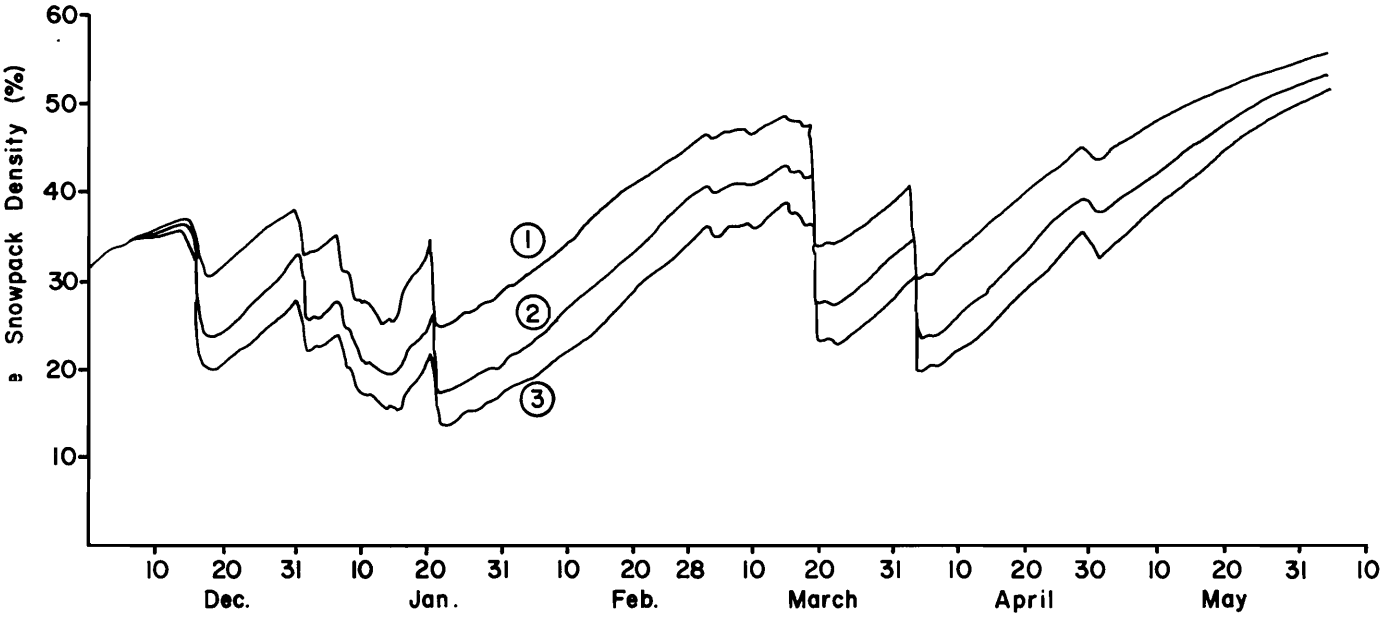

Figure 5.12. Plot of average snowpack density as a function of the three new snow densities of Figure 5.11.

laboratories. The Corps of Engineers studies (6) indicate that a density of 0.10 is a good average density to use for all new snow that accumulates regardless of the temperature of the air at the time of deposition. This value was used, and the effect can be seen in Figure 5.13, which also shows the calculated average pack density for the new snow density curve in Figure 2.5(b) and a constant new snow density of 0.1. The points placed on the graph are from actual measurements taken in the field. The new snow density of 0.1 gives the best results for average snowpack density. This density was used to verify the model for the CSSL and the WBSL simulation.

Maximum density

The maximum average density of the snowpack can be controlled by varying a value in Equation 2.16. The denominator of the fraction $k_{sc}/0.6$ is the value that controls the maximum density. By changing 0.6 to 0.5, the maximum average density will be reduced to 0.5 for the snowpack.

To check the effect on the simulated pack density, data from the UCSL were used. Figure 5.14 shows the snowpack average density for maximums of 0.6 and 0.5. The density given by 0.5 fits the actual field measurements the best. A k_{sc} value of 0.05 was used in the UCSL simulation tests.

Radiation index

The input values for the radiation indexes in the snowmelt and evaporation of Chapter II were checked to see what effect they would have on the quantity of melt at the surface of the pack. To determine the index variation with respect to latitude, slope, and aspect, plots were made (Figure 5.15) showing the radiation index for a south facing basin for a horizontal surface and a surface with a slope of 40 percent at 44.3° and 48.2° north latitude. The figure shows that latitude has little effect, but the slope effect is large compared to a horizontal surface.

The slope aspect and azimuth effect is shown in Figure 5.16, which is for a latitude of 48.2° north and shows a plot of radiation index for a horizontal and sloped surface. For a slope of 40 percent and north facing surface the radiation index varies from zero on December 1 through February 1 to a maximum of 58 on June 21. For the south facing slope of 40 percent the radiation index is more constant. It ranges from a minimum of 55 to a maximum of 60 in March. The 40 percent north facing slope index is greater than for the south facing slope for a short period of time during June and part of July. The radiation index reflects the slope, aspect, and latitude of a basin.

The effect of slope on snowmelt for a given aspect can be seen by comparing runoff from the pack. For the south facing slope of 40 percent the radiation index ratio RI_s/RI_h is greater than for lower slopes and the runoff is increased during December, January, February, March, and April. This can be seen by comparing the runoff from the south facing slope shown in Figure 5.17 to the normal albedo runoff of Figure 5.18 for a slope of 13 percent. The slope is important in calculating the runoff from a watershed or drainage basin and should be defined accurately. Figures 5.17 and 5.18 represent parameter sensitivity changes and assume that sufficient snow is available to satisfy the melt potential. The runoff amounts shown do not necessarily represent actual conditions.

The effect that aspect, or the direction of slope, has on the water equivalent of the pack can be seen in Figure 5.19. On the south facing slope of 40 percent, all of the snow melted by May 30. On the same day, the north facing slope of 40 percent still had a water equivalent of 25 inches. Projecting at the current melting rates, it would take approximately 15 more days or until June 14 for the snow to be gone from the north slope. When comparing Figure 5.19 with the actual water equivalent of Figure 4.19 of the Central Sierra Snow Laboratory, the importance of

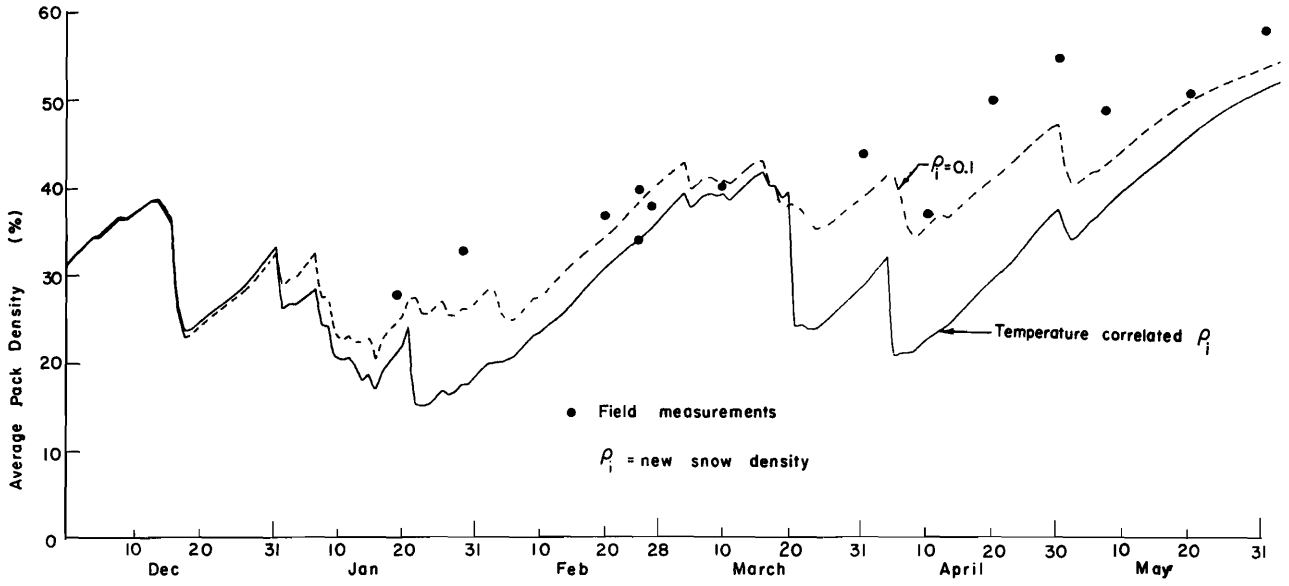

Figure 5.13. Average pack density for constant density of 0.1 and temperatures relationship of Figure 2.5(b).

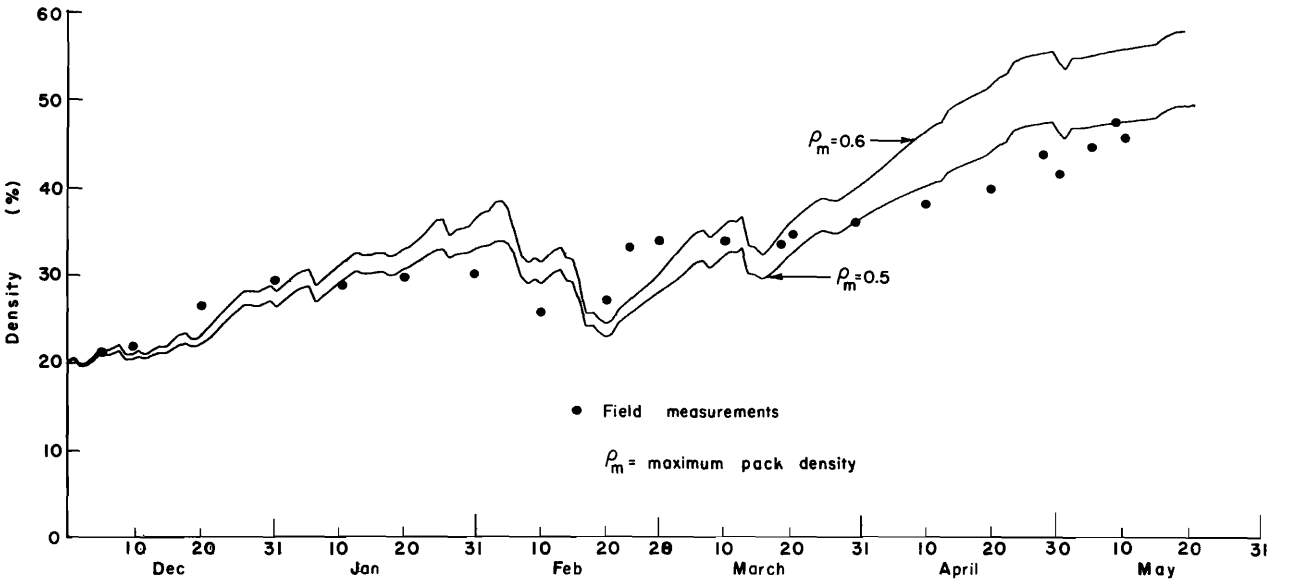

Figure 5.14. The variation of average snowpack density for two values of maximum density for the year 1948-49, UCSL.

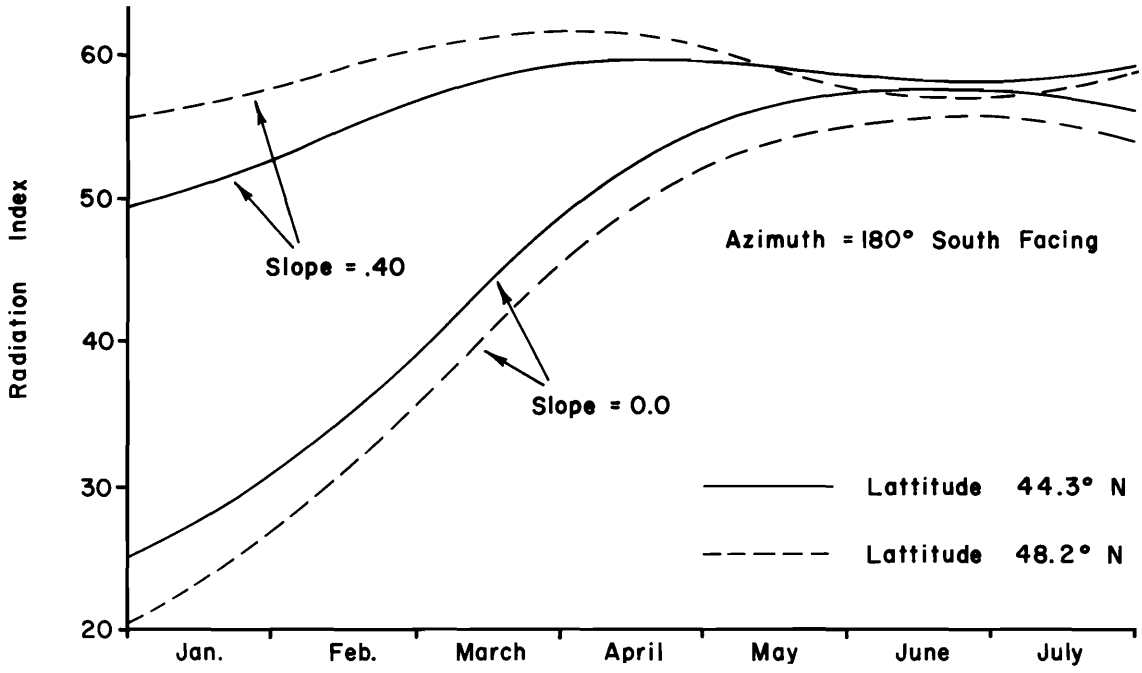

Figure 5.15. Radiation index for a south facing slope as a function of slope and latitude.

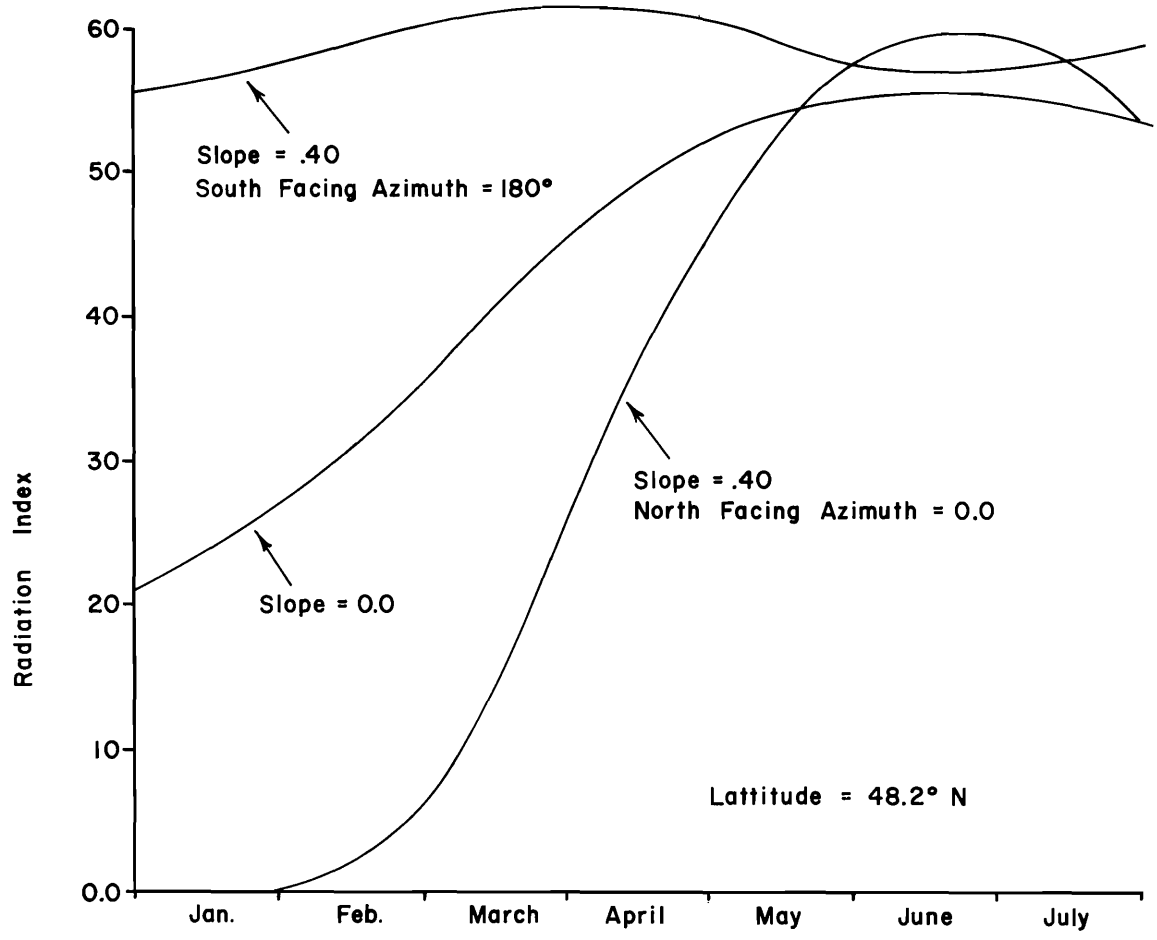

Figure 5.16. Radiation index as a function of aspect for north and south facing slopes.

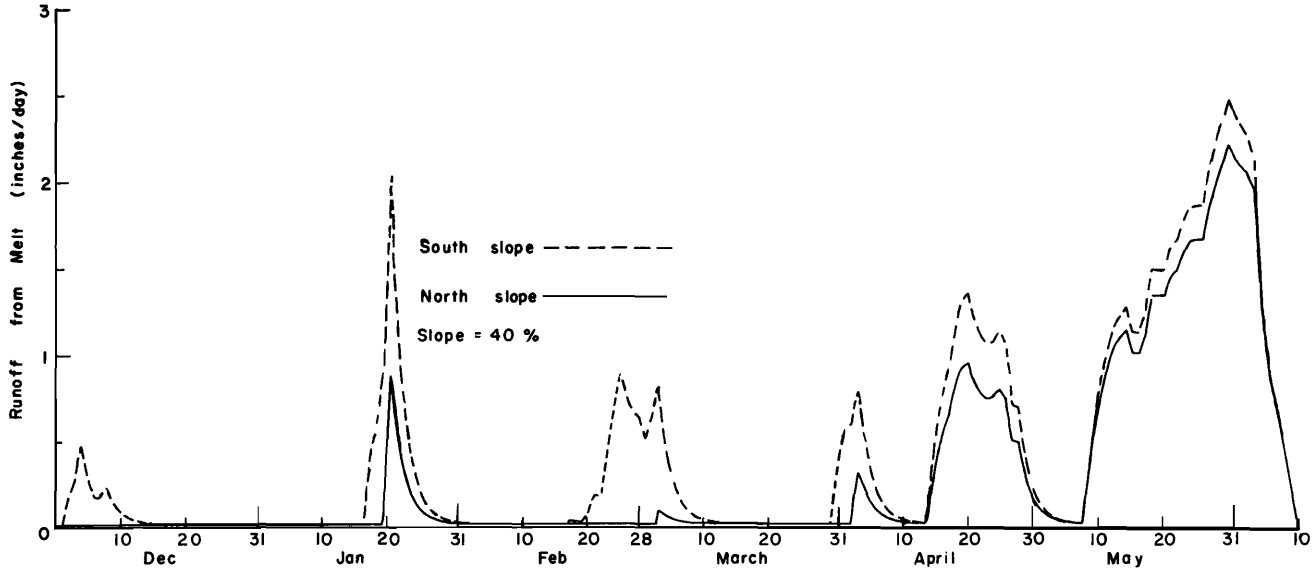

Figure 5.17. Runoff from a snowpack as affected by radiation index.

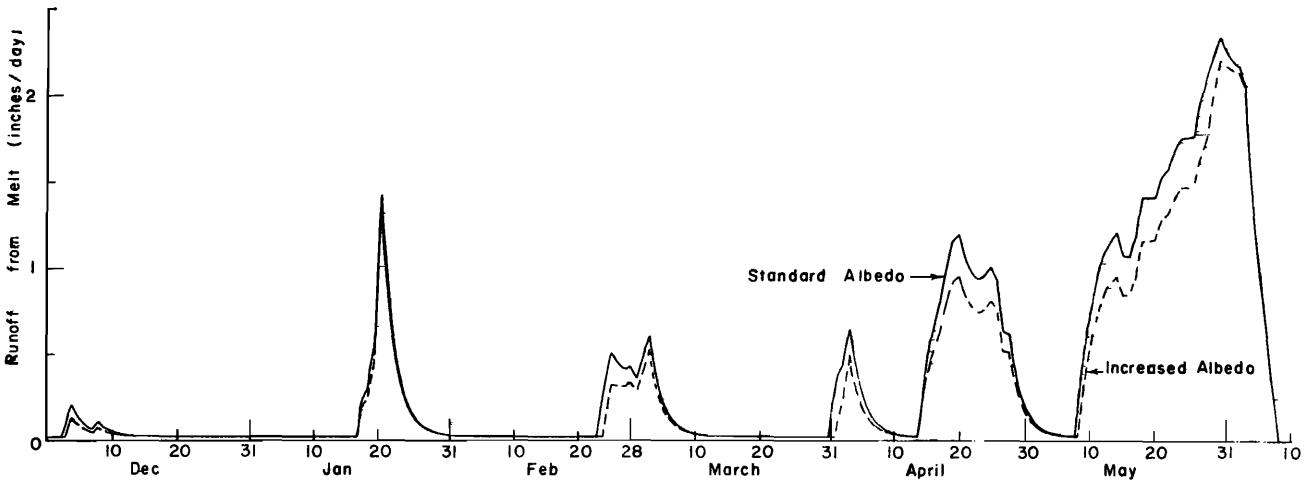

Figure 5.18. Runoff due to snowmelt for two albedo relationships for the year 1949-50, CSSL.

having the average slope and aspect of a basin defined correctly can be seen. The snow is completely melted by June 6 which is about midway between the two curves of Figure 5.19. The reduced water equivalent for the south facing slope is caused by increased snowmelt runoff from the pack. The effect of aspect on runoff from the pack can be seen in Figure 5.17. Data from the CSSL were used because snowmelt is obtained in all periods of time and shows the effect during all months of the snow season. For the north facing slope there was no melt for December and only a small amount near the first of March. The high peak on January 20 is caused by a rain on snow situation. During April and May the runoff generated is almost equal to that for a south facing slope.

With the slope and aspect of a basin defined accurately, the radiation index ratio for the snowmelt equation will be accurate. The slope and aspect can be calculated from the basin characteristics. Figures 5.14 through 5.19 demonstrate the importance of the radiation index to the model for the calculation of snowmelt and evaporation.

Albedo

Variation of albedo was checked to see what effect it had on the runoff and snowmelt for the Central Sierra Snow Laboratory. Figure 5.20 shows the albedo curves used in the sensitivity check. The runoff generated from them is shown in Figure 5.18. The lower runoff rate is shown with broken lines and is for the increased albedo curve with a minimum value of 0.5. The runoff from January shows little difference in actual magnitude because it was generated from a rain on snow event. The runoff that starts on April 13 is reduced by 21 percent with the new albedo curve. The albedo is a significant part of the snowmelt equation and needs to be defined properly to get accurate results. Figure 5.21 shows the effect of albedo on the water equivalent of the snowpack. The time the snow is on the ground is lengthened by 6 days which would change the flood peak for a basin.

Rain on snow events

The sensitivity of the melt rate to rain on snow was shown by modeling 14 days of arbitrary data shown in Table 5.1. These data were modeled in two ways, one without any precipitation and the other with the same daily temperature plus precipitation in the form of rain. Comparisons were made of the runoff rates as shown in Figure 5.22.

The snowmelt runoff hydrograph from a ripe pack without any rain is shown in curve 3 of the figure. Curve 1 shows the combined runoff from the precipitation and snowmelt, while curve 2 shows the precipitation input hydrograph. The delay of the surface melt and precipitation can easily be seen in this case since there was no precipitation or surface melt after the end of the eleventh day. At the end of 14 days, 3 days after melt ceased, there is still 0.155 inches per day runoff draining from the pack. This is quite insignificant when compared to 1.88 inches/day at the end of the eleventh day.

The runoff from each of the plots of Figure 5.22 was accumulated over the runoff period as shown in Figure 5.23. This was done to determine the runoff contribution from each of the factors. The accumulated precipitation of curve 2 at the end of 14 days is equal to 7.31 inches of runoff. The runoff due to surface melt shown in curve 3 is equal to 7.52 inches of runoff. These two amounts equal 14.83 inches of runoff which is 0.39 inches less than the accumulated runoff from the combined melt and precipitation of curve 1. The additional melt of curve 1 is generated from the heat released to the snow in cooling the rain from the air temperature to 32°F in the pack. The amount melted by the rain is quite small compared to the total runoff from the pack. It is 2.6 percent of the total rain plus surface melt of curve 1.

Rain on snow events are also affected by the cutoff temperature below which precipitation falls in the form of snow. For the CSSL and the UCSL data, the cutoff temperature was 35°F. It was found that this value was not low enough during simulation of the WBSL data.

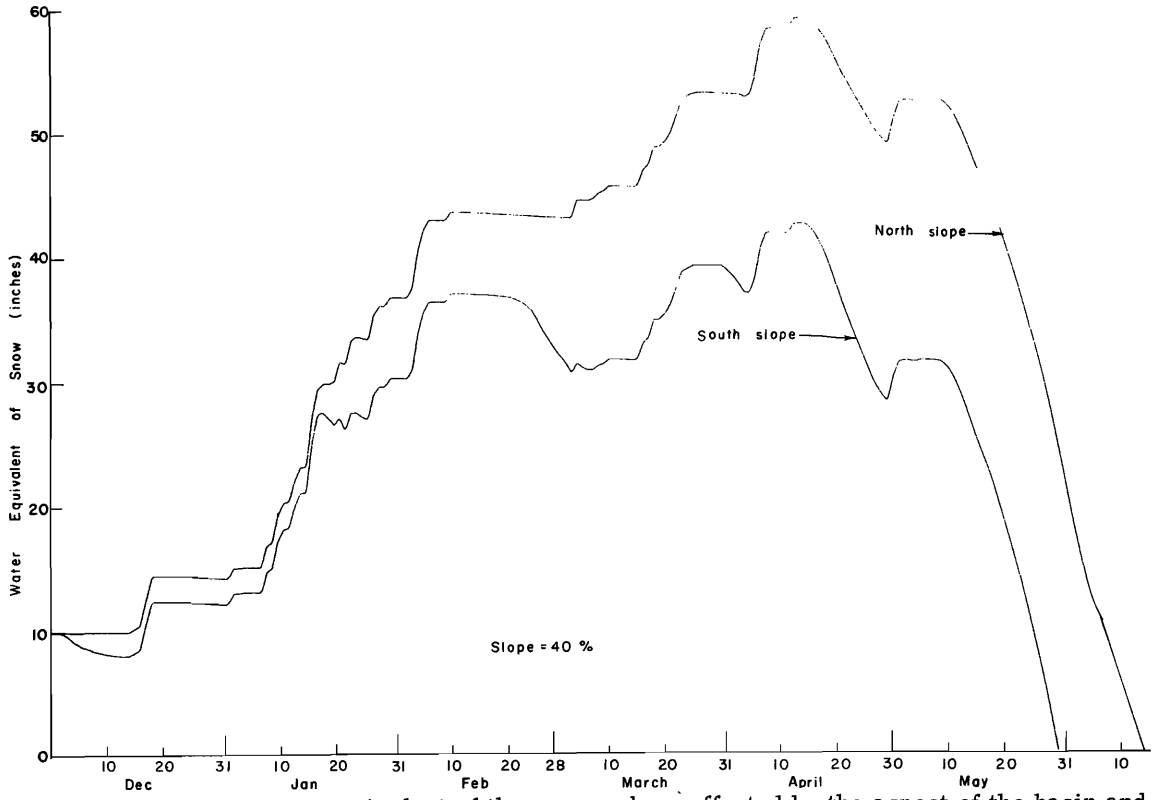

Figure 5.19. The water equivalent of the snowpack as affected by the aspect of the basin and a 40 percent slope for the year 1949-50, CSSL.

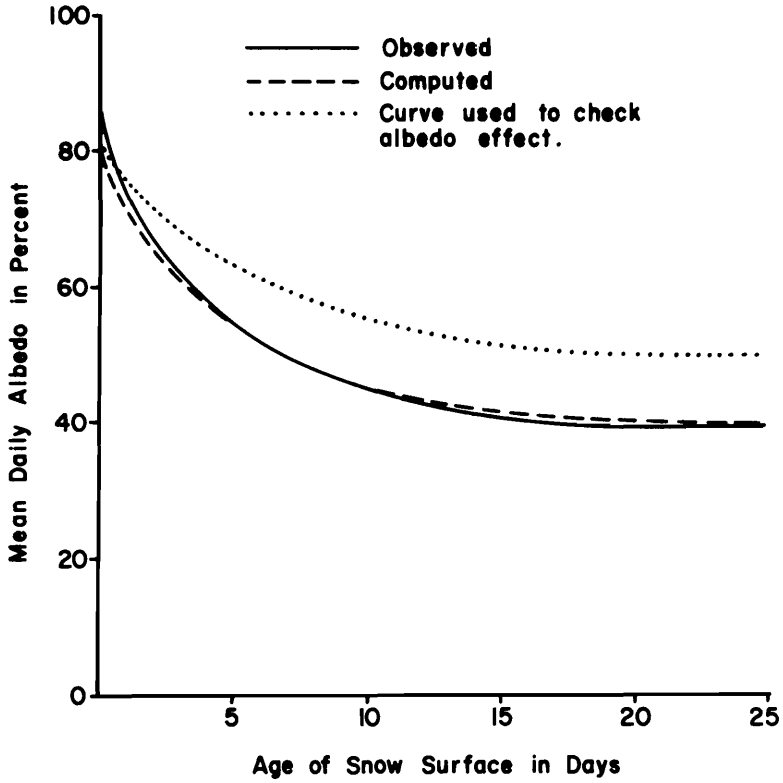

Figure 5.20. The two albedo curves used to produce Figure 5.18.

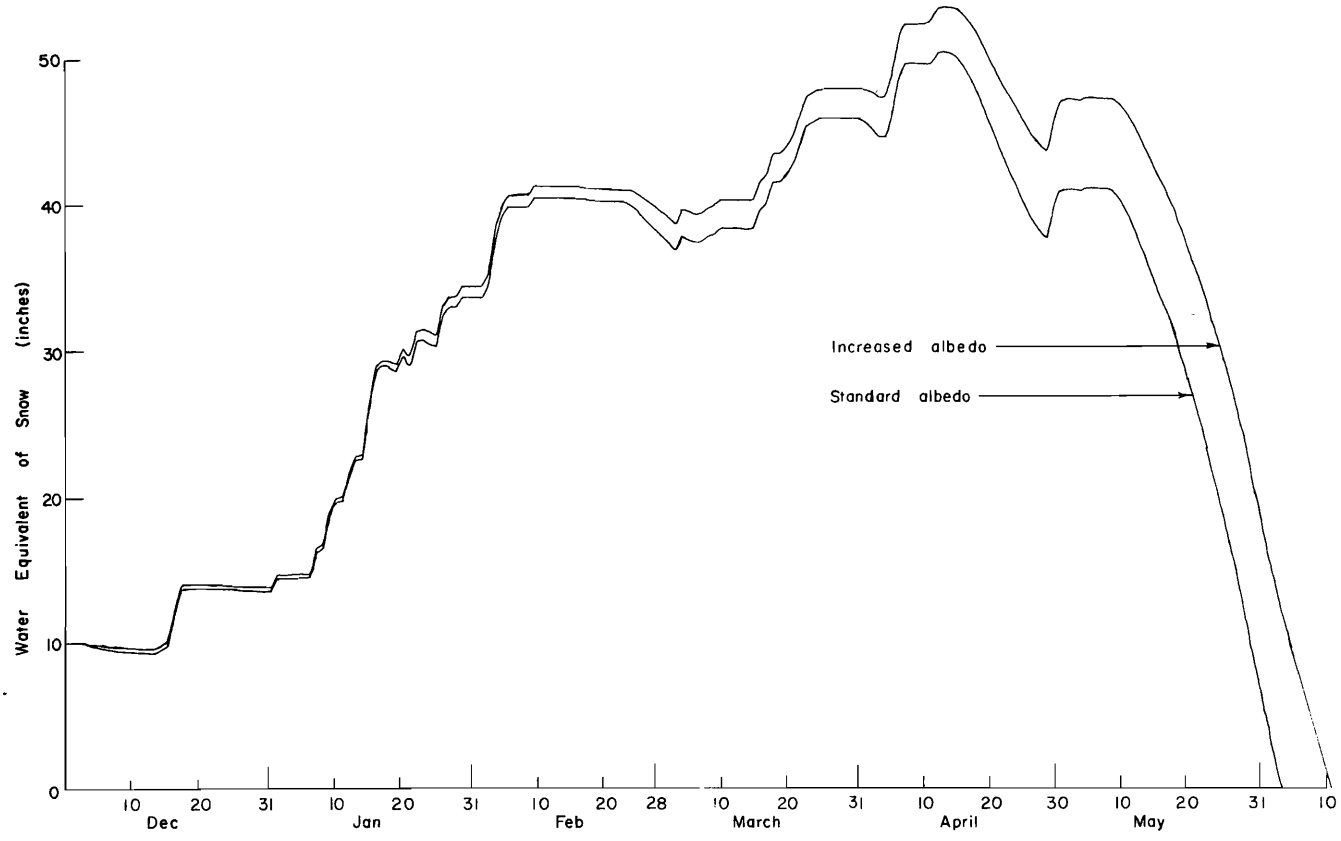

Figure 5.21. Plot of water equivalent as affected by increased albedo of Figure 5.20.

	With Rain		Without Rain
Day	Temperature	Precipitation	Temperature
1	37	0.34	37
2	39	0.54	39
3	40	1.54	40
4	38	1.00	38
5	42	0.39	42
6	35	0.20	35
7	40	0.60	40
8	41	0.80	41
9	45	0.15	45
10	50	0.50	50
11	37	1.25	37
12	32	0	0
13	32	0	0
14	32	0	0
		7.31	

Coefficients used in the simulation. $k_v = 0.40$, $k_m = 0.40$, $k_f = 0.05$, $k_s = 0.9$, $k_{sc} = 0.05$, $RI_h = 0.55$, $RI_s = 0.57$.

Table 5.1. Input data to model for rain on snow simulation.

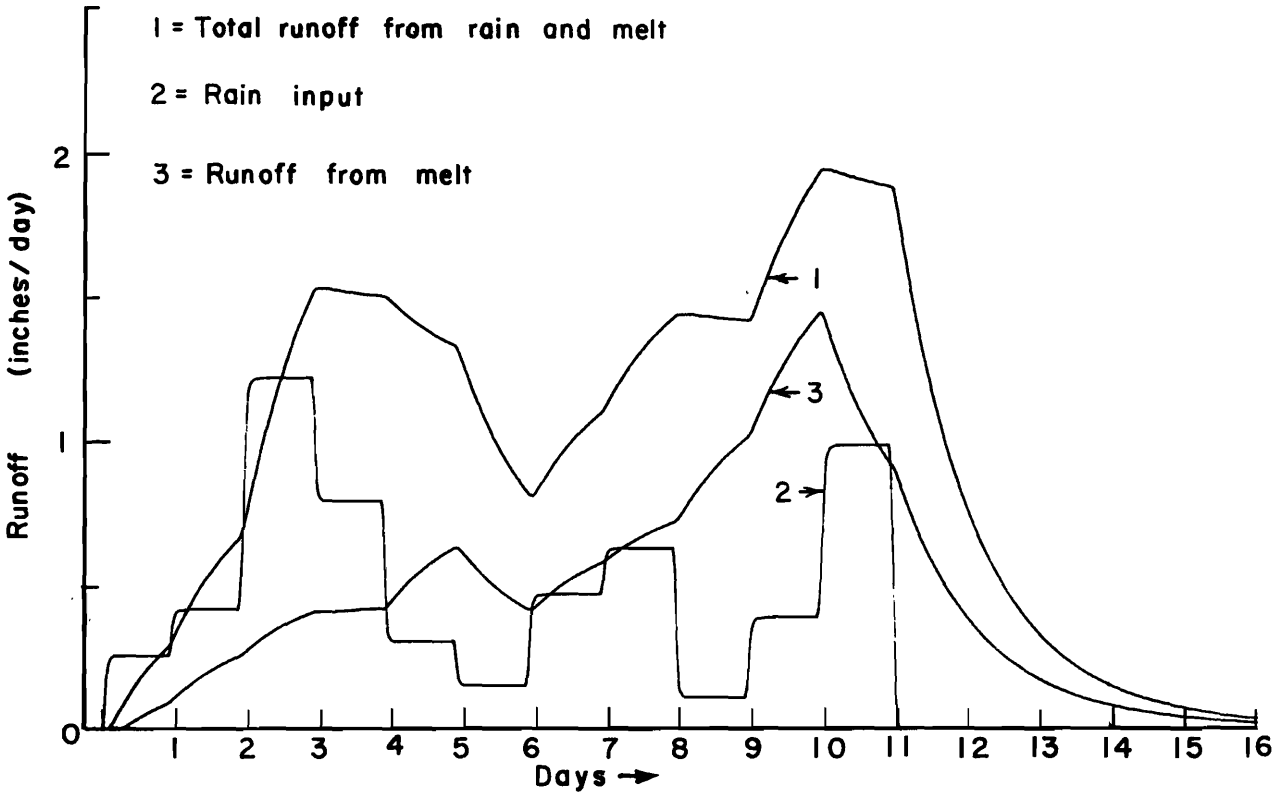

Figure 5.22. Plot of precipitation and snowmelt for a hypothetical simulated rain on snow event.

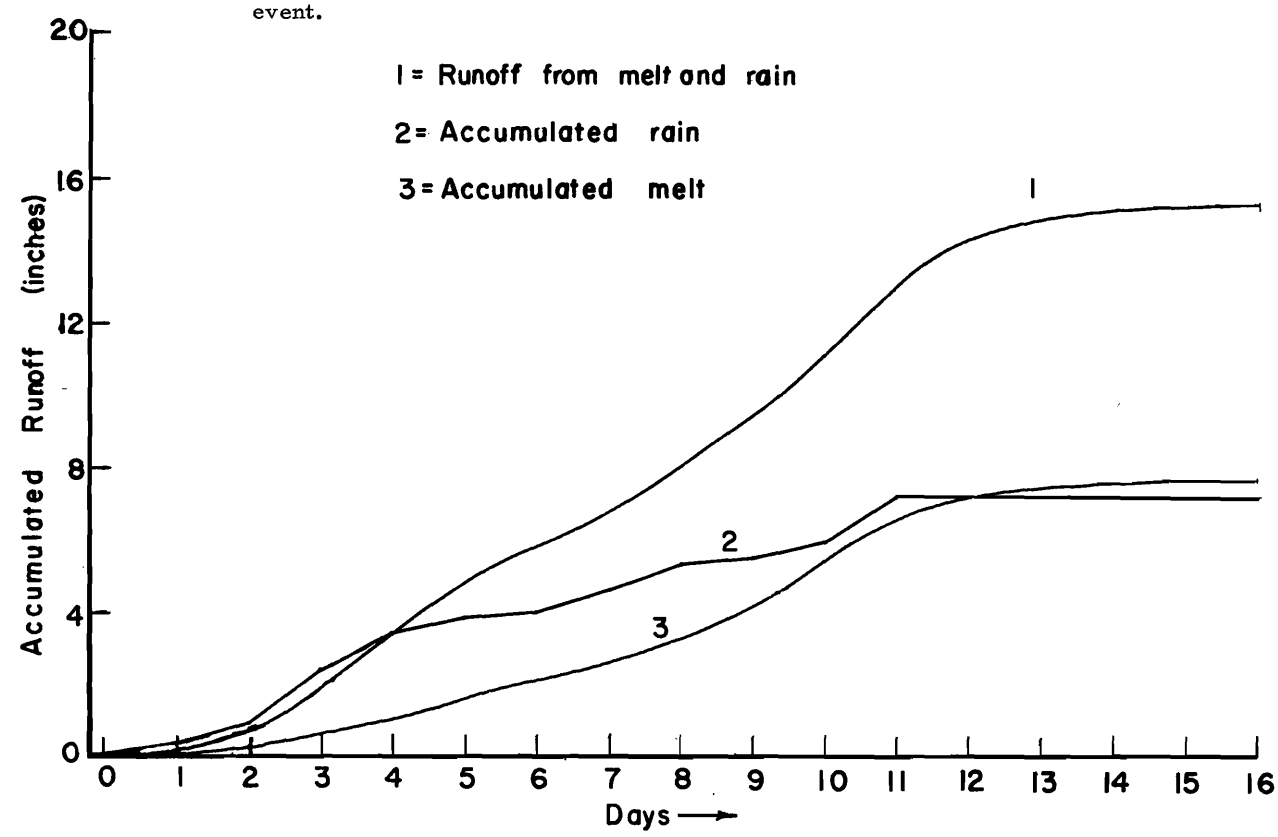

Figure 5.23. Accumulated precipitation and snowmelt for Figure 5.22.

In Figure 5.24 the effect of this cutoff temperature on the water equivalent of the pack is shown. The curves are shown for cutoffs of 35^{o}, 32^{o}, and 31^{o}F, with all other variables being held constant. This shows that the cutoff temperature is significant and needs to be evaluated for each basin. This temperature is important where much of the winter precipitation falls as rain and for low elevation watersheds like the WBSL.

Evaporation

Evaporation for the model was calculated from Equation 2.11. This is an evapotranspiration type equation which related evaporation to mean daily temperature. The results of evaporation calculated on the snowpack water equivalent are shown in Figure 5.25.

Figure 5.25 shows evaporation as calculated for the CSSL for the years 1946-47. For the period December 1 to April 1, the model evaporated 2 inches of water equivalent from the snowpack and caused the snow to disappear 2 days earlier than without evaporation. The 2 inches evaporated represented a loss of 11 percent of the maximum water equivalent.

West (39) found at the CSSL that the net evaporation for the snow seasons of 1958, 59, 60 was less than 1 inch for forested areas with 70 percent canopy cover. For small open areas in the forest the total evaporation was 1.68 inches or less. This study would indicate a value for net evaporation of about 1.0 inch of water from the pack for 1946-47, which is about 6 percent of the maximum water equivalent. For years with higher water equivalents the evaporation would not be as significant to the total runoff from the basin area.

In using Equation 2.11 to calculate evaporation from the snowpack, condensate was added to the snowpack if the mean temperature was below 18^{o}F. During the snowmelt period, when the new point is high, considerable condensation takes place. The equation used does not add any condensate during the melt period and cannot be used if the mean daily temperature is below 0^{o}F.

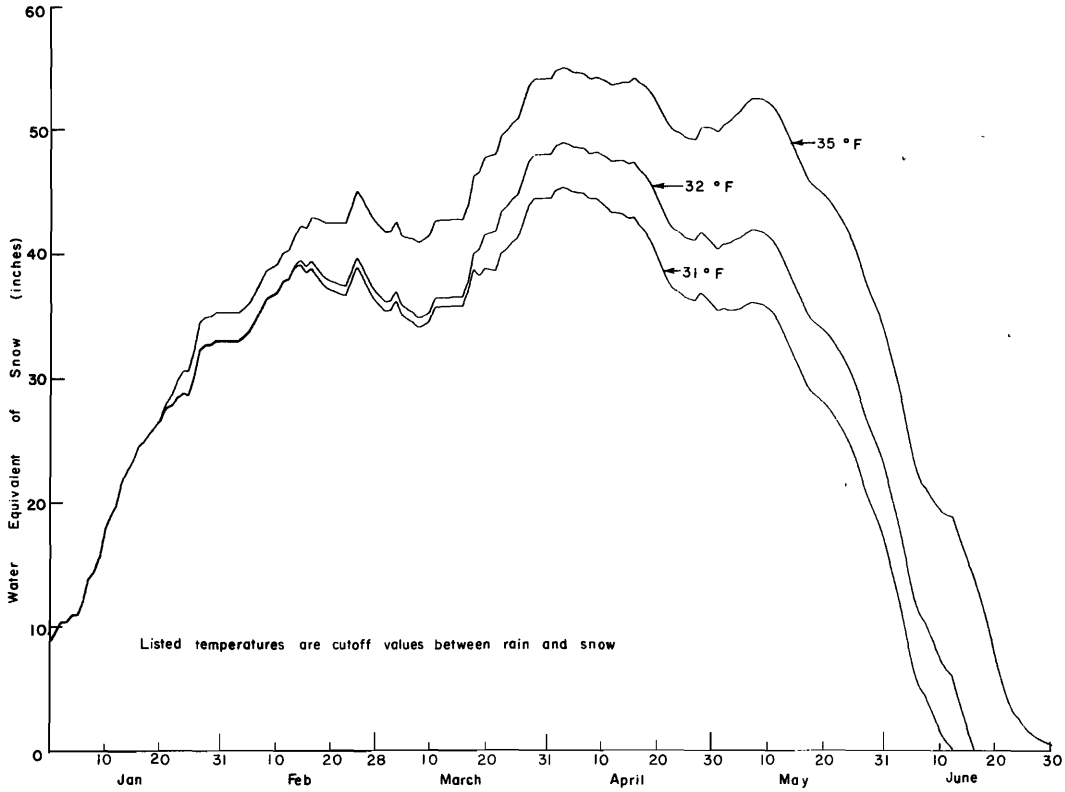

Figure 5.24. The effect of varying the temperature threshold between rain and snow on the water equivalent to the snowpack for 1948-49, WBSL.

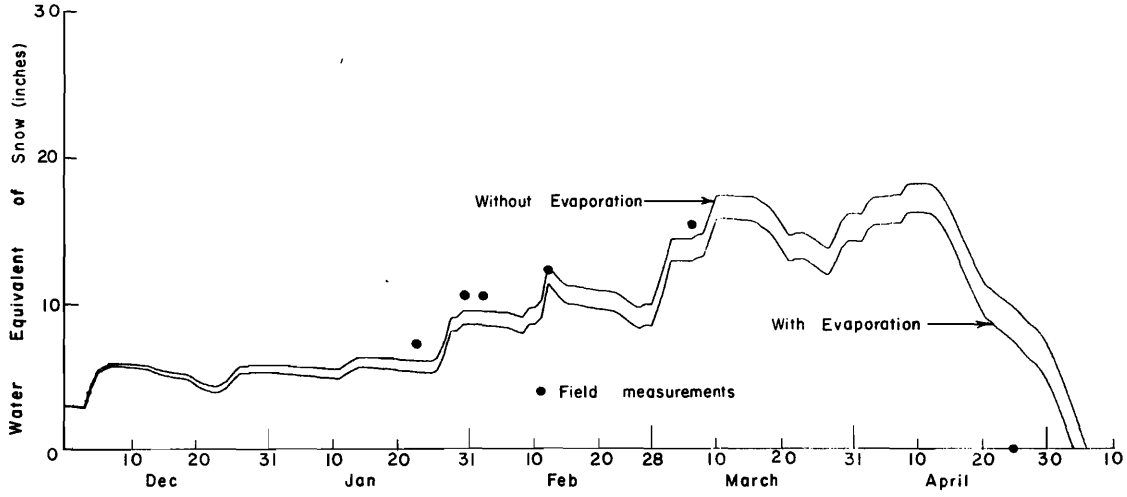

Figure 5.25. The effect of evaporation on water equivalent as calculated by the model for the year 1946-47, CSSL.

CHAPTER VI

CONCLUSIONS AND RECOMMENDATIONS

This report presents the findings of the simulation study of the snow accumulation and ablation processes. The basic components of the hydrologic model considered are temperature and precipitation. Other recorded data such as snow depth, density, water equivalent, and snow temperature were used to check intermediate points in the model.

An important aspect of this study is that the simulation model requires only those data which are usually available on a watershed or which can be readily computed for that watershed. Certainly a more sophisticated model could be constructed but its application would be limited to a few highly instrumented experimental watersheds. The model proposed in this report can be applied to any watershed where precipitation, temperature, elevation, and vegetative cover data are available.

The model was verified with field data from the Central Sierra Snow Laboratory, CSSL. It produced snowmelt each time that the stream flow indicated runoff from snowmelt for each of the three years simulated. The model was also tested on two other basins, the Upper Columbia Snow Laboratory, UCSL, and the Willamette Basin Snow Laboratory, WBSL. For these two basins, adjustments were made in the model to reflect variance in basin characteristics so that the snowpack conditions could be simulated. These adjustments included changes in the allowable maximum density, ground melt rate, density of new snow correlated to temperature, and snowmelt parameters to fit the slope, aspect, latitude, and vegetation of the basin. These changes demonstrated that the model can be readily applied to other basins if appropriate minor adjustments are made.

Conclusions

The model was used to simulate the conditions reflected by data collected at points in three different basins, and sensitivity tests were made. From this information the following conclusions were made:

1. A practical computer model for the snow accumulation and melt processes was developed.

2. The model can be applied to other regions with minor adjustments in the model coefficients.

3. The average density of the snowpack can be calculated from an apparent snow depth plus the accumulated precipitation and is a function of the compaction coefficient, maximum pack density, and new snow density. A good value of the compaction coefficient was found to be equal to 0.05. The value of maximum density was 0.6 for the CSSL and WBSL areas and was 0.5 for the UCSL area. It was found that for regions of cold temperatures such as those encountered at UCSL, new snow density correlated to air temperature gave better results than when a constant density was used.

4. The behavior of the model with reference to the major snowmelt equation parameters is summarized as follows:

   (i) A value of 0.4 for the proportionality constant, k_m, as used in the snowmelt equation was found to be applicable for all basins simulated.

   (ii) The variation of thermal diffusivity as a function of density was not important when compared to changes in snow depth.

   (iii) The model proved to be insensitive to the storage coefficient, k_s, and a value of 1.0 was found to be satisfactory for this parameter.

5. The amount of melt created by rain cooling to 32°F was insignificant under normal conditions when compared to the total runoff created by the surface melt plus rainfall at the same temperatures.

Recommendations

From the summary and conclusions drawn from the study, the following recommendations are made.

1. The snowmelt model should be included in a basin model and tested on an areal basis.

2. Rain on snow events should be modeled and the snowmelt examined more closely on the basis of a short-time increment of, for example, one hour. The system of differentiating between rain and snow needs to be improved, perhaps by using maximum daily temperature or mean temperature for a shorter time period than one day.

3. Thermal diffusivity for the model should be investigated more closely.

4. Consideration might be given to modifying the evaporation equation to include condensation of water on the pack during the snowmelt season. This modification, however, would probably involve the humidity and dew point temperatures which are not commonly measured information on most watersheds.

5. An investigation is recommended in which the snowpack is divided into several depth increments and the snowpack density is computed for each increment. In this way density and temperature stratification within the pack would be more realistically represented by the model.

BIBLIOGRAPHY

1. Amorocho, J., and B. Espildora. 1966. Mathematical simulation of the snow melting processes. Department of Water Science and Engineering, University of California, Davis. February.

2. Anderson, E. A. 1968. Development and testing of snow pack energy balance equations. Water Resources Research. 4(1):19-37.

3. Anderson, E. A., and N. H. Crawford. 1964. The synthesis of continuous snowmelt runoff hydrographs on a digital computer. Technical Report No. 36, Department of Civil Engineering, Stanford University.

4. Bergin, James D., and Robert H. Swanson. 1964. Evaporation from a winter snow cover in the Rocky Mountain forest zone. Proceedings, 32nd Annual Western Snow Conference. pp. 52-59.

5. Bertel, Fredwick A. 1965. Snow compaction method for the analysis of runoff from rain on snow. Proceedings, 33rd Annual Western Snow Conference. pp. 11-18.

6. Corps of Engineers, U.S. Army. 1956. Snow hydrology, summary report of snow investigations. North Pacific Division, Portland, Oregon. 437 p.

7. Corps of Engineers, U.S. Army, and U.S. Department of Commerce. 1952. Weather Bureau, Cooperative Snow Investigations. Hydrometeorological Log of the Central Sierra Snow Laboratory. Water Year 1949-50. South Pacific Division, Corps of Engineers, U.S. Army, San Francisco, California.

8. Corps of Engineers, U.S. Army, and U.S. Department of Commerce. 1952. Weather Bureau, Cooperative Snow Investigations. Hydrometeorological Log of the Central Sierra Snow Laboratory, Water Year 1950-51. South Pacific Division. Corps of Engineers, U.S. Army, San Francisco, California.

9. Corps of Engineers, U.S. Army, and U.S. Department of Commerce. 1952. Weather Bureau, Cooperative Snow Investigations. Hydrometeorological Log of the Upper Columbia Snow Laboratory. Water Year 1948-49. South Pacific Division, Corps of Engineers, U.S. Army, San Francisco, California.

10. Corps of Engineers, U.S. Army, and U.S. Department of Commerce. 1952. Weather Bureau, Cooperative Snow Investigations. Hydrometeorological Log of the Willamette Basin Snow Laboratory. Water Years 1949-50 and 1950-51. South Pacific Division, Corps of Engineers, U.S. Army, San Francisco, California.

11. Corps of Engineers, U.S. Army, and U.S. Department of Commerce. 1952. Weather Bureau, Cooperative Snow Investigations. Hydrometeorological Logs. Central Sierra Snow Laboratory. Water Year 1946-47. South Pacific Division, Corps of Engineers, U.S. Army, San Francisco, California.

12. Chow, Ven Te (Ed.). 1965. Handbook of applied hydrology. McGraw-Hill Company, New York.

13. Diamond, Marvin, and W. P. Lowry. 1953. Correlation of density of new snow with 700 mb temperature. Spire Research Paper 1, Snow, Ice, and Perm. Res. Estab., Corps of Engineers, Willamette, Illinois. August.

14. Frank, Ernest C., and Richard Lee. 1966. Potential solar beam irradiation on slopes: Tables for 30° to 50° latitude. Research Paper RM-18, Rocky Mountain Forest and Range Experiment Station, Fort Collins, Colorado. March. 116 p.

15. Garstka, W. U., L. D. Love, B. C. Goodell, and F. A. Bertle. 1958. Factors affecting snowmelt and streamflow. U.S. Bureau of Reclamation and U.S. Forest Service, U.S. Government Printing Office, Washington, D.C. 189 p.

16. Gay, Lloyd W. 1962. Measuring snowpack profiles with radio-active sources. Proceedings, 30th Annual Western Snow Conferences. pp. 14-19.

17. Gerdel, R. W. 1954. The transmission of water through snow. Trans. Amer. Geo. Un. 35(3):475-485. June.

18. Gray, Howard L. 1967. Density variation in a snowpack of Northern New Mexico. Proceedings, 35th Annual Meeting, Western Snow Conference, Boise, Idaho. April.

19. Hildebrand, R. B. 1962. Advanced calculus for applications. Prentice-Hall, Inc., Englewood Cliffs, New Jersey. 646 p.

20. Kennedy, J. M., R. T. Sakamoto, and A. T. Edgerton. 1967. Microwave radiometric sensing of the physical parameters of snow. Proceedings, 30th Annual Western Snow Conference. pp. 18-23.

21. Kuroiwa, Diasuke. . Snow permeability tests with a subfreezing liquid. Institute of Low Temperature Science, Hokkaido University, Sapporo, Japan. pp. 380-391.

22. Leaf, Charles F. 1966. Free water content of snowpack in subalpine areas. Proceedings, 34th Annual Western Snow Conference. pp. 17-24.

23. Lee, Richard. 1963. Evaluation of solar beam irradiation as a climatic parameter of mountain watersheds. Hydrology Papers No. 2, Colorado State University, Fort Collins, Colorado. 50 p.

24. Linsley, R. K., M. A. Kohler, and J. L. H. Paulhus. 1949. Applied hydrology. McGraw-Hill Company, New York.

25. McCallister, John P., and Ray Johnson. 1962. An objective forecast of the snowmelt hydrograph in the plains region. Proceedings, 30th Annual Western Snow Conference. pp. 78-85.

26. Peak, George W. 1962. Snow pack evaporation. Proceedings, 30th Annual Western Snow Conference. pp. 32-37.

27. Peak, George W. 1963. Snow pack evaporation factors. Proceedings, 31st Annual Western Snow Conference. pp. 20-27.

28. Rantz, S. E. 1962. Diurnal fluctuations of free-water content and density in a snowpack. Proceedings, 30th Annual Western Snow Conference. pp. 30-31.

29. Rikhter, G. D. 1945. Snow cover, its formation and properties. Spire Translation 6, Snow, Ice and Perm. Res. Estab., Corps of Engineers, Willamette, Illinois. August. (Translation by William Mandel from "Snezhnyi pokrov, ego formirovanie i svoistra," Izdatel stvo Akademiia Nauk SSSR, Moskva, 1945.)

30. Riley, J. Paul. 1967. Application of an electronic analog computer to the problems of river basin hydrology. Dissertation, Department of Civil Engineering, Utah Water Research Laboratory, Utah State University, Logan, Utah.

31. Riley, J. Paul, and Duane G. Chadwick. 1967. Application of an electronic analog computer to the problems of river basin hydrology. Project Report 46-1, Utah Water Research Laboratory, Logan, Utah. December. 199 p.

32. Riley, J. Paul, Duane G. Chadwick, and Keith O. Eggleston. 1969. Snowmelt simulation. Proceedings, 37th Annual Western Snow Conference. (Publication Pending)

33. Rowe, P. B., and T. M. Hendrix. 1951. Interception of rain and snow by second-growth Ponderosa Pine. Transactions, American Geophysical Union 32(6). December.

34. Swift, Lloyd W., Jr. 1960. A method for computing the effect of mountain topography upon available solar energy. Southeastern Forest Experiment Station Inservice (FS-1-wl-7-SE), North Carolina State College, Raleigh, North Carolina. 25 p.

35. Swift, Lloyd W., Jr., and C. H. M. van Bavel. 1961. Mountain topography and solar energy available for evapotranspiration. Presented before the Section of Hydrology, American Geophysical Union, North Carolina State College, Raleigh, North Carolina. April. 7 p.

36. U.S. Army Corps of Engineers. 1957. Flood prediction techniques. Department of the Army Technical Bulletin, TB 5-550-3, Department of the Army. February. 215 p.

37. U.S. Army Corps of Engineers. 1960. Runoff from snowmelt. Engineering and Design Manual 1110-2-1406. 75 p.

38. U.S. Civil Works Investigations. 1950. Technical Bulletin No. 6, Project CE-171. April. 7 p.

39. West, A. J. 1962. Snow evaporation from a forested watershed in the Central Sierra Nevada. Journal of Forestry 60(7):481-483.

40. West, A. J. 1959. Snow evaporation and condensation. Proceedings, 27th Annual Western Snow Conference. pp. 66-74.

41. Williams, G. P. 1955. A field determination of free water content in wet snow. National Research Council, Canada, Report No. 69 of the Division of Building Research, Ottawa. August.

42. Wilson, W. T. 1941. An outline on the thermodynamics of snowmelt. Transactions, American Geophysical Union I:182-205.

43. Wilson, W. T. 1941. Some factors in relating the melting of snow to its causes. Proceedings, Central Snow Conference 1:33. December.

44. Yosida, Z. 1963. Physical properties of snow. Proceedings, Massachusetts Institute of Technology, W. D. Kingery, Editor, MIT Press, February 12-16, 1962.

APPENDIX A

Snowmelt Simulation Program

```
C       SNOWMELT SIMULATION PROGRAM PREPARATION

        DIMENSION L(6),P(6),ALBED(25),RIS(6),RIH(6)
        DO 50 N=1,25
        READ(4,500) ALBED(N)
500     FORMAT(F6.4)
 50     CONTINUE
        PAUSE  1
        READ(4,600)CKV,CKM,DIN
600     FORMAT(3F6.4)
        PAUSE  2
        DO 210 K=1,6
        READ(4,100)L(K),P(K),RIS(K),RIH(K)
100     FORMAT(I5,3F10.6)
210     CONTINUE
        PAUSE  3
        M=0
        DO 410 K=1,6
        J=L(K)
        DO 400 I=1,J
        READ(4,200)TEMP,PRG
200     FORMAT(2F10.5)
        DEGD=TEMP-32.
        IF(DEGD.LT.0.0) DEGD=0.0
        EVAP=.25*P(K)*TEMP*RIS(K)/RIH(K)*(TEMP*.0173-.314)*.0167
        IF(TEMP.LE.32.) GO TO 230
        TEMSS=.32
        GO TO 240
230     TEMSS=TEMP/100.
240     IF(TEMP.LT.35.) GO TO 250
        SNAC=0.0
        PRM=PRG
        GO TO 260
250     SNAC=PRG/(DIN*200.)
        PRM=0.0
C       ALBEDO FORMULATED TO CREATE 1-A TO MULTIPLY BY THE DEGREE DAY
260     IF(SNAC.GT.0.0) GO TO 300
        M=M+1
        ALB1=ALBED(M)
        GO TO 310
300     M=1
        ALB1=ALBED(M)
310     IF(M.GT.25) ALB1=.60
320     CONTINUE
C       SUMATION OF HEAT FROM ALBEDO AND RAIN
        HOS2=(DEGD*(ALB1*CKV*CKM*RIS(K)/RIH(K)+.0067*PRM)+PRM)*.2
        PRG=PRG*.01333
        WRITE(5,440) EVAP, TEMSS,SNAC, HOS2,PRG
440     FORMAT(5F8.6)
400     CONTINUE
410     CONTINUE
        PAUSE  4
        STOP
        END
@
```

APPENDIX B

Snowmelt Control Program

```
C          SNOWMELT CONTROL PROGRAM EGGLESTON
        DIMENSION A(5),B(5)
        CALL  QSHYIN(IERR,580)
        CALL  QSC(1,IERR)
        CALL  QSSECN(IERR)
        CALL  QSDLY(10)
30      NCO=-5
        I=0
        B(1)=0.
        B(2)=0.
        B(3)=0.
        B(4)=0.
        B(5)=0.
        CALL  QWBDAR(B,00,05,IERR)
        CALL  QSTDA
        CALL  QSIC(IERR)
        PAUSE 1
160     CALL  QRLBB(ITEST,IERR)
        IF(ITEST.NE.'200) GO TO 160
        CALL  QSOP(IERR)
50      READ(4,100)(A(I),I=1,5)
100     FORMAT(5F8.6)
        B(1)=A(2)
        B(2)=A(3)
        B(3)=A(4)
        B(4)=A(5)
        B(5)=A(1)
140     IF(ABS(B(1)).GT.0.0) GO TO 150
        GO TO 300
150     CALL  QWBDAR(B,00,05,IERR)
        CALL  QSTDA
        I=I+1
        CALL  QRBADR(CDIN,0,1,IERR)
        IF(CDIN.GT..4) GO TO 200
      LA  /'100000
      OCT 5042
        GO TO 250
200   LA  /'40000
      OCT 5042
250     IF(NCO)260,270,270
260     CALL  QRLBB(ITEST,IERR)
        IF(ITEST.NE.'100) GO TO 260
        NCO=5
        GO TO 280
270     CALL  QRLBB(ITEST,IERR)
        IF(ITEST.NE.'200) GO TO 270
        NCO=-5
280     READ(4,100)(A(I),I=1,5)
        B(1)=A(2)
        B(2)=A(3)
        B(3)=A(4)
        B(4)=A(5)
        B(5)=A(1)
        GO TO 140
300     CONTINUE
        CALL  QSH(IERR)
        TYPE 5,I
5       FORMAT(6X,13HTOTAL DAYS = ,I4)
        PAUSE  2
        STOP
        END
@
```